Investigations into interferon response of novel bat cell cultures upon alphavirus infection

Dissertation

zur

Erlangung des Doktorgrades (Dr. rer. nat.)

der

Mathematisch-Naturwissenschaftlichen Fakultät

der

Rheinischen Friedrich-Wilhelms-Universität Bonn

vorgelegt von

Susanne Elisabeth Zweerink, geb. Biesold

aus

Leverkusen

Bonn, Januar 2013

Angefertigt mit Genehmigung der Mathematisch-Naturwissenschaftlichen Fakultät

der Rheinischen Friedrich-Wilhelms-Universität Bonn

am

Institut für Virologie des Universitätsklinikum Bonn

1. Gutachter: Prof. Dr. Christian Drosten
2. Gutachter: Prof. Dr. Hans-Georg Sahl
Tag der Promotion: 28.05.2013
Erscheinungsjahr: 2013

Für meine Lieben.

Wer immer tut, was er schon kann,

bleibt immer das, was er schon ist.

- Henry Ford

Contents

List of Tables

List of Figures

1 Introduction

1.1 Chiroptera (bats)

The class of mammals comprises more than 5,000 species. They all share the characteristics for classification like a coat which goes along with an endothermic living, breast feeding, and almost all are live bearing [39]. Most of the mammals are terrestrial, some are aquatic and some are even able to fly [39]. Flying mammals are represented by the order Chiroptera (bats), which form the second largest order within the mammals (20%) [179, 169]. The highest abundance of bats with the greatest species diversity can be found in the tropical regions [104]. With the development of special skills like active flying and the echolocation for orientation and hunting, bats were able to settle on all continents except Antarctica [179]. They can form colonies in highly diverse ecological niches (Figure 1.1) [89].

(a) (b)

Figure 1.1: **Examples of typical bat quarters.**
(a) The Kalkberg Cave in Bad Segeberg, Germany, is a hibernation side for around 20,000 bats (®Noctalis). (b) In tropical regions, some bat species form quarters in trees like in Kumasi, Ghana (® Institute of Virology, Bonn).

Chiroptera are subdivided into two suborders *Yango-* and *Yinpterochiroptera*.

Yangochiroptera comprise three bat super families: *Emballonuroidea*, *Noctilionoidea* and *Vespertilionoidea*. These include the insectivorous species *Myotis daubentonii* (*M. daubentonii*), *Pipistrellus spec.* (both *Vespertilionidae*), *Tadarida brasiliensis* (*T. brasiliensis*, *Molossidae*) and *Hipposideros cf. caffer/ ruber* (*H. cf. caffer/ruber*, *Hipposideridae*). The suborder *Yinpterochiroptera* includes frugivorous/nectarivorous bats (flying foxes) with species like *Rousettus aegyptiacus* (*R. aegyptiacus*), *Pteropus alecto* (*P. alecto*) and *Eidolon helvum* (*E. helvum*) as well as the insectivorous bat *Rhinolophus cf. landeri* (*R. cf. landeri*, *Rhinolophidae*)[195][89]. The neotropical fruit bat species *Artibeus jamaicensis* (*A. jamaicensis*) belongs also to the suborder *Yinpterochiroptera,* family *Phyllostomidae*. It is distributed in Middle and South America as well as regions of the Caribbean [179].

Migration of bats is closely related to their habitat. Seasonal migration is encountered particularly in the temperate zone covering a flying distance between 50 to 1,800 km [104]. Generally, seasonal migration is based on prospecting for summer quarters for the breeding of pups, and for winter quarters to hibernate in an environment with a constant temperature [8]. A typical hibernation cave is located in Bad Segeberg (10°18´57´´E; 53°56´09´´N), Germany, and is inhabited by 20,000 bats from eight different species every winter (Figure 1.1a) [63]. With a constant temperature of 9°C, it offers optimal hibernation conditions [63]. In the tropical zones, migration is influenced by the availability of food [104]. Figure 1.1b shows a roosting bat colony where the animals sleep during the day in trees and go hunting at night. With the absence of drastic seasonal climate change, hibernation does not occur in the tropical regions [104].

The second special skill of bats, which enabled the colonization of highly diverse niches, is the echolocation. Echolocation mainly occurs within the *Yangochiroptera* [173]. Bats produce high frequency sounds that are echoed off objects in the surroundings, giving the bats an accurate impression of the landscape, and objects in their surroundings [89]. The development of this ability has enabled night hunting and cave-dwelling. The *Yinpterochiroptera* lack the ability to echolocate, with the exception of the genus *Rousettus* [131].

High life expectancy, low reproduction rates and demanding living requirements make it challenging to use Chiroptera as a model organism in the laboratory. Therefore, more suitable models like cell cultures are desirable.

1.1.1 Description of bats relevant to this work

The straw-coloured fruit bat *E. helvum* belongs to the family of the flying foxes (*Pteropodidae*), accounts for the largest bat population in Africa [136] and is widely spread. These flying foxes are found in the forest and savannah zones south of the Sahara desert, on the south western part of the Arabian Peninsula and on the island of Madagascar [136]. The yellowish colour of their coat led to their name [136] (Figure 1.2a).

(a) (b)

Figure 1.2: **Pictures of two bat species relevant to this work.**
(a) The flying fox *Eidolon helvum* (*E. helvum*) is wide spread over the African continent with incidences at the Arabian Peninsula and the Island of Madagascar (® Institute of Virology, Bonn). (b) The Franquet´s epauletted fruit bat, also called *Epomops buettikoferi* (*E. buettikoferi*), is mainly found in western Africa (® Matschie. 1899. Megachiroptera Berlin Museum: 45).

The social interaction habits between members of *E. helvum* present a typical example of the social life of the bats in general [136]. They live in colonies of several hundred thousand to one million animals and sleep during the day in trees, caves or buildings in their roosts, while searching for food at night in smaller groups [136]. Their common diet is based on fruits from the Palmyra palm or the date palm, mangos and ceibas [136]. During foraging bats can cover a distance of 30 km per night [136].

Due to their widespread occurrence bats often come into contact with human [8]. They are, for example, often encountered close to food markets or plantations where bats sometimes destroy the harvest [8]. In some regions bats are also part of the human food chain and are consumed as protein source [216, 73].

The second bat species of importance in this work is the Franquet´s epauletted fruit bat, also called *Epomops buettikoferi* (*Epo. buettikoferi*). Like *E. helvum,* it belongs to the family of *Pteropodidae* but its distribution is limited to Ivory Coast, Ghana, Guinea, Guinea-Bissau, Liberia, Nigeria, Senegal, and Sierra Leone [8]. The primary diet of *E. buettikoferi* is fruits, like mangos, bananas, figs and guava fruits [8]. Franquet´s bats are solitary or live in small groups in lowland forests near bodies of water [8]. Normally they prefer tropical forests and roost in trees [98] (Figure 1.2b).

The species *Myonycteris torquata* (*M. torquata*) is distributed in West and Central Africa and known to roost as singles or in small groups, preferring lowland tropics and primary and secondary forest [133]. However, the species also appeared to migrate to grassland regions during rainy seasons and, due to their high capacity to adapt, also in city gardens [133]. The species *R. aegyptiacus* is spread throughout Africa, except in the desert regions of the Sahara, and the Middle East, as far east as Pakistan and in the southern part of Turkey [14]. They occasionally roost in trees and primarily in natural or man-made caves in large colonies and forage for food during the night [14]. Both bat species show antibody prevalence for Ebola viruses and are most likely the reservoir for this virus [150, 151].

1.1.2 Bats as reservoir for human pathogenic viruses

Bats have been shown to host relevant human pathogens like Rabies, Ebola, Marburg, Henipaviruses (Hendra-, Nipah-) and severe acute respiratory syndrome (SARS)-like Coronaviruses [24].

The human pathogenic SARS-CoV is one example for a zoonosis originating from bats [108, 149]. First serological studies on wildlife markets identified masked palm civets (*Paguma larvata*), racoon dogs (*Nyctereutus procyonoides*) and hog badger (*Artonyx collaris*) to have antibodies to SARS-CoV-like virus [66]. In the following SARS-CoV-like viruses were identified in the Chinese horseshoe bats (*Rhinolophus*) [108] and phylogenetic analysis proved close relation to the human SARS-CoV. The close contact between human, civets and bats on the wild life markets enabled effective transmission between reservoir and alternate hosts as well as the dead end host [184]. In the following years CoV antibodies could be detected in African and European bat species [63, 134].

The family *Paramyxoviridae* comprises a large number of human and veterinary pathogens including measles-, mumps-, parainfluenza- and rinderpest virus as well as Sendai-, Hendra- ((HeV) in Australia) and Nipah virus ((NiV) in Asia) (genus

Henipavirus) [99]. First associations with bats (genus *Pteropus*) as reservoirs were found for *Henipaviruses*, which cause fatal encephalitits in humans [73, 49]. Related viruses exist in a colony of *E. helvum* fruit bats in Ghana [41] and most recent studies identified new virus species belonging to the genus *Henipavirus* found in six bat species collected in five different African countries [42].

Certain alphaviruses were found in several bat species like Egyptian rousette (*R. aegyptiacus*), Sundevall´s leafnosed bat (*H. caffer*) or the vampire bat (*Desmodus rotundus*) [24]. The bats were most probably infected by arthropods. If they play a role in the life cycle of alphaviruses needs to be analysed. First connections between bats and SINV were described by Blackburn *et al.* in 1982 [19], who were able to isolate the virus from bat organs. ONNV, CHIKV and SINV are primarily associated with polyarthritis and rash [99]. The representative of the New World alphaviruses, VEEV, belongs to the Venezuelan equine encephalitis complex [99]. It was first isolated in brains of horses in the Guajira region of Venezuela in 1936 [212]. The outbreak spread to the central valleys of Colombia and later the virus was also isolated in South America, Central America, the Caribbean islands and the southern regions of the United States [212]. The main vector of the virus belongs to the *Culex* genus [48]. As the name already implicates the virus belongs to the encephalitis causing alphaviruses [99]. Interestingly, first detections of VEEV in neotropical bats were described in 1939 by Kubes *et. al* [101]. In the following years similar discoveries were made in Equador, Colombia and Mexico as well as in Texas (USA) [202]. Seymour *et al.* could identify antibodies against VEEV in bats from Mexico and Guatemala in 1973 and postulated a role of bats in transmission during the enzootic cycle of the virus [168]. The serological survey of neotropical bats for at least 10 different virus antibodies including WEE, EEE and VEEV by Ubico *et al.* confirmed earlier findings of antibodies against VEEV in bats for Guatemala, underlining the evidence of the role of bats in the enzootic cycle of the virus [202].

1.1.3 Cell cultures of bats

The role of bats as reservoirs implicates the question how these mammals deal with virus infections. Bats are difficult to breed making live animal studies challenging (1.1). Cell culture systems are a good alternative and are a favoured model to answer fundamental questions. Commercially available are only the bat cell lines Tbl-Lu (ATCC number CCL-88, generated from the lung of *Tadarida brasiliensis*) and Mvi/It (ATCC number CRL-6012, originated from inter scapular of *Myotis velifer incautus*). Crameri et al. presented *P. alecto* immortalised bat cells, which

were characterized and could be used for virus-host interaction studies [32]. They described that the commercially available cells were not infectable with their viruses of interest [32]. The generation of specific bat cell lines like primary fetal cells from the Egyptian fruit bat (*R. aegyptiacus*) traced back on the idea that isolation and characterization of viruses may be more efficient in the reservoir [90]. For in-depth studies and virus-host interaction studies in the reservoir, the establishment of specific cell lines is essential.

1.2 Alphaviruses

Alphaviruses belong to the family *Togaviridae* and are mainly arthropod-borne viruses. Based on the geographic location from which they were originally isolated, these viruses could be classified as either New World alphaviruses or Old World alphaviruses [189]. Old World Alphaviruses include Chikungunya virus (CHIKV), O´nyong-nyong virus (ONNV), Ross River virus (RRV), Semliki Forest virus (SFV) and Sindbis virus (SINV). They cause fever, rash and arthralgia syndrome which is rarely fatal [99]. The representatives of the New World alphaviruses, such as Eastern equine encephalitis virus (EEEV), Venezuelan equine encephalitis virus (VEEV) and Western equine encephalitis virus (WEEV), commonly cause encephalitis in horses, humans and other mammals [158]. Initial studies on alphaviruses focused on the prototypic SFV and SINV, because both grew to high titers in cell cultures and were not pathogenic for humans [158]. Recently attention has been directed towards investigations on CHIKV due to the 2005 outbreak of CHIKV in La Reunion resulting in over 300,000 cases of infection and 250 fatalities [180].

1.2.1 Genomic composition and virion structure

The alphavirus genome is a single-stranded, positive-sense, RNA genome and comprises approximately 12 kb [176, 188]. Subgenomic mRNAs, which encode the structural proteins are generated during viral replication [176, 188]. Both genome species contain a 5´cap and a poly (A) tail [99]. Within the coding sequence there are two open reading frames (ORFs) [74]. The ORF located at the N-terminus encodes for the nonstructural polyprotein, whereas the C-terminally located ORF is encoding the structural polyprotein (Figure 1.3) [74].

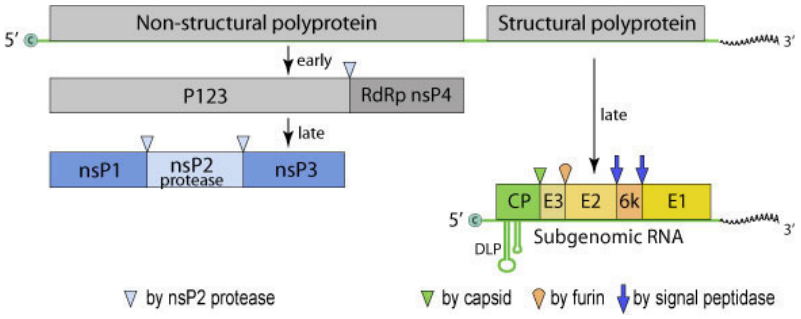

Figure 1.3: **Alphavirus genome and variations during replication.** Single-stranded, positive-sensed RNA forms the alphavirus genome. It encodes two open reading frames. In this scheme the early and late processing of the polyproteins is highlighted with the identified proteases. nsP, non-structural protein; P123, non-structural polyprotein of nsP1, 2 and 3; RdRp, RNA-dependent RNA polymerase; CP, capsid; E2 and E1, glycoprotein; 6K, 6K protein (ViralZone:www.expasy.org/viralzone, Swiss Institute of Bioinformatics).

Viral and host proteases cleave the two polyproteins [74]. The RNA replication is performed by the four nonstructural proteins and their intermediates (nsP1 to 4), and for viral encapsidation and budding the five structural proteins (C, E3, E2, 6K, E1) are needed (Figure 1.3) [74].

In general alphaviruses are found to be small, icosahedral-shaped and enveloped viruses with approximately 70 nm in diameter [123, 135]. The lipid membrane surrounding the alphavirus virion is host-cell acquired and has 80 spikes arranged in a $T = 4$ icosahedron [56]. The spike protrusions are formed by trimers, which in turn are assembled by heterodimers of the glycoproteins E1 and E2 (Figure 1.4) [209].

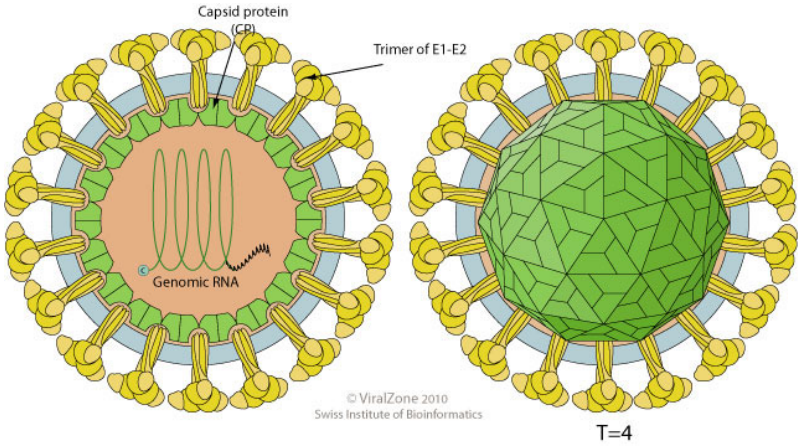

Figure 1.4: **Scheme of the alphavirus virion.**
The scheme depicts the icosahedral structure with highlighted structural alphavirus proteins and the genomic RNA. Capsid protein and the genomic RNA are coloured in green and the spikes are coloured in yellow (ViralZone:www.expasy.org/viralzone, Swiss Institute of Bioinformatics).

Newly synthesized viral genomic and subgenomic RNAs are capped and methylated by the nsP1 protein [4, 132], which is assumed to anchors replication complexes to cellular membranes during RNA replication [142]. The nsP2 combines three activities and is mainly active as protease in processing of the nonstructural polyprotein (Figure 1.3) [64, 206, 154, 74]. ADP-ribose 1-phosphate phosphatase, as well as RNA binding activity were identified with the help of crystal structures of the CHIKV and VEEV nsP3 N-terminus [122]. An RNA-dependent RNA polymerase (RdRp) function was described for the nsP4 protein [69][170].

Viral genomic RNA is bound by the alphavirus capsid protein (CP), during nucleocapsid formation [138, 214]. The role of the structural protein E3 varies between the different alphaviruses and is, therefore, undefined [112][61][175]. The glycoprotein E2 mediates receptor binding [183, 60, 118]. The 6K protein plays an important part in the alphavirus particle assembly [86, 57] and has also been described as a viroporin [163, 162, 129]. E1 protein is defined as a fusion protein for all alphaviruses [21, 137].

1.2.2 Alphavirus Life-Cycle

Alphaviruses enter the cell via receptor-mediated endocytosis [99]. By fusion with the endosomic membrane the nucleocapsid is released into the cytoplasm (Figure 1.5).

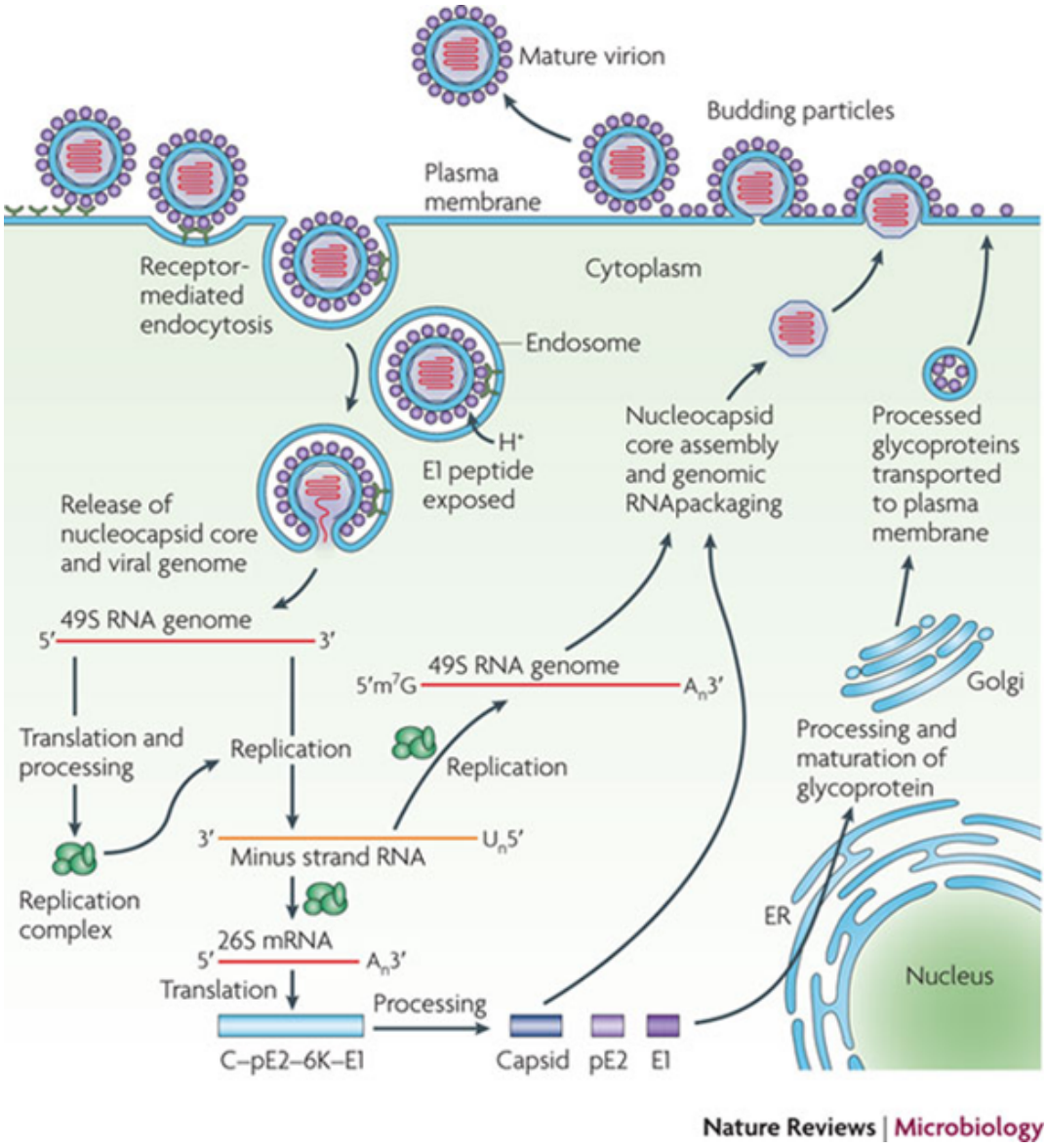

Figure 1.5: **Replication cycles of alphaviruses.**
The virus enters a cells via receptor mediated endocytosis. After release of the nucleocapsid and the viral genome, translation of the nonstructural proteins starts. Formation of a replication complex allows replication of minus strand RNA, which serves as template for subgenomic RNA. Here the structural proteins are translated and processed. Final processing and maturation of pE2 and E1 takes place in the endoplasmic reticulum (ER) and the Golgi apparatus. Meanwhile the nucleocapsid core assembly and genomic RNA packaging takes places in the cytosol. The processed structural proteins are transported to the plasma membrane and form together with the nucleocapsid budding particles, which are released as mature virions into the intracellular space [166].

Here the viral genome is set free and translation of the nonstructural (P1234) and structural polyproteins starts immediately [62][36]. Together, the nsps build an unstable initial replication complex, which starts to synthesize negative-strand RNA

[189, 110, 171, 33]. When cleavage is completed to nsP1, nsP2, nsP3 and nsP4, synthesis of negative-strand RNA is inhibited and the stable replication complex starts the synthesis of postitive-strand genomic and subgenomic RNA [110, 171]. The replication mechanism is controlled by a leaky termination codon located behind nsP3 resulting in a read-through efficiency of 10-20 % [116]. The structural polyprotein is cleaved cotranslationally and starts with the autoproteolytic cleavage of the CP (Figure 1.3) [127, 7, 61]. CP binds to newly synthesized RNA, leading to RNA packaging and nucleocapsid assembly (Figure 1.5) [214, 138]. The remaining polyprotein is inserted into the endoplasmic reticulum and is processed by a host signal peptidase [127, 121]. The budding process is driven by interactions between CP and the cytoplasmic domain of the E2 protein, leading to envelope formation around the nucleocapsid-like particles by E1-E2 heterodimers [139, 130, 207]. The membrane bilayer of the virions is obtained upon release from the host cell plasma membrane (Figure 1.5) [56, 3, 106, 209].

The early phase of infection is characterized by high virus titers at the primary infection site and leads to fever which is accompanied by a strong increase of interferon (IFN) (Figure 1.6) [99].

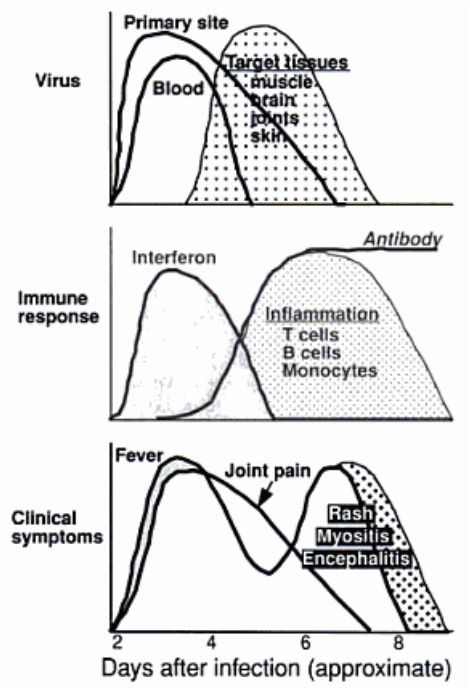

Figure 1.6: **Alphavirus infection and clinical consequences.**
The three schematic diagrams describe virus replication, immune response to it and the clinical symptoms of the human body over time illustrating the connectivity between the three factors [99].

During late phase of infection the virus replication is concentrated on the target

tissues (like muscle, brain, joints and skin) inducing symptoms like joint pain, rash, myositis and encephalitis [99]. The adaptive immune response is in parallel activated (Figure 1.6) [99].

1.2.3 Alphaviruses transmission cycles

ONNV and CHIKV are closely related and belong to the Semliki Forest antigenic complex [94]. While ONNV is distributed in the central east part of Africa, CHIKV outbreaks are found in sub-Saharan Africa, South-east Asia, Indonesia and the Philippines [99]. Although the two viruses are closely related, they have different mosquito hosts [205]. CHIKV is transmitted by several species of the genus *Aedes* [92], ONNV is the only alphavirus known so far to be transmitted by *Anopheles* mosquitoes, which is the main vector for Malaria [218, 30]. SINV is a member of the Western equine encephalitis complex and was isolated in Europe, the Middle East, Africa, India, Asia, Australia and the Philippines [99]. Its vectors are species of two different mosquito genera, *Culex* and *Culiseta* [99].

Viruses, which are transmitted by arthropod vectors (like ticks or mosquitoes), are summarized as **ar**thropod-**bo**rne viruses (*Arboviruses*) [99]. *Arboviruses* have a natural transmission cycle (Figure 1.7).

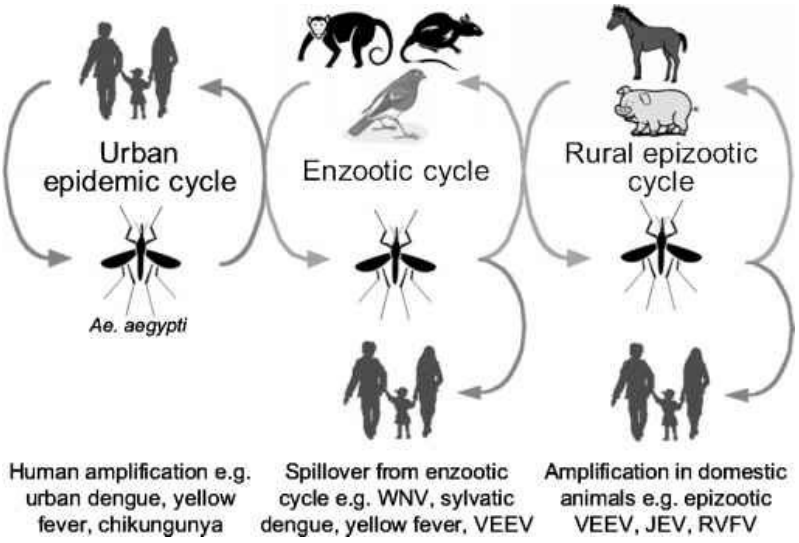

Figure 1.7: **Transmission cycles of arboviruses.**
Three different transmission cycles have been described for arboviruses. The enzootic or sylvatic cycle involves wild animals, mostly small mammals or birds and a vector mosquito and rare human infections. Crossing to a epizootic or epidemic cycle includes a host change and can additionally include a vector change. The rural epizootic cycle includes non-wild animals like horses or pigs, while the urban epidemic cycle has humans as new host (http://explow.com/sylvatic).

This is called sylvatic or enzootic cycle, in which the virus cycles between wild animal populations and the lifelong infected vector and humans are normally dead-end hosts infected by vectors [99]. Often small mammals like rats, opposums, birds or monkeys are ´hosts‘ [47, 88]. In most cases the defined vector is only one mosquito species, but in some cases several mosquito species serve as vectors in the sylvatic cycle [48]. When a virus changes host, it enters the epizootic cycle [197]. This can be caused by the usual vector with a mutated virus or it can be due to a so called bridge vector mosquito (introduction of the virus in a different mosquito, which has e.g. less specialized feeding habits) [99]. The epizootic cycle is divided in the domestic or the urban epidemic cycle [99]. In the first case domestic animals like horses and pigs are involved, in the latter case, humans are the new host [99]. At this stage humans are the host for the virus and transmission is limited between vectors and humans (Figure 1.7) [99]. Viruses in the epizootic cycle are highly infectious and trigger disease in several thousand people or domestic animals [99].

For VEEV it was shown that species of the genus *Culex* are part of the enzootic cycle [48]. It was described that the primary vectors during epizootic cycles are *Psorophara confinnis* and *Aedes sollicitans* (*Ae. sollicitans*), which suggests that a change in the transmission cycle has taken place [212]. For CHIKV monkeys and two mosquito species (*Ae. africanus*, *Ae. furcifer*) were identified to be involved in

the sylvatic cycle, while the mosquito *Ae. aegypti* could be identified to be involved in the urban epizootic cycle between human and mosquito in Africa [37, 197]. It is postulated that CHIKV has no enzootic cycle in Asia and, therefore, remains in the urban cycle (Figure 1.7)[102]. During epidemics of ONNV human-mosquito-human transmissions have been described [205, 174]. The enzootic vector and vertebrate reservoir host remain unidentified [205, 174]. For SINV the main mosquito vectors of the sylvatic cycle belong to the genus *Culex* and *Culiseta* with birds as the major vertebrate host [99]. Entering the urban epidemic cycle is most probably based on the introduction of the virus into the bridge vector mosquito of the genus *Aedes [22].*

1.3 IFN response to virus infections

The innate immune response is composed of physical and chemical barriers as well as cellular response mechanisms (including the IFN response) to prevent viral and bacterial infections [87]. The first line of intracellular defence to virus infections are intrinsic immune-related proteins that recognize either viral proteins or viral nucleic acids (Figure 1.8) [87].

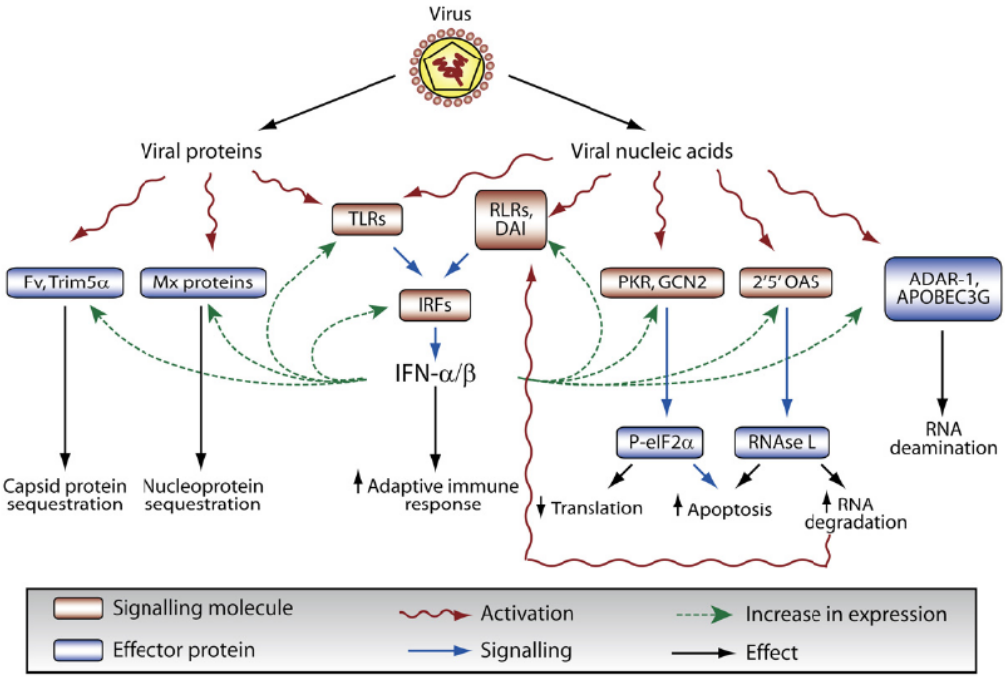

Figure 1.8: **Innate response to virus infection.**
The first innate response to viruses can be distinguished between viral proteins and viral nucleic acids. Viral proteins are recognized by cytoplasmic restriction factors like Fv (mouse), TRIM-5α (human), or myxovirus resistance (Mx) proteins and by TLRs. Viral nucleic acids activate kinases protein kinase R (PKR), the general control non-derepressible -2 (GCN2) and additional kinases which phosphorylate the eukaryotic translation initiator factor 2 (eIF2α), resulting in the downregulation of translation. Activation of 2´-5´oligoadenylate synthetase (OAS) is caused by viral RNA and triggers RNase L and thereby inducing unspecific RNA degradation. Apoptosis can be induced by both PKR and 2´-5´-OAS. Additionally, mutations in viral genomes are caused after viral RNA recognition by the adenosine deaminase acting on RNA (ADAR1) and the apolipoprotein B mRNA-editing enzyme catalytic polypeptide-like editing complex (APOBEC3G). Viral nucleic acids activate Toll-like receptors (TLRs), (RIGI-like) receptors (RLRs) and DNA-dependent activator of IFN regulatory factors (DAI), which induces a signalling cascade with final activation of IRFs and transcritpion of IFN-$\alpha$and IFN-β genes. This triggers the expression of antiviral proteins and thereby the antiviral status.[146]

Capsid proteins of retroviruses are targeted by Fv (murine) or tripartite motif protein (TRIM) 5α and nucleoproteins of bunya- and orthomyxoviruses are recognized by myxovirus resistance (Mx) proteins [71, 17]. The apolipoprotein B mRNA-editing enzyme catalytic polypeptide-like editing complex (APOBEC) 3G entail mutations causing subsequent virus replication by deamination retroviral genomes (Figure 1.8)[72, 17]. Additional antiviral mechanisms can be activated by viral presence [160]. The presence of viral RNA activates the kinases protein kinase R (PKR) and/or the general control non-derepressible -2 (GCN2), causing phosphorylation of

the α subunit of the eukaryotic translation initiator factor 2 (eIF2α), that leads to downregulation of mRNA translation (Figure 1.8) [16, 217]. The 2´-5´oligoadenylate synthetase (2´-5´OAS) is also activated by viral RNA and stimulates RNAse L, which induces RNA degradation [147]. Finally, viral replication intermediates are deaminated by adenosine deaminase acting on RNA (ADAR)-1 (Figure 1.8) [160]. Taken together these effects (decreasing protein translation, RNA degradation and RNA deamination) have strong effects on the cell viability and can lead to apoptosis [160]. Notably these antiviral responses are only active when a cell is infected and are directed by pattern-recognition receptors (PRRs), which lead to the expression of proinflammatory cytokines and chemokines arranging the innate and adaptive immunity [87]. They recognize lipopolysacchride (LPS) or viral nucleic acids taken together as pathogen-associated molecular patterns (PAMPs) and can be divided in three classes, namely Toll-like receptors (TLRs), retinoic acid-inducible gene I (RIGI-like) receptors (RLRs) and nucleotide oligomerization domain (NOD)-like receptors (NLRs) [126, 6]. TLRs and RLRs play a major role in regulating the expression of type I IFNs and several other cytokines. NLRs mainly lead to the production of interleukin-1β (IL-1β) through caspase-1 activation [152, 93]. On cellular level viral infection can trigger natural killer (NK) cells to stimulate dendritic cell (DC) activation, resulting in the induction of the adaptive immune response (Figure 1.8) [109].

1.3.1 Induction of IFN and cytokines

The intracellular response upon infections consists of gene-regulatory networks that allow prompt alternations in gene expression [198]. While TLR3, 7 and 9 recognize PAMPs in the endosomes, the RLRs are located in the cytosol (Figure 1.9).

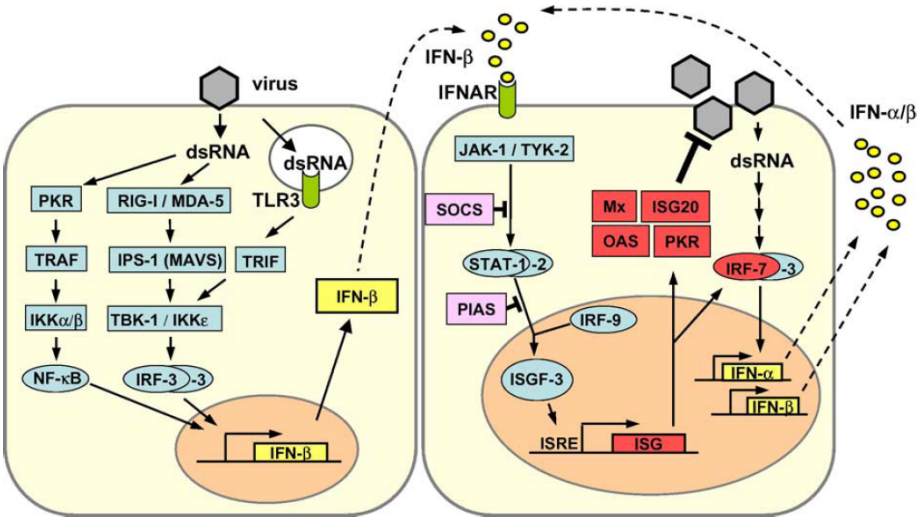

Figure 1.9: **Scheme of the IFN response of the cell.**
After viral entry (for enveloped viruses via endocytosis or fusion with the plasma membrane) single or double-stranded RNA molecules are released. They are recognized by Toll-like receptors in the endosomes or MDA5 or RIG-I as well as PKR in the cytoplasm. The recognition actives a cascade of phosphorylation leading to IRF3 dimerization and its translocation to the nucleus. Here the complex binds to the IFN promoter and induces IFN-β mRNA expression. The protein is secreted and activates in an auto- and paracrine way the JAK/STAT-pathway, which induces an antiviral state of the cell by expressing IFN stimulated genes (ISG). ISGs can either interact directly by inducing degradation of viral RNA or by inhibiting the host transcription and in the end by inducing apoptosis [70].

Representatives of the RLRs are RIG-I and the melanoma differentiation-associated gene 5 (MDA5) and also the laboratory of genetics and physiology 2 (LGP2) [221]. The signalling activity of RIG-I and MDA5 is mediated by two caspase activation and recruitment domains (CARDs) located N-terminally [193]. All three molecules share an internal DExD/H-box RNA helicase domain that has ATPase activity [222]. It was shown that the ATPase activity, activated by ligand binding, is crucial for signalling [222, 193]. The C-terminal region of RIG-I and LGP2 consists of a repressor domain (RD), which keeps the molecules inactive until ligand binding occurs. This triggers conformational changes resulting in CARD domain release and induces signalling [159]. RIG-I and MDA5 bind via the released CARD domain to the signalling-adaptor molecule, IPS-1, which is located in the outer mitochondrial membrane (also known as MAVS, VISA or Cardif) [167, 97]. IPS-1 activates in the following the TANK-binding-kinase 1 (TBK-1) and IκB kinase ϵ (IKKϵ) [50]. This step was detected in both TLR-dependent and RLR-dependent IFN-inducing pathways [77]. The phosphorylation of the interferon regulatory factors (IRF) 3 and/or 7 results in homo- or heterodimers. Dimerization allows nuclear transloca-

tion and leads to induction of type I IFNα/β expression [165]. Additionally IPS-1 triggers the activation of the kinase IKKα-IKKβ-transcription factor that stimulates the nucleus-translocation of the nuclear factor-κB (NF-κB). Type I IFN-β and inflammatory gene chemokine (C-C-motif) ligand 5 (CCL5), also known as RANTES (Regulated upon Activation, Normal T-cell Expressed and Secreted), are both induced by NF-κB [128]. Although RIG-I and MDA5 show a high similarity in structure and induce type I IFN expression, they recognize different dsRNA molecules. RIG-I recognizes positive and negative stranded RNA viruses (like Hepatitis C virus, vesicular stomatatis virus (VSV) and influenza A virus) and plays a role in recognition of DNA viruses [1], while MDA5 is responsible for the recognition of picorna viruses as well as dsRNA and Polyinosin:Polycytidyl acid (poly IC) [194, 96]. Both helicases response to reoviruses, West Nile virus and Dengue virus [96].

1.3.2 IFN secretion and signalling

Three different IFN types have been identified. The type I IFNs have multiple subtypes with 1 IFN-β and at least 14 known IFN-α substypes. In several species additional subtypes are known [143]. They can be induced in all nucleated cells upon viral infection, in contrast to type II IFN (IFN-γ), which can only be secreted by T lymphocytes and NK cells in response to T cell receptor (TCR) or NK cell receptor signals [186]. The type III IFNs (IFN-λI, IFN-λ2 and IFN-λ3) are expressed by separate intron-containing genes [100]. The type I, II and III IFNs have separate signal receptors, but the downstream signalling molecules are similar. They regulate many identical genes [186], therefore, only the signalling cascade of type I IFN -β is described subsequently.

The secreted IFN-β binds to the IFN-α/β receptor. The receptor consists of two subunits IFNAR-1 and IFNAR-2. The signalling is mediated by the *Janus* family of tyrosine kinase (JAK) enzymes together with the signal transducer and activator of transcription (STAT) family (JAK-STAT) pathway [35]. The STAT family has at least seven members with *stat-1* and *stat-2* relevant for the IFN-dependent response, and the JAK family has in total four, with *jak-1*, *jak-2* and *tyk-2* kinases [34, 111]. JAK-1 and TYK-2 kinases mediate the signalling of IFN -β, with TYK-2 interacting with IFNAR-1 and JAK-1 with IFNAR-2 subunit. After IFN -β binding to the receptor, the bound kinases are activated and phosphorylate the cytoplasmic STAT transcription factors. Phosphorylated STAT1 and STAT2 assemble with IFN-regulatory factor 9 (IRF9) to the IFN-stimulated gene factor 3 (ISGF3) [114, 12]. The heterotrimer translocates into the nucleus and binds to the

IFN-stimulated response element (ISRE), which is a region of the promoter region of a great number (> 300) of IFN stimulated genes (ISGs) [81, 20, 54]. The described intrinsic proteins (section 1.3) belong to this large group of ISGs and IFN triggers their expression upon viral infection. One of the first described ISGs is ISG56 gene (the protein is called p56). It belongs to a family of proteins that mediate protein-protein interactions [113, 107]. p56 inhibits the initiation of translation and protein synthesis by binding to eIF3 [196]. The Mx protein is a member of the dynamin superfamily of large GTPase [72] and is strictly dependent on IFN signalling. It blocks early stages of transcription of specific human and animal viruses by binding to nucleocapsid proteins [71].

1.3.3 Bioassays to measure secreted IFN

Since the discovery of IFN in 1957 by Isaacs and Lindemann [85], it has been a challenge to find an appropriate way to determine biologically active IFN concentrations secreted by virus infected cells. The first established assays were based on reduction of virus replication due to IFN-mediated protection of the cells [187, 157]. In 1969 Stewart *et al.* revealed in the discussion about the relative sensitivity of viruses to type I IFN that the origin of the IFN is critical [187]. The comparison between mouse, hamster, human, bat and rabbit IFN indicated that the origin of the type I IFN was critical to its ability to suppress virus growth [187]. The compared type I IFN was gained differently for each cell line, the following IFN assays were based on plaque reduction assays [187]. Their work showed the relevance of the IFN source and might have been one of the first ideas of viral-host interactions.

The most favoured assays to determine bioactive IFN are still based on antiviral activity. The classical VSV-bioassay is based on the reduction of the cytopathic effect (CPE), which describes in this case the degree of cell destruction. VSV is highly sensitive to the antiviral effect of IFN [155] and replicates in cell cultures derived from many animal species [46]. These characteristics made the virus a tool for IFN detection. First approaches to determine IFN titers by reduction of CPE caused by VSV were performed by Rubenstein *et al.* in 1981 [157]. Although VSV was reported to have been spread by direct contact among infected animals [185] and caused devastating epidemics in a range of domestic animals [153], the risk of biological transmission between infected humans and domestic animals was found to be very low [2]. Nevertheless, this virus provided an essential tool to the IFN-bioassay sector. In this study, bioactive IFN, a recombinant pan-species IFN-α (IFN-α B/D *bgl*II) (synthesized by PBL Biomedical Laboratories) was introduced

as standard to achieve comparable measurements of secreted [105].

In the presented thesis the focus therefore was put on a virus system that is widely applicable and can be used in any biosafety level (BSL) 2 laboratory.

1.3.4 IFN response in bats

Since bats host human pathogenic viruses and show the ability to control them, it was hypothesized that bats might have evolved particularly effective mechanisms of immune control [191, 213, 220]. Little is known about the immune system of bats. Development of immunoglobulins after infection and lymphoid development similar to that in other mammals were detected in bats [124, 26, **?**] but in particular information on the innate immune response of bats is rare. In *R. leschenaulti* and *P. alecto* toll-like receptor genes have been identified [83, **?**]. Stimulation with the dsRNA analogue poly IC, and infection with the bat-associated paramyxovirus (Tioman) induced high amounts of IFN in cells from *Pteropus* species [223]. Interestingly, infection with the highly pathogenic paramyxovirus Hendra virus did not induce IFN expression and IFN signalling, suggesting the presence of specific viral IFN antagonists [208]. Earlier it was described that different mammalian cell cultures including the bat cell lines Tb1-Lu have a conserved functionality of IFN signalling [68, 67]. Still, knowledge of the mechanisms by which type I IFNs are induced and IFN signals are processed in bat cells is limited and further studies are needed.

1.3.5 Alphavirus antagonism to cellular defence mechanisms

The nsP2 protein of Old World viruses like ONNV, CHIKV and the capsid protein of VEEV were shown to induce a general transcriptional shutoff [59]. The nsP2 is translocated into the nucleus, where it impairs the function of the DNA-dependent RNA-dependent polymerase I and II [58]. Additionally it was shown that nsP2 blocks cellular mRNA translation [51, 53]. The translational shutoff can be PKR-independent or PKR-dependent [215, 51, 52].The capsid protein of the New World alphaviruses forms a complex with the importin-α/β and nuclear export receptor CRM1, that inhibits protein trafficking through the nuclear pore and thereby initiates transcriptional shutoff [10, 11, 9]. Nevertheless, alphaviruses provoke a strong IPS-1 mediated IFN response *in vivo* [215], which is most likely due to the incomplete inhibition of the cellular antiviral response [59]. The inhibition of STAT1 phos-

phorylation was recently described for representatives of the Old and New World alphaviruses but the precise mechanism is not yet analysed, showing that the knowledge of alphavirus antagonism is not understood completely and further studies are needed [178, 177].

Aim of the thesis

The number of viruses related to severe human diseases found in bats is continuously growing. Although bats are mammals, it is still not understood how they can cope with these viruses. The research on IFN response of bats is still at the outset because adequate tools, which are already at hand for commonly used laboratory animals, are required to be designed first.

The aim of the present study was to compare the IFN response in bat cell lines to reference murine (MEF) and human (MA104) cell lines on IFN-induction, -secretion and -signalling after virus infection. The purpose of this comparison was the evaluation of bat IFN response to virus infection, .

First immortalized bat cell lines were to be established. These cell lines should be IFN competent which should be tested by challenging the cells with commonly used IFN inducers. In addition, virus replication efficiency was to be analysed on genome equivalence concentration and viral particle formation to guarantee equal infection behaviours in the different cell lines.

A serological survey on prevalence of alphaviruses in bats should be performed with serum samples collected on three different continents, underlining the distribution of alphavirus prevalence in bats around the world.

All cell lines were to be challenged with ONNV, because it is as alphavirus a strong IFN-inducer. To investigate IFN-secretion, the classical VSV-bioassay was to be adapted to and to be optimized for bat cell lines, enabling unique species-specific bioactive IFN determination and allowing comparison between different species.

SINV and CHIKV infections were additionally to be performed, to differentiate if the results with ONNV were virus-specific or were general antagonizing mechanisms of alphaviruses in bats. SINV was chosen because it belongs to the Old World alphaviruses and is widespread around the world, while CHIKV was chosen because of the close relation to ONNV.

2 Materials and Methods

2.1 Materials

2.1.1 Technical equipments

Table 2.1: **Technical equipment with design type and source**

Equipment	**Type designation**	**Source**
Autoclave	Varioklav® Typ 500	H+P Labortechnik, Oberschleisheim
Balance	TP-214	Denver Instrument Bohemia, New York, USA
	EW2200 - 2NM	Kern, Balingen-Frommern
	PM1200 precision scale	Mettler- Toledo, Giessen
Bioluminescence, Luciferase-System	Synergy2, Multi-detection Reader	BioTek, Vermont, USA
Biosafety cabinet	HERAsafe®KS12	Thermo Scientific
	HERAsafe® KS18	Brunswick
Biotainer	1.8 L	E3 cortex, Thieux, France
Blue screen table	VB-26	UVP, Upland, Californien, USA
Centrifuges	5410 R	Eppendorf, Hamburg
	5415	Eppendorf, Hamburg
	5416	Eppendorf, Hamburg
	5418	Eppendorf, Hamburg

	5429	Eppendorf, Hamburg
	5430	Eppendorf, Hamburg
	5810	Eppendorf, Hamburg
	Galaxy MiniStar	VWR, Darmstadt
Chemiluminescence Detection, Western Blot	FusionFx7	PeqLab/Vilber Lourmat, Erlangen
Freezer	LB 750 (Liquid nitrogen)	Taylor-Wharton, Alabama, USA
	- 20°C	AEG, Frankfurt a. Main, Kirsch, Offenburg
	- 80°C	Kaltis international, Taiwan
Gel electrophoresis documentation	E-Box 3028, WL/26	Vilber Lourmat, Marne-la-Vallee, France
Gel electrophoresis chambers nucleic acids	PefectBlue Gelsystem Mini S- 50 mL	PeqLab, Erlangen
	PefectBlue Gelsystem Mini L- 100 mL	PeqLab, Erlangen
	PerfectBlue Gelsystem Maxi S- 200 mL	PeqLab, Erlangen
Gel electrophoresis chambers for proteins	Mini Protean Tetra System	BioRad, Hercules, Californien, USA
Glass bottles	Duran® Flasks; different Volumina	Schott, Mainz
Incubator	Heraeus® B6126	Thermo Scientific, Brunswick
Incubator CO_2	HERAcell® 240	Thermo Scientific, Brunswick
Microscopes	Inverse TELAVAL 31	Zeiss, Jena
	Fluorescence Axio Imager M1	Zeiss, Jena

Power supply	Standard Power Pack P25	Biometra, Goettingen
	EV202	Consort Turnhout, Belgium
Pipettes (0.1-2.5µL/ 0.5-10µL/ 10-100µL/ 100-1000µL)	Research® Plus	Eppendorf, Hamburg
	Research® Plus Multi channel pipette	Eppendorf, Hamburg
Pipette assistance	Accujet® pro	Brand, Wertheim
PCR-Cycler	Master cycler ep. gradients S	Eppendorf, Hamburg
	Master cycler Pro vapo.protect	Eppendorf, Hamburg
pH-meter	766 Calimatic	Knick, Berlin
Real-time PCR-Cycler	LightCycler® 480 II	Roche Diagnostics Basel, Switzerland
Refrigerator	4°C	AEG, Frankfurt a. Main, Kirsch, Offenburg
Magnetic stirrer	MR2000	Heidolph, Schwabach
Shaker	MiniRocker MR-1	PeqLab, Erlangen
Spectrophotometer	NanoDrop 2000c	PeqLab, Erlangen
Thermo mixer	comfort 5355	Eppendorf, Hamburg
Thermo mixer	PHMT SC-18	Grant-bio, Cambridgeshire, Great Britain
Water purification system	Milli-Q® Biocel	Millipore, Schwalbach
Vortex	VV3	VWR, Darmstadt
Western blot	FastBlot B44	Biometra, Goettingen
Water bath	51221029	Precision Westlock, Alberta, Canada
Water bath	1092	GFL, Burgwedel

2.1.2 Disposable materials

Table 2.2: **Description of the disposable material and source**

Material	Description	Source
Cell culture flasks	25 cm^2 (T25), 75 cm^2 (T75), 162 cm^2 (T150)	Corning, VWR, Darmstadt
Cell culture plates	96-, 24-, 12-, 6-well	TPP® Trasadingen, Switzerland
Cell culture scraper	24 cm	TPP® Trasadingen, Switzerland
Centrifugation tubes (conical)	Falcon™-Typ, 15 mL	Greiner bio-one, Frickenhausen
	Falcon™-Typ, 50 mL	Sarstedt, Nuembrecht
Counting chamber	C-Chip Neubauer Improved, disposable	Digital Bio, TPP®Trasdingen, Switzerland
Filter paper for western blots	Gel Blot Paper	Whatman, Dassel
Cryotubes	Cryo tubes 1.8 mL	Sarstedt, Nuembrecht
Mikrotiterplates for Luciferase-System	LUMITRAC 600 Micro-Plates, 96-well	VWR, Darmstadt
Glass slide	76 x 26	Menzel Glaeser, Brunswick
Parafilm		Brand, Wertheim
PCR reaction plates, 96 well	LightCycler® 480 Multiwell Plate 96	Roche Diagnostics, Basel, Switzerland
Pipette tips (0.1 mL, 0.5 mL, 1.0 mL, 2.5 mL, 5.0 mL)	Combitips plus	Eppendorf, Hamburg
Pipette tips (0.1-10 µL, 2-100 µL, 20-300 µL, 50-1000 µL)	epT.I.P.S. LoRetention Dualfilter	Eppendorf, Hamburg
Reaction tubes	0.2 mL	Brand, Wertheim
	0.5 mL	Sarstedt, Nuembrecht

	0.5 mL, Safe-Lock	Eppendorf, Hamburg
	1.5 mL	Sarstedt, Nuembrecht
	1.5 mL, Safe-Lock	Eppendorf, Hamburg
Serological Pipettes	1 mL, 2 mL, 5 mL,10 mL, 25 mL	Sarstedt, Nuembrecht
Western blot membrane	Westran Clear Signal PVDF, 0.45 µm	Whatman, Dassel

2.1.3 Chemicals

Table 2.3: **Source of chemicals**

Chemical	**Source**
2-Mercaptoethanol (β-ME)	Roth, Karlsruhe
β -Propiolacton (β-PL)	Ferak® Berlin, Berlin
2-Propanol, Isopropanol, 99.5%	Roth, Karlsruhe
6 x Loading Dye (Loading buffer)	Fermentas, St. Leon-Rot
Acetic acid	Roth, Karlsruhe
Agarose, Broad Range	Roth, Karlsruhe
Agarose, GTQ	Roth, Karlsruhe
Ampuwa®, Sterile pyrogenic free Water	Fresenius Kabi, Bad Homburg
Ammonium persulfate (APS)	Roth, Karlsruhe
Bovine serum albumin (BSA)	Roth, Karlsruhe
Bromphenol blue	Roth, Karlsruhe
Calcium chloride	Roth, Karlsruhe
di-Sodium hydrogen phosphate dihydrate	Merck, Darmstadt
di-Sodium hydrogen phosphate Heptahydrate, 98%	Roth, Karlsruhe
Dithiothreitol (DTT)	Life Technologies, Darmstadt
dNTPs, 100 mM Set	Invitrogen, Karlsruhe
Ethanol, 99.5%	Roth, Karlsruhe
Ethidium bromide solution, 10 mg/mL	Sigma-Aldrich® Munich

Formaldehyde (Roti®-Histofix 4% Formaldehyde)	Roth, Karlsruhe
Glycerine, 99.5%	Roth, Karlsruhe
Glycine, 99%	Roth, Karlsruhe
Hexaquart plus	Braun, Melsungen
Histofix	Roth, Karlsruhe
Hydrochloric acid, fuming, 37% concentrated	Merck, Darmstadt
Igepal CA-630	Sigma-Aldrich® Munich
IMMUMOUNT (Dakocytomation)	Dako, Hamburg
Incidin® Extra N	Ecolab, Dusseldorf
Potassium chloride	Merck, Darmstadt
LB-Agar (Lennox)	Roth, Karlsruhe
LB-Medium (Lennox)	Roth, Karlsruhe
Methanol	Merck, Darmstadt
Milk powder	Roth, Karlsruhe
Mycoplasma-Off®	Minerva Biolabs, Berlin
poly IC	Sigma-Aldrich® Munich
Poly-L-Lysin, 0.01% solution	Sigma-Aldrich® Munich
Protease Inhibitor Cocktail Set III , EDTA-free	Merck, Darmstadt
Re-Blot Plus-Strong® , 10 x	Millipore, Billerica, Massachusetts, USA
Rotiphorese® Gel 30 (Acrylamid)	Roth, Karlsruhe
Sample buffer IIFT (Albuminazid)	Euroimmun, Luebeck
Sodium chloride, 94%	Roth, Karlsruhe
Sodium dodecyl sulfate (SDS), Ultra Pure, 99%	Roth, Karlsruhe
S.O.C. Medium	Invitrogen, Karlsruhe
SuperSignal® West Femto Maximum Sensitivity Substrate	Thermo Scientific, Brunswick
SYBR Green, Gel stain (1:1000)	Lonza, Cologne

Tetramethylethylenediamine (TEMED), 99%	Roth, Karlsruhe
Tris, Ultra Quality Pufferan, 99.9%	Roth, Karlsruhe
Triton X 100	Roth, Karlsruhe
Tween® 20	Roth, Karlsruhe

2.1.4 Buffers and solutions

10% APS - 10 mL

1 g APS
add 10 mL H_2O
1 mL Aliquots
Stored at -20°C

Blocking solution for Western blot

5% Milk powder
1 x PBS
0.1% Tween® 20

1 M DTT - 20 mL

1 M DTT
0.01 M Sodium acetate, pH 5.2
sterile filtered
1 mL Aliquots
Stored at -20°C

10 x Phosphate buffered saline (PBS) - 1 L (solution in use 1 x)

1.37 M NaCl
0.03 M KCl
0.1 M Na_2HPO_4
0.02 M KH_2PO_4

Radio immunoprecipitation assay (RIPA) lysis buffer

0.15 M NaCl
1% Igepal CA-630
0.5% Sodium Deoxycholate
0.1% SDS
0.05 M Tris (pH 8.0)
add right before use:

Proteinase Inhibitor (PI) III (1:100)
Benzonase® Nuclease (1:1000)
0.005 M DTT

10% SDS - 1 L
100 g SDS
900 mL H_2O
heated to 68°C to dissolve SDS crystals
adjusted pH to 7.2 with HCl
Stored at RT

10 x SDS polyacrylamide gel electrophoresis (PAGE) running buffer (solution in use 1 x)
0.5 M Tris
1% SDS
3.84 M Glycine
Stored at RT

4 xβ-ME sample buffer (solution in use 1 x)
0.5 M Tris (pH 6.8)
40% Glycerine
8% β-ME
4 g/L Bromphenolic blue
80 g/L SDS
Stored at -20°C
0.01 M DTT added before use

50 x TAE buffer - 1 L (solution in use 1 x)
2 M Tris
1 M acetic acid
0.05 M Na_2 EDTA (pH 8.0)
Stored at RT

10 x Transfer buffer - 1 l (solution in use 1 x)
0.25 M Tris
1.5 M glycine in H_2O
Stored at RT
10% MeOH added before use

1.875 M Tris HCl buffer (pH 8.8)
Adjusted to pH 8.8 with 37% HCl (concentrated)
Stored at RT

0.6 M Tris HCl buffer (pH 6.8)

Adjusted to pH 6.8 with 37% HCl (concentrated)

Stored at RT

Dilution solution for antibodies during western blot

1% milk powder

1 x PBS

0.1% Tween® 20

Washing buffer for western blot

1 x PBS

0.1% Tween® 20

2.1.5 Cell culture media

Table 2.4: **Media and reagents used in cell culture experiments with source**

Media and reagents	Source
Amphotericin B	PAA, Pasching, Austria
DMEM[1] High Glucose (4.5 g/L), with L-Glutamine	PAA, Pasching, Austria
Dulbecco's PBS (1 x), without calcium and magnesium	PAA, Pasching, Austria
L-Glutamine (200 mM, 100 x)	PAA, Pasching, Austria
MEM with Earle´s salts, with L-Glutamine	PAA, Pasching, Austria
Imipenem	Zienam, MSD, Haar
Nanofectin®	PAA, Pasching, Austria
Non essential amino acids (NEAA) (100 x)	PAA, Pasching, Austria
Sodium Pyruvate solution (100 mM, 100 x)	PAA, Pasching, Austria
Penicillin/ Streptomycin GIBCO™	Invitrogen, Karlsruhe
Trypsin-EDTA (1 x)	PAA, Pasching, Austria
Fetal calf serum (FCS), standard quality	PAA, Pasching, Austria
OptiPRO™SFM, Serum free medium GIBCO®	Invitrogen, Karlsruhe

Legend: Dulbecco's Modified Eagles Medium (DMEM)1.

2.1.6 Cell lines

Table 2.6: **Cell lines and description**

Designation	**Tissue**	**Source**	**Organism**
A549	Lung adeno-carcinoma	IVB	*Homo sapiens*
EidNi/41.3	Kidney	IVB	*Eidolon helvum*
EidNi41.2	Kidney	IVB	*Eidolon helvum*
EidNi/41	Kidney	IVB	*Eidolon helvum*
EpoNi/22.1	Kidney	IVB	*Epomops torquata*
293 lp	Kidney	F.W.	*Homo sapiens*
HeLa	cervix carcinoma	IVB	*Homo sapiens*
Hep2	Larynx carcinoma	IVB	*Homo sapiens*
MA104	Kidney	F.W.	*Chlorocebus sabaeus*
MEF Rigi-/-	Embryonic	IVB	*Mus musculus*
RoNi/7	Kidney	IVB	*Rousettus aegyptiacus*
Vero E6	Kidney	BNI	*Chlorocebus sabaeus*

Legend: EidNi= *E. helvum*, Ni= Niere (kidney), EpoNi= *E. torquata*, Ni= kidney; IVB, Institute of Virology, Bonn; BNI, Bernhard-Nocht-Institute, Hamburg; F.W., Prof. Friedemann Weber, University of Marburg, Department of Virology.

2.1.7 Viruses

Table 2.7: **Viruses used in this work**

Virus	**Abbr.**	**Genus, Family**	**Source**
Recombinant Rift Valley fever virus *Renilla* luciferase del NSs	RVFV 13	*Phlebovirus*, *Bunyaviridae*	F.W.
O´nyong-nyong Virus	ONNV	*Alphavirus*, *Togaviridae*	IVB
Chikungunya Virus	CHIKV	*Alphavirus*, *Togaviridae*	IVB
Sindbis Virus	SINV	*Alphavirus*, *Togaviridae*	IVB
Vesicular Stomatitis Virus	VSV	*Vesiculovirus*, *Rhabdoviridae*	IVB

Legend: F.W., Prof. Friedemann Weber, University of Marburg, Department of Virology, IVB, Institute of Virology, Bonn.

2.1.8 Bacterial strains

For cloning and expression of plasmids used in this work TOP 10® Chemical competent *E.coli* bacteria from Life Technology (Karlsruhe, Germany) were used.

2.1.9 Kits

Table 2.9: **Kits used for extraction ans analysis**

Name of used Kit	Source
Renilla-Luciferase Assay Systems	Promega, Mannheim
NucleoSpin ®RNA Virus	MACHEREY-NAGEL, Dueren
NucleoSpin ®8 RNA Virus	MACHEREY-NAGEL, Dueren
NucleoSpin ®RNA II	MACHEREY-NAGEL, Dueren
NucleoSpin ®8 RNA	MACHEREY-NAGEL, Dueren
QIAEX® II Gel Extraction Kit	Qiagen, Hilden
QIAprep® Spin Mini Kit	Qiagen, Hilden
QIAshredder™	Qiagen, Hilden
RNeasy® Mini Kit	Qiagen, Hilden

2.1.10 Oligonucleotides

Table 2.5: **Forward and reverse PCR primer and probes**

Assay	Name	Sequence	GenBank ID Reference
Actin-β (ACTB)			
Bat	qRT-bACTB_for	GGCTCCCAGCACAATGAAGA	JN613815
	qRT-bACTB_prb	6-FAM-CAAGATCATTGCGCCC CCTGAGC-BHQ-1	JN613816
	qRT-bACTB_rev	GGAGCCGCCGATCCA	JN613817; JN613818
Mouse	mACTb_for	AAATCGTGCGTGACATCAA AGA	NM_008331.3
	mACTb_prb	6-FAM-ATGGAAAGATCAAC CTCACCTACAGGGCG-BHQ-1	
	mACTb_rev	GGATGGCAAAGGCAGTGT AACT	

Human	qRT_hpmACTB_fwd	GAGGCATCCTCACCCTGAAG	NM_001101.3
	qRT_hpmACTB_prb	6-FAM-CCCCATCGAGCACGGCATCG-BHQ-1	NM_001009945.1
	qRT_hpmACTB_rev	TCCATGTCGTCCCAGTTGGT	NM_001033084.1
IFN-β (IFNB1)			
Bat	bIFN-B1-F	CAGCTATTTCCATGAGCTACAACTTG	JN613819
	bIFN-B1-Prb	6-FAM-TCGATTCCAACAAAGAAGCAGCAATTTAGC-BHQ-1	JN613820; JN613821
	bIFN-B1-R	TTAACTGCCACAGGAGCTTCAG	JN613822
Mouse	mIfnb1_for	AGAAAGGAGGAACATTCGGAAAT	NM_010510.1
	mIfnb1_prb	6-FAM-ATGGAAAGATCAACCTCACCTACAGGGCG-BHQ-1	
	mIfnb1_rev	GGATGGCAAAGGCAGTGTAACT	
Human	IFN F	GAACTTTGACATCCCTGAGGAGATT	[80]
	IFN P	6-FAM-CAGCAGTTCCAGAAGGAGGACGCC-BHQ-1	
	IFN R	GGAGCATCTCATAGATGGTCAATG	
ISG56/ IFN-induced protein with tetra-tricopeptide repeats 1 (IFIT1)			
Bat	qRT-bISG56_for	TTGAAGAAGCTCTGGCCAACA	JN613823
	qRT-bISG56_prb	6-FAM-ACAGACCTACGTCTTTCGATATGCAGCCA-BHQ-1	JN613824
	qRT-bISG56_rev	GCGCCTTTTCTTCGGTAAAA	JN613825; JN613826
Mouse	mIsg56_for	TGCCTGGCTGCATTACCA	NM_008331.3
	mIsg56_prb	6-FAM-TTGGCAGAAGCCCAGATCTACCTGGAC-BHQ-1	

	mIsg56_rev	TGAAAATTCCTTGCACACCT TCT	
Human	ISG56 F	CCTGGAGTACTATGAGCGGGC	[80]
	ISG56 P	6-FAM-ACAGAGTTCTCAAAG TCAGCAGCCAGTCTCAGT -BHQ-1	
	ISG56 R	TGGGTGCCTAAGGACCTTGTC	
MX1/ MxA/ IFN-inducible protein p78			
Bat	qRT-bMxA_for	CCGATC TGACCC TCATCGA	JN613827
	qRT-bMxA_prb	6-FAM- TGGGCAACCAGCCC CAGG AC-BHQ-1	JN613828
	qRT-bMxA_rev	ATGGTCTGCTGCCTCTGGAT	JN613829; JN613830
Mouse	mMxA1_for	TGAATAATCTGTGCAGGCAC TATG A	NM_010846.1
	mMxA1_prb	6-FAM- TGCGGCCCTGTTTGAC CTCATCG-BHQ-1	
	mMxA1_rev	CTGAACTCTGGTCCCCAATGA	
Human	MxA F	TTCAGCACCTGATGGCCTATC	[80]
	MxA P	6-FAM- CAGGAGGCCAGCAAG CGCC ATC-BHQ-1	
	MxA R	TGGATGATCAAAGGGATG TGG	
TATA box binding protein (TBP)			
Bat	qRT-bTBP_for	TTGCTGCTGTGATCATGAGA ATT	JN613831
	qRT_bTBP_prb	6-FAM- CCCGGACCACGGC CCTGA-BHQ-1	JN613832
	qRT_bTBP_rev	CCCGGACCACGGCCCTGA	JN613833
Mouse	mTbp_for	TGTACCGCAGCTTCAAAA TATTGT	NM_013684.3
	mTbp_prb	6-FAM-TCCCAAGCGATTTG CTGCAGTCATC-BHQ-1	

	mTbp_rev	AGTTGTCCGTGGCTCTCT TATTCT	
Human	qRT_hTBP_fwd	GCTGCGGTAATCATGAGG ATAAG	NM_003194.4
	qRT_hTBP_prb	6-FAM-AGCCACGAACCAC GGCACTGATTTT-BHQ-1	
	qRT_hTBP_rev	TGCACACCATTTTCCCAG AA	
ONNV, Gulu strain			
	ONNV-S	TGATCCAGACTCAACCATTCT	M20303.1
	ONNV-P	6-FAM-ACCAGCTAGGAGG ATGATGTCTGA-BBQ-1	
	ONNV-AS	GGCAGACGCAGTGGTATT TTCT	
CHIKV			
	CHIK-S	TGATCCCGACTCAACCATCCT	[140]
	CHIK-P	6-FAM- GCCAGCAAGGAGGATG ATGTCGGA-BBQ-1	
	CHIK-AS	GGCAAACGCAGTGGTACT TCCT	
SINV			
	SINV-S	AAGAACGAGGACGGAGATG TCA	in house assay [161]
	SINV-P	6-FAM- CGGGCACGCACGCAC TGGCCATG-BBQ-1	
	SINV-AS	TTTCACGTGCAGAGGTTTCAT TAC	
Simian virus 5 (SV5)/ Parainfluenza virus 5 (PIV5)			
	SV5-F	CGTGGGGGATCCCTTCA	AF052755
	SV5-P	6-FAM-CCCACCAGCAGATA CCAGTCAATTTGATC-BHQ-1	
	SV5-R	CCACCTCTGGGTGATACAA TGA	
Genotyping (mitochondrial cytochrome b)			

L14724	CGAAGCTTGATATGAAAAA CCATCGTTG	[84]
H15149	AACTGCAGCCCCTCAGAAT GATATTTGTCCTCA	

Legend: Human (h); bat (b); mouse (m); Forward primer (F, for, S); reverse primer (R, rev, AS); probe(P, prb); β-Actin (ACTB); TATA box binding protein (TBP); Simian virus 5 (SV 5).

2.1.11 Plasmids

Table 2.12: **Plasmids for cloning and transfection**

Name	**Type**	**Source**
pCAGGS-MCS	Eukaryotic Vector	S.B.
pRL-SV40	Eukaryotic Vector	F.W.
p-125 Luc	p55C1B-Luc	T.F.

Legend: RL, *Renilla*-Luciferase; S.B., Prof. Stephan Becker, University of Marburg, Department of Virology; F.W., Prof. Friedemann Weber, University Marburg, Department of Virology; T.F., Prof. Takashi Fujita, Institute for Virus Research Kyoto University.

2.1.12 Software

Table 2.13: **Computer programs**

Name	Description	Version	Source
BioEdit	Sequence Alignment Editor	7.0.5.3	©1997-2005 Tom Hall
DNASTAR Lasergene 7	EditSeq, SeqMan, Protean	7.2.1	©1989-2007 DNASTAR
Gene 5		1.04.5	©2006-2007 BioTek Instruments Inc
Oligo Calc			http://www.basic.northwestern.edu/biotools/oligocalc.htmL
AxioVision		4.8.1.0	©2006-2009 Carl Zeiss Imaging Solutions GmbH

2.2 Methods

2.2.1 Tissue culture conditions

Cell culture was performed under sterile conditions, which were accomplished by the use of laminar flows and decontamination of surfaces and working equipment with Incidin® (0.5% for BSL-2 or 3% for BSL-3 laboratories, respectively) or Hexaquart® plus and Mycoplasma-OFF®. Cultivation of the cell lines listed in 2.6 was performed at 37 °C and 5% CO_2 with DMEM with 4.5 g/L Glucose supplemented with 1% Penicillin/ Streptomycin 100 x concentrate (Penicillin 10,000 units/mL, Streptomycin 10 mg/mL), 1% MEM NEAA 100 x concentrate, 1% Sodium Pyruvate 100 mM, 1% L-Glutamine 200 mM and 10% of FCS.

2.2.2 Harvesting, counting and seeding cells

In order to expand the cell lines, the old supernatant was discarded and washing of the cells was performed by carefully adding 5 to 10 mL of PBS. Cells were detached by incubating in trypsin solution for 5 to 10 minutes and when complete detachment was observed, the cells were resuspended in DMEM.

All cells were commonly split in ratios 1:2 to 1:10 at 90% confluence. Cells were counted with a Neubauer® cell counting chamber. The number of cells per mL was calculated with the following equation:

$$\frac{counted\,cells}{number\,of\,chambers} * dilution_{factor} * 10^4 = cells/mL$$

Cell suspensions were usually adjusted to cell densities of 4 x 10^5 cells per mL.

2.2.3 Generation and immortalisation of bat cell cultures

Under the auspices of Ghana authorities bats were caught with mist nets, anaesthetized with a standard Ketamine/Xylazine mixture and euthanised to perform organ preparations. Organs from *E. helvum* (embryo kidney and lung), *E. buettikoferi* (kidney) and *R. aegyptiacus* (kidney) were cut into pieces, trypsinized and cultured in DMEM medium as described previously [79]. Additionally, Imipenem and Amphotericin B were added to minimize contamination risks. Immortalization was done with the help of lentiviral transduction of the large T antigen of Simian Virus (SV) 40 [208]. Immortalized cells were expanded and either stock-frozen or processed further for subcloning. Three morphologically distinct cell clones were then chosen for expansion and either further used in culture or frozen. All cell cultures were genotyped by amplification of mitochondrial cytochrome b as previously described using primers L14724 and H15149 [208, 67] and were controlled for mycoplasma [190], SV5 (in-house assay, see 2.1.10), lyssaviruses [76] and filoviruses [141] contaminations. In this study cell clones EidNi/41.3, EidNi/41.2, EpoNi/22.1 and the mixed cell cultures EidNi/41 and RoNi/7 were used.

2.2.4 General procedure of tissue culture infections

The general infection procedure was similar in all experiments to obtain reproducible results. The medium was discarded and the cells were inoculated with a virus stock dilution (6 well: 1 mL; 12 well: 0.5 mL; 24 well: 0.25 mL; 96 well: 50-100 µL) for one hour at 37°C. Thereafter, the supernatant was removed, cells were washed twice with PBS and fresh medium was applied. The incubation time of the infected cell differed between experiments and/or cells. Depending on the virus, experiments were performed under either BSL-2 or -3 conditions. Inactivation of virus samples were ensured by incubating in 8% formaldehyde (plaque assays) or incubation with inactivating buffers (AVL (Viral RNA isolation kit), RLT (total RNA isolation kit) or RIPA + SDS-loading buffer with in the following heat inactivation at 90°C for 10 minutes).

2.2.5 Virus infection and titration

ONNV, SINV, CHIKV and RVFV 13 infections were performed at multiplicity of infection (MOI) of 1 or 2.5 and 0.0025, respectively. The viruses were diluted in serum-free medium OptiPRO™. Cells were inoculated for 1 h and washed twice after infection. Samples were taken at time points 0, 8 and 24 hours post infection (hpi) or 4 and 10 hpi. Titrations of the viruses were performed by plaque assay as previously described [79, 90]. Briefly, Vero E6 cells were seeded in 24-well plates at a density of 4 x 10^5 cells per mL. Cells were inoculated with virus samples and after 1 h incubation the inoculum was removed. Subsequently the cells were washed with PBS and 0.5 mL (per well) of an overlay solution of 2 x MEM, supplemented with 0.44% (w/v) $NaHCO_3$, 20% FCS and 2% Penicillin/ Streptomycin, was mixed in a 1:1 ratio with 2.4% Avicel. After 48h of infection the overlay was discarded and cells were stained with a 0.2% cristal violet and 20% EtOH containing solution. The virus replication of RVFV 13 is proportional to the expression of the *Renilla* luciferase expression and therefore to the chemiluminescence read-out measured with Multi-Detections-Reader (Synergy 2, BioTek). The assay was performed as described before [105] with the following minor modifications: Cells were seeded at a density of 4 x 10^5 cells per mL and 20 µL of the cell lysate were added to the plate for read-out. The calculation of the Relative Light Units (RLU) by dividing the mean value of the sample of interest by the mean value of the negative virus control.

2.2.6 Virus inactivation by β-PL treatment

In case experiments were carried out with supernatants containing ONNV, SINV, CHIKV or RVFV 13 virus was inactivated by β-PL treatment. The supernatants were transferred to a 12-well plate and β-PL was added at a final concentration of 0.05% for RVFV 13 and 0.1% for the alphaviruses. The 12-well plate was wrapped in a plastic bag and incubated for 16 h at 4°C. Subsequently the β-PL was inactivated by hydrolysis, which was achieved by exposing the samples to 37°C for 2 h.

2.2.7 IFN induction by infection and transfection

The sensitivity of *E. helvum* cells to commonly used IFN inducers, was tested by transfection of poly IC and infection with RVFV 13, which carries a *Renilla* luciferase reporter gene instead of the non-structural protein NSs [105]. Both experiments were performed in 6-well plates at a density of 4 x 10^5 cells per mL. The transfection

of poly IC and the empty vector pCAGGS, which was used as negative control, was executed with the Nanofectin® transfection reagent. To determine optimal induction conditions 5, 2.5 and 1 µg poly IC per well were transfected to EidNi/41.3 cells according to the manufacturer´s instructions. The final IFN induction with poly IC was done with 5 µg poly IC per well and 24 h after transfection cells were lysed and total RNA was extracted (see 2.2.10.1). In a second approach, IFN-induction was stimulated by infection with RVFV 13 with an MOI of 1 as described in 2.2.4. After 24 h, all supernatants were harvested and treated with β-PL (see 2.2.6).

2.2.8 VSV-bioassay

A classical VSV bioassay was performed as described previously [200]. Briefly, EidNi/41.3, EpoNi/22.1, MEF and MA104 cells were seeded in 12-well plates at a density of 4 x 10^5 cells per mL. After 24 h the inactivated supernatants and a pan-IFN-α (pan-IFN, a universal recombinant type I human IFN-α A/D hybrid) standard dilution series was added to the respective cell lines. An internal standard curve comprising five concentrations (0.5, 1, 10, 20 and 40 U/mL) of pan-IFN diluted in medium of mock treated cells was applied in every experiment. The external pan-IFN standard curves for the EC_{50} calculation were performed in quadruplicates and comprised pan-IFN concentrations between 0.25 and 150 U/mL diluted in DMEM. 24 h post treatment, IFN containing supernatants were removed and cells were washed with PBS. The cells were then infected with VSV at an MOI of 0.025. After a 1 h virus adsorption, cells were washed and an Avicel overlay was added as described in 2.2.5. As depicted in 3.1(in results) the optimal incubation time varied between 24 and 48 h for the different cell lines. When the corresponding time for incubation was achieved, the overlay was removed and the cells were fixed and stained as described in 2.2.5.

2.2.9 Calculation of EC_{50} values and determination of normalized IFN concentrations

The amount of plaques of the applied pan-IFN standard curves or of the test samples was calculated in % (maximal plaque count from the negative control was set to 100%). The equation of the internal standard was used to calculate IFN amounts in the samples (Table 3.2). EC_{50} values were defined as IFN concentrations which re-

duces the number of plaques up to 50%. Thereafter, the values of IFN concentration were multiplied by the dilution factors and figures were normalized to the amount of IFN per mL. To define comparable, species-independent IFN concentrations the calculated amount of IFN was divided by the EC_{50} of each internal standard curve. Thus, the normalized amount of IFN could directly be compared.

$$n.o.p.\ \ relate\ \ to\ \ standard * dilution_{factor} * mL_{factor} = IFN/mL$$

$$\frac{IFN/ml - n.c.}{EC_{50}} = corr.\ \ IFN/mL$$

Legend: n.o.p. = number of plaques; n.c.= negative control; corr.= correlated.

2.2.10 Preparation and analyses of nucleic acids

2.2.10.1 Isolation of total RNA

Isolation of total RNA was the first step to allow investigations on changes in messenger RNA (mRNA) abundance in cells upon infection or other stimuli. The RNeasy® Mini kit, NucleoSpin® RNA II or the NucleoSpin® 8 RNA was used for total RNA extractions. Basically, cells were treated with the RLT solution, which is a highly denaturing guanidine isothiocyanate lysis buffer, and detached by pipetting a few times. For final homogenisation the lysates were applied to the QIAshredder® spin column system, before the RNA was applied to the silica gel-based membranes. The extraction and washing steps that followed were performed as described in the manufacturer's manual and the RNA elutions were done using 50 µL RNase-free water pre-heated to 70°C. Nucleic acid concentrations were determined by spectrophotometrical measurement and for final qRT-PCR assays adjusted to 80 ng/µL.

2.2.10.2 Isolation of viral RNA

Viral RNA (vRNA) was extracted from supernatants to determine viral replication based on real-time PCR. The extractions of vRNA was performed with the QIAamp® Viral RNA Mini kit, NucleoSpin® RNA Virus or the NucleoSpin® 8 RNA Virus. The AVL buffer which is provided by the kit, is able to lyse viral particles under denaturing conditions, thus inactivating infectious agents and RNases.

Stabilizing carrier RNA was added to prevent vRNA from RNase degradation. Thereafter, vRNA was applied to a silica gel-based membrane and procedure was finished according to the manufacturer's manual. The AVE buffer was pre-heated to 70°C and all samples were eluted in 50 µL. In this case the concentration of the resulting vRNA was not measured due to the presence of carrier RNA but was either used directly or stored at -80°C.

2.2.10.3 Spectrophotometric determination of nucleic acid concentrations

Nucleic acids are able to absorb monochromatic light at a specific wavelength (= 260 nm) which is based on their chemical structure. The phenomenon allows the determination of the concentration of nucleic acids within a sample by photometric measurements. Spectrophotometric determination of nucleic acid concentrations were performed with a NanoDrop® and 1 µL of the corresponding diluting liquid was used as a reference.

2.2.11 Polymerase chain reaction

The polymerase chain reaction (PCR) amplifies the nucleic acid sequence of interest and thereby increases its amount up to detectable level. In brief, amplification of the sequence of interest is achieved by cycles of denaturation of the double stranded DNA, annealing of specific oligonucleotides (primers) flanking the area of interest and elongation of the 3'-hydroxy moiety of the primers with the help of a thermostable DNA-dependent DNA polymerase of bacterial origin (*Thermus aquaticus*).

2.2.11.1 Quantitative real-time RT-PCR for detection of IFN, MxA, ISG56 and TBP mRNA

The addition of a fluorescently labelled probe to the PCR enables real-time monitoring of the exponential amplification. Exponential amplification above the background fluorescence signal determines the crossing point (cp). The measured cp values can be used for relative or absolute quantification mRNA concentrations. IFN, MxA and ISG56 as well as TBP mRNA abundance was quantified from total RNAs.

PCR assays were performed as one-step reverse transcription PCRs, using the SuperScript® III One-Step RT-PCR System with Platinum Taq® DNA polymerase.

The reaction volume of the amplications was 12.5 µL, including 6.25 µL 2 RXN-buffer, 0.25 µL one-step RT-PCR kit enzyme mix (both provided by the kit), 400 nM of each primer, 200 nM probe, 1 µg BSA, Ampuwa® water and 1 µL sample RNA. The species-specific primers and probes are listed in 2.1.10. The reverse transcriptase reaction was performed for 15 minutes at 55°C. The initial denaturation was done for 2 minutes at 95°C. In the following 45 cycles of 15 seconds denaturation at 95°C and 30 seconds annealing/elongation at 58°C were performed. To determine the fold-induction of the different target genes (IFN, MxA, ISG56) the $2^{-\triangle\triangle Ct}$ method was applied with TBP as housekeeping gene [119].

2.2.11.2 Real-time RT-PCR for detection of ONNV, SINV and CHIKV

The quantification of viral genome equivalents from tissue culture supernatants was performed with the isolated vRNA as described previously (see 2.2.10.2) and tested by one-step RT-PCR with reactions set up as in 2.2.11.1.

For the quantification of ONNV, SINV and CHIKV genome equivalents (GE) the dilution end-point were defined as one PCR unit. Log PCR units per mL for each experimental sample were calculated from the linear equations of the dilution series as described [144].

2.2.12 Eukaryotic protein isolation

After the induction of ISGs by either RVFV 13 or poly IC, total protein extraction was performed by lysis of cells with RIPA buffer supplemented with DTT, Benzonase, and proteinase inhibitor III (PI-III) before use. After the supernatant was discarded and the cells were washed with PBS, 100 µl of the RIPA-based solution was added to the 6 well. Homogenisation was achieved by scraping off the monolayer and repetitive pipetting, which was followed by an incubation of 20 minutes on ice (4°C). Samples were either stored at -80°C or directly analysed by SDS-PAGE and Western blot analysis.

2.2.13 SDS-PAGE and Western blot analysis

Proteins can be detected with specific antibodies by Western blot analysis. Here, the expression of the ISGs p56 and MxA proteins after viral infection with RVFV 13 or ONNV, SINV as well as CHIKV were compared to expression levels of non-treated

cells. Protein samples were diluted 1:10 with RIPA buffer and 15 µl of the dilution was supplemented with 5 µl 4 x loading buffer (NuPage®) containing β-ME for protein denaturation. The mixture was heated to 90°C for 10 minutes. 10 µl of the samples and 5 µl marker (Page Ruler® Prestained Protein ladder) were loaded on a 10% SDS polyacrylamide gel electrophoresis (PAGE) (see Tab. 2.10). The intrinsic charge of the polypeptides is overcome by SDS binding, resulting in polypeptides being only negatively charged. They can subsequently be separated by an electric field according to their molecular weight.

Table 2.14: **Compounding of a 10% SDS PAGE components stacking gel separation gel**

ingredients	separation gel	stacking gel
30% acrylamide	3.33 mL	0.5 mL
1.875 M Tris (pH 8.8)	2.0 mL	
0.6 M Tris (pH 6.8)		0.6 mL
Ampuwa® water	4.51 mL	1.85 mL
10% SDS	100 µL	30 µL
10% APS	50 µL	15 µL
TEMED	10 µL	3 µL

SDS-PAGE were run at 80 volts until the proteins reached the separation gel. The voltage was then adjusted from to 100 volts. The SDS-PAGE was followed by semi-dry blotting with a transfer of the proteins to a membrane of polyvinyliden uorid (PVDF) with a pore diameter of 0.45 µm. Activation of the membrane with methanol enabled immobilization of the proteins by hydrophobic interactions. The transfer of the proteins from the gel to the PVDF membrane was achieved by an electric field of 200 mA per membrane and with a maximum of 25 volts for 1.5 h. After the proteins were transferred to the membrane, unspecific antibody-binding during the immuno detection was limited by incubating the membrane in blocking buffer (5% milk powder diluted in PBS-Tween (PBS-T; 0.1% Tween20)) for at least one hour. Specific proteins were detected by exposing the membrane to the primary antibody. In this case mouse anti-MxA, p56 and actin, at a dilution of 1:5000 in PBS-T containing 1% dry milk, for 1 h respectively. To minimize unspecific antibody binding five washing steps with PBS-T of 5 minutes were performed before the membrane was incubated with the secondary antibody (goat-anti-mouse diluted 1:20000 in 1% milk powder PBS-T) for 45 minutes. The membrane was washed five times with PBS-T to remove residual antibodies for five minutes. The linkage of the secondary antibody to a horseradish peroxidase (HRP) enabled detection of bound proteins by chemiluminescence. 150 µl SuperSignal R Femto Maximum Sensitivity

substrate was added to the membrane and incubated for 5 minutes in the dark. The chemiluminescent signals were detected by the FusionFx7 from PeqLab.

2.2.14 Immunofluorescence

In cooperation with the company EUROIMMUN (EU38, Lubeck), a mosaic immunofluorescence chip harbouring cells infected with 15 various human pathogenic viruses was used. VEEV and CHIKV infected cells represented New and Old World alphaviruses. Each slide contained acetone fixed and γ-radiated infected cell with an approximate infection of 30 to 50%. The cells were initially treated with diluted bat sera (1:40). Thereby allowing the bat antibodies to bind to viral antigens that were present in infected cells. Next, the bound bat antibodies were recognized by an goat anti-bat immunoglobin (Ig) (Bethyl Laboratories, Montgomery, TX, USA) directed to the constant region of the bat antibody. To detect positive sera via IF, the following antibody was a donkey anti-goat Ig conjugated to a cyanine 3 (Cy 3) (Dianova, Hamburg) or to fluorescein isothiocyanate (FITC). Final observation was performed with the Fluorescence Axio Imager M1® microscope from ZEISS.

3 Results

Technical preliminary work

As a technical prerequisite bat cell cultures of African fruit bats like *E. helvum*, *R. aegyptiacus* and *Epo. buettikoferi* had be to established. Secondly the established VSV-bioassay was optimized to enable the comparison of secreted bioactive IFN after infection with the same virus. The IFN response, - induction, - secretion and - signalling was investigated and compared to mammalian model cell lines like MEF and MA104.

3.1 Generation of cell cultures

3.1.1 Immortalised and subcloned bat cell lines

E. helvum, R. aegyptiacus and *Epo. buettikoferi* belong to the Old World frugivorous/ nectarivorous bats or flying foxes (Pteropodidae; formerly classified as Megachiroptera). Whereas *E. helvum* was shown to harbour Henipa-like viruses [41], *R. aegyptiacus* is a known reservoir for the Marburg virus [199, 200, 192]. *Epo. buettikoferi* was found to carry Lagos bat virus (LBV) [75]. Bats carry these pathogenic viruses without showing overt clinical symptoms implying specific immunological defence mechanisms. Cell culture systems as a basic tool in molecular virology could help to identify cellular mechanisms. So far only for *R. aegyptiacus* and *Tadarida brasiliensis* cell cultures are commercially available. In cooperation with M. A. Mueller *E. helvum* and *Epo. buettikoferi* bats roosting in Kumasi, Ghana, were investigated shortly before the parturition season in 2009. Pregnant females were euthanised by injection of Ketamine/Xylazine according to approved protocols, under a license from the veterinary services and the Ministry of Food and Agriculture, Accra, Ghana. Primary cell cultures from embryonic kidney tissue of all three bat species were generated at the Kumasi Collaborative Center for Research in Tropical Medicine, Kumasi (Figure 3.1). Immortalisation of the cells was per-

formed by lentiviral transduction of the SV40 large T antigen [79]. While primary cells could only be passaged twice, immortalised cells could be passaged continuously (> 30 passages). Clonal cell lines were achieved by end point dilution out of the second passage. In Figure 3.1 cell lines of EidNi/41.3 for in-depth characterisation are shown. To exclude subclone specific differences, two additional clonal cell lines from the same preparation (EidNi/41.1 and EidNi/41.2) and one mixed culture (EidNi/41) were included in some experiments. The different subclones and the mixed culture showed the same phenotype (Figure 3.1). In addition kidney cell cultures (4th passage) from adult *R. aegyptiacus* (RoNi/7) and *Epo. buettikoferi* (EpoNi/22.1) from bats were prepared as described for EidNi/41.3 cell lines to investigate putative differences between related frugivorous bats. Genotyping of all bat cell cultures was performed by amplifying the mitochondrial cytochrome b fragments [84] followed by a BLAST analysis.

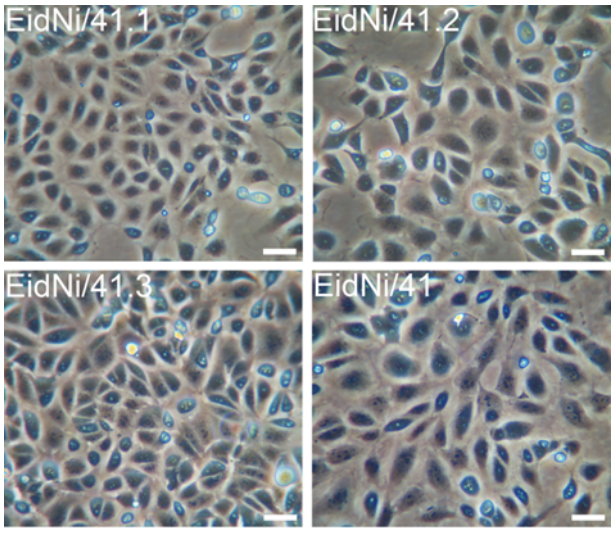

Figure 3.1: **Generation of immortalized bat cells.**
Example of primary bat cell cultures which were generated from an embryonic kidney of *E. helvum*. Cell cultures were immortalized by lentiviral transduction of SV40 large T antigen. Three subclonal cell lines (EidNi/41.1, 41.2 and 41.3) were prepared from a mixed culture (EidNi/41) by end point dilution plating. Bar indicates 20 µm.

3.1.2 IFN induction of established bat cell cultures

The generated cell cultures were used to study intracellular signalling cascades in particular the IFN response. IFN induction and secretion could previously be shown for primary bat cells of the *Pteropus* species [208, 187, 32, 223]. Immortalisation

of cells can result in dysfunctional signalling pathways by damaged cytokine genes. Therefore the reactivity of EidNi/41.3 to IFN stimuli was tested. Two methods were chosen to analyse the IFN induction in EidNi/41.3 cells. First, cells were transfected with three different concentrations of poly IC, which is a synthetic analogue of dsRNA [95]. In a second approach, cells were infected with RVFV 13 which is lacking the NSs protein, its main IFN antagonist. It was previously shown that this virus induces IFN response in epithelial cells [105, 18]. After IFN induction by these methods, the upregulation of IFN mRNA was examined by real-time RT-PCR.

For the applied prototype cell cultures (MA104, MEF) specific RT-PCRs were already available [80]. To enable comparison of mRNA expression levels between bat and other mammalian cell lines, specific quantitative RT-PCR for bat cells had to be designed. In cooperation with Daniel Ritz (Institute of Virology, Bonn) the IFN beta gene was amplified by nested RT-PCR from cell cultures of a phylogenetically representative range of bats differing in main diet and hunting strategies including the insectivorous *M. daubentonii*, *Pipistrellus spec.* (Vespertilionidae), *H. cf. caffer/ruber* (Hipposideridae) and *R. cf. landeri* (Rhinolophidae) as well as the frugivorous/nectarivorous bats *R. aegyptiacus* and *E. helvum* (Pteropodidae) (Figure 3.2a). RT-PCR primers were designed after alignments of available IFN-β genes from horses, swine, cattle, humans, mice and rats (Table 2.1.10). A conserved region among bats was identified and used to design forward and reverse primers as well as probes (Figure 3.2b) for the quantitative real-time RT-PCR analysis by Primer Express 3.0.

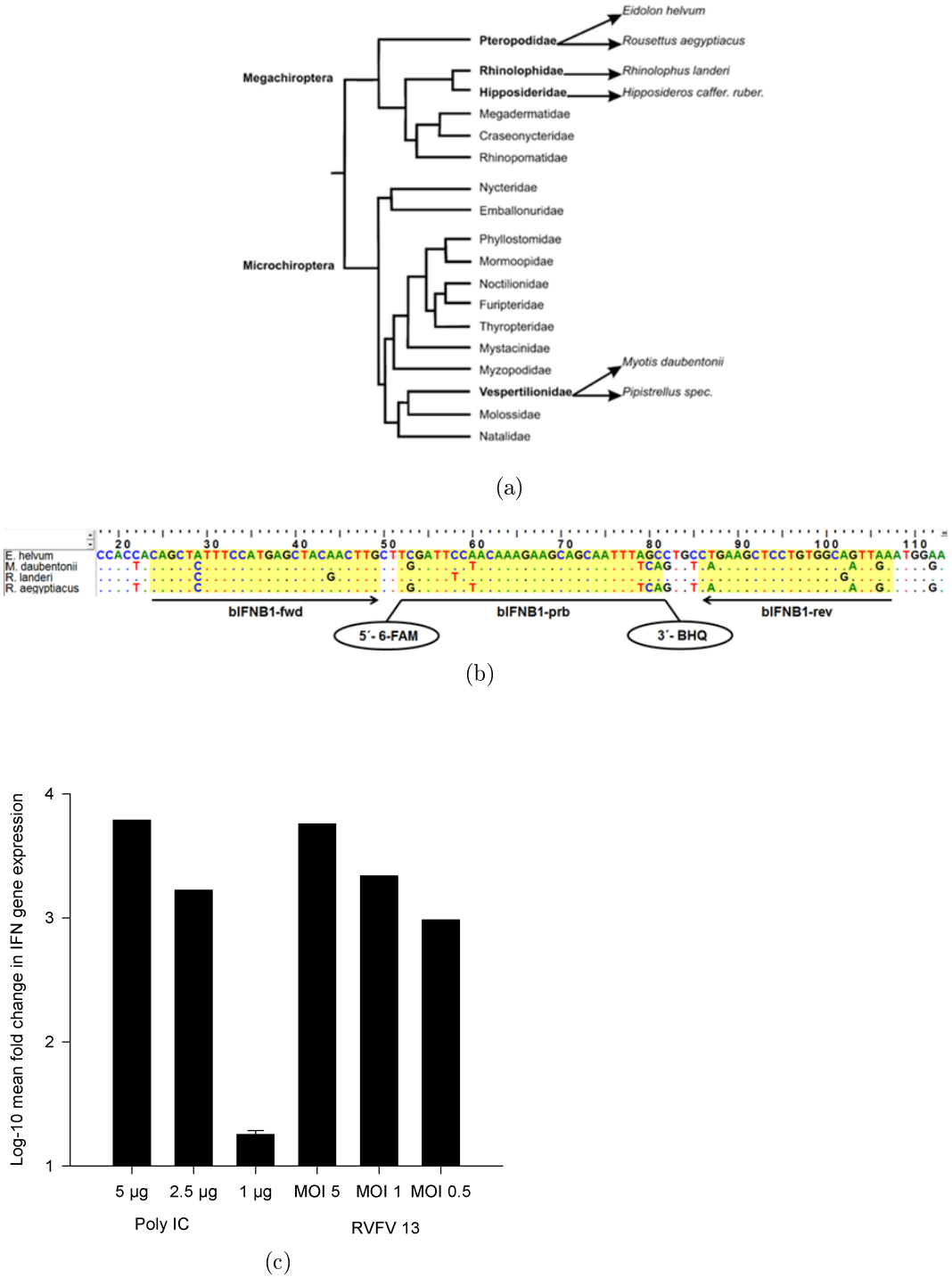

Figure 3.2: **Design of bat-specific RT-PCRs and IFN response of infected bat cells.** (a) Phylogenetic relationships of different selected bat species for the generation of target gene sequences (adapted from [89]). (b) For the IFN-β gene four species were selected. Alignment of bat IFN-β genes (*E. helvum, M. daubentonii, R.cf. landeri* and *R. aegyptiacus*) and positions of primers and probe for a pan-bat real-time RT-PCR. (c) Sensitivity to different amounts of commonly used IFN inductors like poly IC or RVFV 13. Cells were transfected with poly IC at 3 different concentrations or infected with RVFV 13 at three different MOI´s. 24 hpi cells were lysed and IFN mRNA was measured with RT-PCR. In parallel TBP mRNA levels were determined as a reference for cellular gene expression. Experiments were performed in triplicates.

Next, the designed RT-PCR was evaluated by applying two methods to induce IFN response. IFN mRNA levels were detected after treatment with three different concentrations of poly IC and RVFV 13. The bat specific RT-PCR assay was sensitive for the IFN-β mRNA of EidNi/41.3 cells and detected a high expression (>1000-fold) of the IFN-β gene upon stimulation (Figure 3.2c). IFN induction by poly IC was dose-dependent. The highest expression levels of IFN mRNA were found after stimulation with 5 µg poly IC (6150-fold) per well of a 6 well plate, followed by a lower stimulation observed efficiency for 2.5 µg poly IC (1672-fold). This result was also found after stimulation with RVFV 13 at MOIs 5 and 1 (5700- and 2180-fold) . To choose comparable conditions for all cell lines and ensure equally strong IFN induction poly IC was used at a concentration of 5 µg per well of a 6 well plate and RVFV 13 was applied at an MOI of 1 in the following experiments.

3.1.3 Sensitivity of different bat and reference cell lines to IFN inductors

Next the IFN response between bat cells and other mammalian reference cells was compared with the optimized stimulation conditions. The bat cell line, EpoNi/22.1, was included in the experiments testing the sensitivity of the different cell lines to commonly used IFN stimulating factors. This cell line was generated from the bat species *Epo. buettikoferi*, which was together with *E. helvum* and other species identified to carry LBV [75]. The IFN response was induced by poly IC and RVFV 13 treatment in EidNi/41.3, EpoNi/22.1, MEF and MA104 cell lines under conditions optimized in EidNi/41.3 as described in paragraph 3.1.2. 24 h post transfection with poly IC, IFN-β mRNA transcription levels were measured by species-specific RT-PCR assay and compared to the transcription levels of the house keeping gene TBP. For all cell lines a 100-fold increase of IFN-β was observed. Upon RVFV 13 infection the bat cell lines showed a stronger IFN induction compared to MEF and MA104 cells (Figure 3.3a).

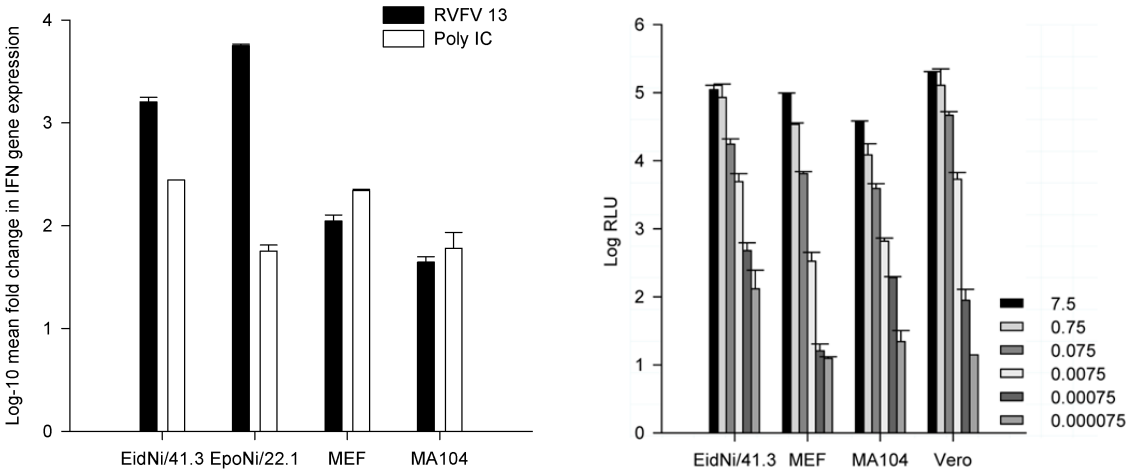

Figure 3.3: **IFN induction in bat cell lines.**
(a) IFN-β mRNA transcription was induced by either RVFV 13 infection (MOI 1) or poly IC transfection (5µg per 6 well). IFN-β and TBP mRNA was quantified by species-specific real-time RT-PCR assays. The fold induction was calculated with the $2^{-\triangle\triangle Ct}$method. (b) Replication of RVFV 13 expressing a *Renilla* luciferase in various cell lines (EidNi/41.3, MEF, MA104 and as reference Vero cells at different MOIs. Cells were infected at different ten-fold diluted MOIs (7.5 until 0.000075) and lysed 24 hpi with *Renilla* lysis buffer (Promega). Replication was detected by *Renilla* luciferase read-out. Experiments were performed in duplicates. Highest replication was found in Vero cells followed by EidNi/41.3, MEF, MA104 (between 10 to 100-fold less compared to Vero cells).

To exclude that differences in IFN induction were due to variable replication a selected bat, a primate and the murine cell line together with a reference cell line (Vero) were infected with RVFV 13 of different MOIs. Since this virus has its IFN antagonist replaced by the Renilla luciferase gene, virus replication could be correlated to the luciferase expression [105]. As depicted in Figure 3.3b, all cell lines were efficiently infectable by RVFV 13. The replication correlated with the virus concentration that was used (Figure 3.3b).

It was concluded that both generated bat cell lines EidNi/41.3 and EpoNi/22.1 were able to react to natural and artificial IFN stimuli and that the pathways were not negatively affected by the immortalisation. The IFN-β transcription was equal or even stronger in comparison to MEF and MA104 cells.

3.2 VSV-bioassay

IFN-β mRNA transcription was a first indicator for type I IFN response. To verify that upregulated mRNA led to measurable amounts of type I IFN proteins, it was

tested whether EidNi/41.3 and EpoNi/22.1 cells were able to produce and secrete effective doses of type I IFN. Therefore it was necessary to compare and calibrate species-specific IFN secretion between primate, rodent, and bat cells, using an appropriate experimental model. To achieve this, a VSV-based IFN bioassay was established. A VSV-bioassay was chosen for two reasons i) the virus is known to enter almost every cell line [29] causing cytopathogenic effects and ii) the virus is highly sensitive to IFN pretreatment of the cells [15]. The IFN induced antiviral state of the cells results in dose-dependent plaque reduction. The optimal conditions for the VSV-bioassay were calibrated for all cell lines.

3.2.1 Optimisation of experimental conditions

First approaches for the development of the VSV-bioassay were focused on handling and proceeding. As shown in Figure 3.4a three various well formats were tested (6, 12 and 24 well). Plaque formation in the 6 well format was detected, but for practical handling reasons this format was excluded. In the 12 well format plaque formation was sufficient and the sample volume was reduced by half. In the 24 well format the number of plaques was too small to generate a standard curve. Therefore in the following experiments the 12 well format was chosen. To gain a countable number of plaques, virus concentration and time of incubation after infection needed to be optimized. All cell lines were infected with three different MOI´s and the incubation time was varied from 24 to 72 h. In Figure 3.4 an example of the optimization for MA104 cells is given. In general, a correlation between plaque size and incubation time was observed. Cells treated with an MOI of 0.125 showed numerous plaques after 24 h incubation which resulted in complete destruction of the cell monolayer after longer incubation times. The second MOI tested was 0.025 and resulted in a countable number of plaques after 24 hpi, 48 and 72 h was found to be too long for proper plaque counting. For the third virus concentration optimal incubation time was identified to be 48 hpi. As depicted for MA104, both virus concentrations (MOI 0.025 and 0.0125) were possible. After infection with an MOI of 0.025 the optimal time of incubation was 24 h, whereas infection with an MOI of 0.0125 optimal plaque formation was achieved after 48 h. To accelerate experimentation MOI 0.025 was further applied. Incubation was increased to 30 hpi to allow formation of easily countable plaques.

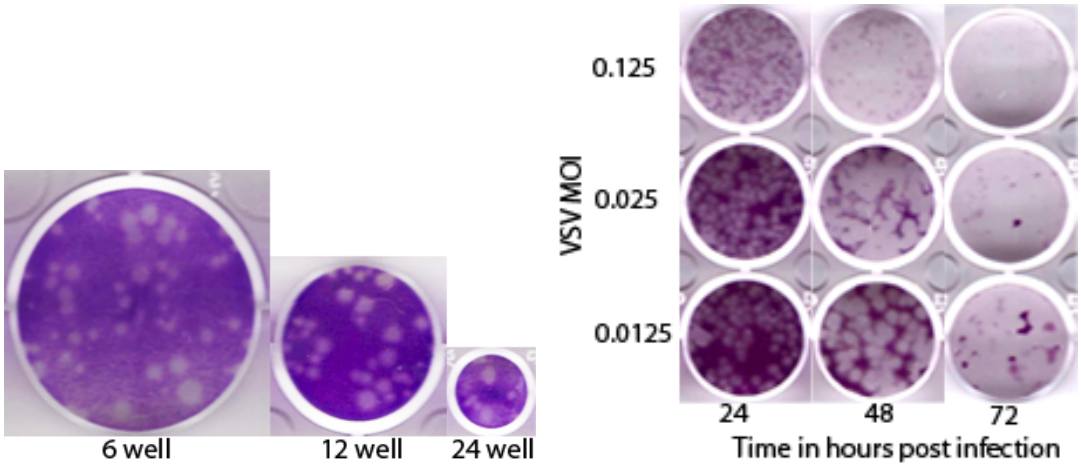

(a) (b)

Figure 3.4: **Optimisation of VSV-bioassay.**
(a) *R. aegyptiacus* kidney cells were seeded in 6, 12 and 24 well plates at a density of 4 x 10^5 cells per mL. After 24 h cells were infected with VSV at an MOI of 0.025. After 1h of incubation supernatants were discarded, cells were washed and overlayed with Avicel. Two days post infection overlay was removed, the cells were fixed and staining was performed with crystal violet solution. Optimal plaque performing conditions for creation of standards were found with the 12 well format. (b) For each cell line virus concentration and incubation time was optimized. Here the example of three virus dilutions and different incubation time points for MA104 cells is shown.

Optimization of virus dilution and incubation time was performed for a number of cell lines that are listed in table 3.1. For most tested cell lines MOI 0.025 was found to be optimal with an incubation time of 24 to 48 h. VSV was not able to infect the HeLa cell line and 293lp cells showed various plaque formations after infection, which made these cells not applicable for this assay. For further experiments the cell lines EidNi/41.3, EpoNi/22.1, MEF and MA104 were selected.

Table 3.1: **Overview of tested cell lines for VSV-bioassay**

Cell line	Species	VSV susceptibility	IFN induction	Plaque formation	Time of incubation MOI 0.025 in h
293 lp	Human	yes	NA	not stable	assay not applied
A549	Human	yes	yes	yes	24
HeLa	Human	no	NA	no	-
Hep2	Human	yes	yes	yes	48
MA104	Primate	yes	yes	yes	30
MEF	Rodent	yes	yes	yes	48
RoNi/7.1	Bat	yes	yes	yes	48
EidNi/41.3	Bat	yes	yes	yes	48
EpoNi/22.1	Bat	yes	yes	yes	24

Legend: NA = not applicable

3.2.2 VSV plaque morphology and sensitivity to pan-IFN

For the selected cell lines the variable VSV plaque morphology was documented as shown in Figure 3.5a. For calibration of IFN secretion across species, cells were incubated with a dilution series of pan-species IFN. The optimal outcome would show complete plaque reduction with highest concentrations of pan-IFN and continuously increasing numbers of plaques at decreasing pan-IFN concentrations. Due to species-specific IFN α/β receptor molecules the sensitivity to pan-IFN was expected to vary between all cell lines. Thus it was crucial to optimize the range of the dilution series for each cell line. In Figure 3.5b the dilution series for EidNi/41.3 is shown. This data were the basis for the determination of individual EC_{50} values.

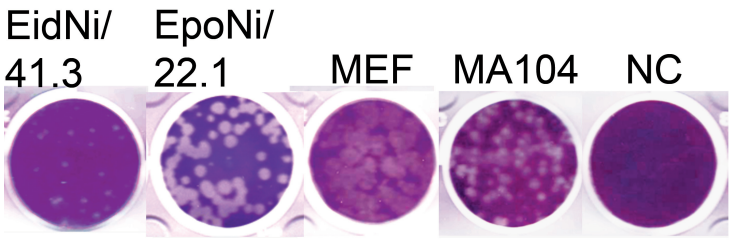

(a)

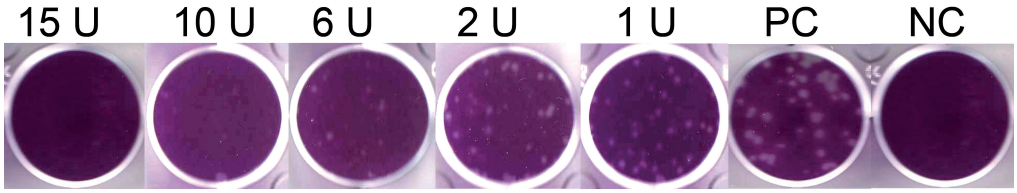

(b)

Figure 3.5: **IFN quantification and calibration by VSV-bioassay.**
(a) VSV plaque morphology was analysed for the bat cell lines EidNi/41.3 and EpoNi/22.1, a rodent cell line, MEF, and a primate cell line, MA104.(b) For the VSV-bioassay standard EidNi/41.3 cells were pre-incubated with various amounts (units per mL; U/mL) of pan-species IFN (pan-IFN). Cells were fixed 24 h after treatment, stained and plaques were counted to estimate the correlation between the amount of pan-IFN and plaques. NC, negative control and PC, positive control.

3.2.3 Generation of standard curves and calculation of EC_{50} values

After determining the optimal range of pan-IFN treatment standard curves had to be generated for EC_{50} calculations. The EC_{50} is the effective dose of pan-IFN to achieve a 50% plaque reduction. All cell lines were incubated with dilution gradients within the determined optimal range of recombinant pan-IFN. The number of plaques expressed in percentage was correlated to the dilution series of pan-IFN concentration in U per mL (Table 3.2).

Table 3.2: **Calculation of the standards**

Cell line	rIFN U/well	n.o.p. in %	equation
EidNi/41.3			
	15	0	
	10	0	
	6	22,56	y = -28,75ln(x) + 78,668
	2	78,04	
	1	95,73	
	0,25	100	
EpoNi/22.1			
	30	1,91	
	25	3,02	
	20	7,23	y = -33,19ln(x) + 121,06
	10	66,73	
	5	98,47	
	1	100	
MEF			
	15	0	
	10	5,1724	
	5	17,2414	y = -31,65ln(x) + 79,861
	4	40,2299	
	1	85,0575	
	0,5	100	
MA104			
	50	0	
	25	3,45	y = -20,02ln(x) + 84,42
	10	53,65	
	5	67,68	
	1	88,41	
	0,25	100	

Legend: n.o.p. = number of plaques

Different sensitivities to pan-IFN among the various cell lines were observed and EC_{50} values ranged between 2.6 and 11.2 U/mL (Table 3.3). At least three pan-IFN concentrations from these defined species-specific standards had be to included in every VSV bioassay that followed. EidNi/41.3 had an EC_{50} value of 3.4 while EpoNi/22.1 showed an EC_{50} value of 11.2 (Table 3.3).

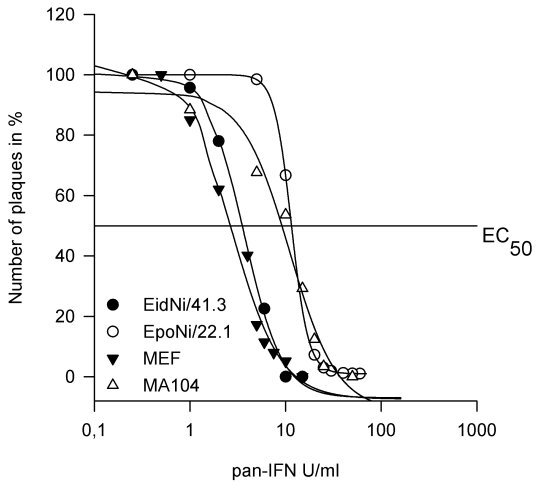

Figure 3.6: **Standard curves and EC_{50} values for VSV-bioassay.**
With pan-IFN dilution series standard correlations between number of plaques as a percentage and pan-IFN U in mL were achieved. EC_{50}values indicate the amount of IFN to reduce the number of plaques to 50 percent. This factor was determined to correlate IFN concentrations between different cell lines.

The sensitivity to pan-species IFN was independent of origin or relation of the cell lines (MEF < EidNi/41.3 < MA104 < EpoNi/22.1). All determined IFN concentrations in the following experiments were normalized with the determined EC_{50} values. This enabled the comparison of secreted IFN concentrations between different cell lines from variable species independently from their IFN receptors and the differential sensitivity to the pan-species IFN.

Table 3.3: **Definition of EC_{50} values**

Cell line	EidNi/41.3	EpoNi/22.1	MEF	MA104
EC_{50} (U/mL)	3.4	11.2	2.6	9.3

3.2.4 Comparison of IFN secretion

With the help of the established VSV-bioassay species-specific secreted bioactive IFN could be measured. As described in chapter 3.2.3 infection with RVFV 13 and transduction with poly IC led to measurable IFN induction on mRNA level (Figure 3.7a). Supernatants from the same cells were now used to measure secreted IFN. In accordance with increased IFN mRNA transcription, elevated levels of secreted IFN were detected for all cell lines starting at a 1,000 fold increase (Figure 3.7a). In

EidNi/41.3 cells the induction with both IFN stimulating factors led to an 100,000 fold increase in secreted IFN. In accordance with the increased mRNA levels (Figure 3.3), EpoNi/22.1 cells showed stronger IFN secretion after RVFV 13 treatment compared to the IFN stimulation with poly IC. Both stimuli induced IFN gene expression as well as secretion (Figure 3.7b).

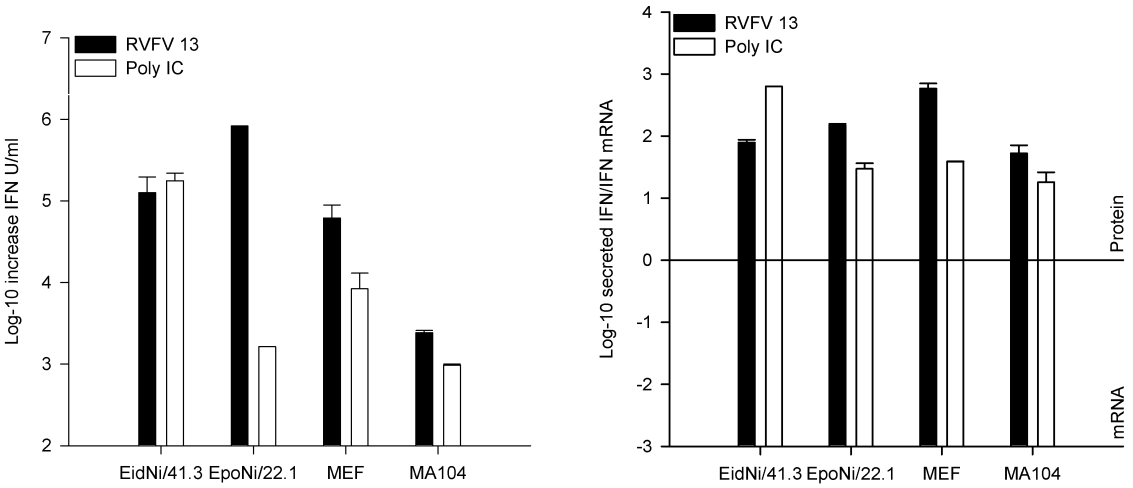

Figure 3.7: **Bat cells produce high levels of secreted IFN.**
(a) Cells were infected with RVFV 13 or transfected with poly IC as described before. With the help of the VSV-bioassay secreted IFN was measured. Each cell line was incubated for 24 h with IFN-containing supernatants (β-PL inactivated) and with pan-IFN standards diluted in medium from untreated control cells. IFN concentrations were normalized with the help of EC_{50} values as described in the methods section. (b) IFN-β mRNA transcription was induced by either RVFV 13 infection (MOI 1) or poly IC transfection (5µg per 6 well). IFN-β and TBP mRNA was quantified by species-specific real-time RT-PCR assays. The fold induction was calculated with the $2^{-\triangle\triangle Ct}$method.

Except for cell line EidNi/41.3, RVFV 13 led to higher IFN secretions. Most applied cell lines thus showed a higher sensitivity to the replicating virus as a ´natural‘ stimulus (Figure 3.7a). In conclusion, EidNi/41.3 and EpoNi/22.1 cell lines were able to express IFN mRNA after induction with natural and artificial stimuli, to secrete measurable, active type I IFN protein leading to an antiviral state and to produce comparable and higher amounts like MEF and MA104 cell lines.

Overview

Bats harbour a multitude of human pathogenic viruses including arboviruses like VEEV, CHIKV and SINV [24]. Their role in the arboviral life cycle has not been investigated yet. Little is known about virus host interaction, particularly host specific defence mechanisms. In this study the prevalence of arboviruses in bats with focus on *Togaviridae* (New and Old World viruses) was analysed by a serological assay. Additionally first insights into the IFN response mechanisms of bat cells were gained by newly developed *in vitro* tools.

3.3 Serological survey of Alphaviruses in bats

A variety of alphaviruses have been detected or isolated from different bat species [24]. So far it is unclear which role bats play in the alphavirus life cycle. Since bats harbour parasites and can be bitten by mosquitoes it can be assumed that they serve as an intermediate host. In order to get insights into the prevalence of alphaviruses in bats we conducted a serological survey. The map in Figure 3.8 shows origin countries of bat sera, namely Germany, Ghana, Gabon and Panama, which were analysed for alphavirus antibody prevalence (Figure 3.8).

Figure 3.8: **Distribution of analysed samples in the world.**
Various bat species were captured with mist nets. Blood and stool samples were taken and frozen until further analysis. Species were determined by field ecologists. The samples used in this study were collected in Germany, Ghana, Gabon and Panama. The countries of origin are marked in red.

In each country an average of four species was collected. Blood, faecal and parasite samples were taken and wing size and bone length were measured by field biologists. In this study only serum samples were included. In cooperation with M. A. Mueller (Institute of Virology, Bonn), 1136 sera from 16 bat species were analysed for antibody reactivity with alphavirus antigen. Bat sera were screened for cross reactive antibodies by IF assay as described in chapter 2.2.14. The IF slides carried either VEEV or CHIKV infected Vero cells. Only 30 to 50% of the cells were infected in order to guarantee non-infected cells to be present as a negative control. In Figure 3.9 an example of positive and negative tested bat sera is given (Figure 3.9).

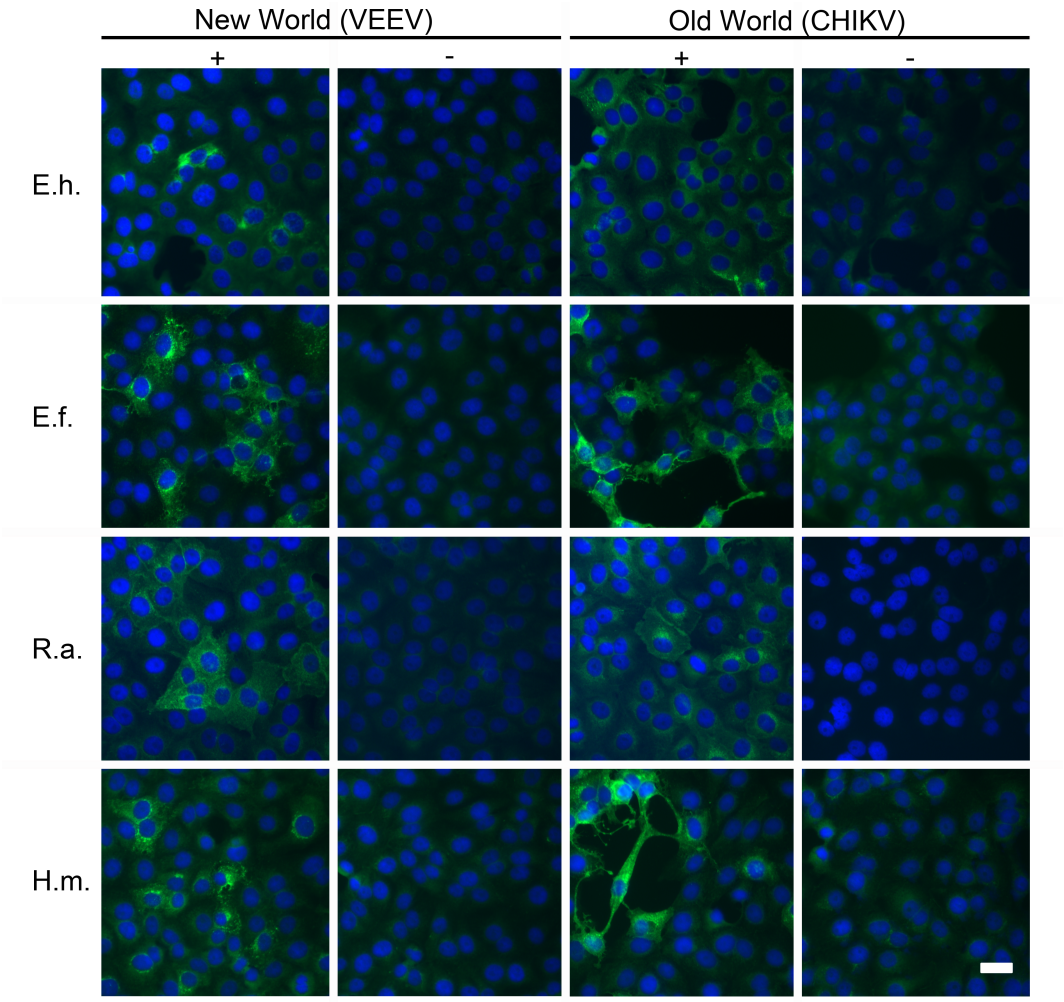

Figure 3.9: **Immunological analysis of bat sera.**
Bat sera were exposed to VEEV or CHIKV infected Vero cells. *Eidolon helvum* (E.h.) (GH85), *Epomops franqueti* (E.f.) (GB3520), *Rousettus aegyptiacus* (R.a.) (GB1558) and *Hypsignathus monstrosus* (H.m.) (CHA431) were found to have cross reactive antibodies with VEEV and CHIKV antigens.

Cross reactions with VEEV and CHIKV antigens were found in *E. helvum*, *Epo. franqueti*, *R. aegyptiacus* and *H. monstrosus* bat sera. All four species with higher prevalence belonged to frugivorous bat species. These cross reactions with VEEV antigens are consistent with earlier findings of VEEV detection in neotropical bats in Mexico, 1970 [19, 31]. In total 5% of all tested bat species were found seropositive (Table 3.4).

Table 3.4: **Bat sera tested for alphavirus reactivity from different species and locations**

Bat species			**Togaviridae**	
Old World fruit bats	**Location**	**Sera tested**	**VEEV** Positive n (%)	**CHIKV**
Eidolon helvum	Ghana	167	1 (0.6)	8.0 (4.8)
Epomops franqueti	Gabon	99	13 (13.1)	13 (13.1)
Hypsignathus monstrosus	Gabon	94	11 (11.7)	14 (14.9)
Micropterus pusillus	Gabon	100	3 (3.0)	3 (3.0)
Myonycteris troquata	Gabon	100	18 (18.0)	16 (16.0)
Rousettus aegyptiacus	Gabon	197	2 (1.0)	4 (2.0)
Insect bats				
Coleura afra	Gabon	14	0 (0.0)	0 (0.0)
Hipposideros caffer	Gabon	48	0 (0.0)	2 (4.2)
Hipposideros gigas	Gabon	129	1 (0.8)	1 (0.8)
Miniopterus inflatus	Gabon	51	1(2)	0 (0.0)
Myotis dasycneme	Germany	26	0 (0.0)	0 (0.0)
Myotis daubentonii	Germany	28	0 (0.0)	0 (0.0)
Nyctalus noctula	Germany	24	0 (0.0)	0 (0.0)
Rhinolophus spec.	Gabon	16	0 (0.0)	1 (6.3)
Neurotropical bats				
Artibeus jamaicensis	Panama	28	1 (3.6)	2 (7.1)
Artibeus lituratus	Panama	15	0 (0.0)	0 (0.0)
Percentage positive (%)			**4.5**	**5.6**
No. total sera positive (n)			51	64
Total sera tested		1136		

Antibody reactivity was 10-fold higher in fruit bats compared to insectivorous

bats. Highest seroprevalence was detected in *Myonycteris troquata* (20%) and lowest prevalence was found in *Miniopterus inflatus* (2%). The geographical distribution of positive bats could be correlated with the abundance of the arbovirus vector-the mosquito species *Aedes aegypti* or *Anopheles gambiae*. These mosquitoes are mainly found in tropical regions. All bat serum specimens collected in Germany were negative. The neotropical bats showed an abundance of approximately 5%, only in *A. jamaicensis*. Interestingly, VEEV antigen reactive sera were found to the same amount as CHIKV, although VEEV belongs to the New World alphaviruses spread in Central- and South America. Likewise CHIKV antibodies were found in sera from neotropical bats. A general cross-reactivity of sera with those related antigens can be excluded as several sera reacted exclusively with only one viral antigen. These findings could be explained by cross reactivity with closely related viruses located in Africa for VEEV and in Central America for CHIKV. As alphaviruses can infect bats and induce sero conversion the generated cell cultures were applied for further investigations.

3.4 IFN response after ONNV infection in EidNi/41.3, EpoNi/22.1, MEF and MA104 cell lines

The Old World alphavirus ONNV was chosen since alphaviruses have been previously detected in bats [19, 31] and induce IFN response [158]. Alphaviruses avoid the antiviral response of cells by initiating a cellular translational shutoff, while the viral translation remains unaffected [158, 215, 23]. Here, it was analysed whether bat cells show the same IFN response to alphavirus infection compared to mammalian reference cell lines MEF and MA104.

3.4.1 ONNV replication

The following experimental considerations were taken into account for infection studies with ONNV. First a high MOI of 2.5 was chosen to ensure a synchronized infection. In addition, incubation times of 0 and 24 hpi were selected to guarantee measurable amounts of increased IFN in supernatant but only slight cytopathic effects (CPE) for all cell lines. Finally, supernatants and cells were harvested at the same time to simultaneously measure genome equivalents (GE) per plaque forming

unit (PFU) and mRNA expression levels as well as secreted IFN protein in the same sample. Virus growth was determined by an ONNV-specific real-time RT-PCR (Figure 3.10a) and by titration of viral particles in supernatants 24 hpi (Figure 3.10b). Virus mRNA and infectious virus were detected in all cell lines. A 1,000-fold increase of GE was detected for infectious virus formation after 24 hpi. However, newly synthesized RNA genome could be degraded, thereby leading to positive RT-PCR values but no infectious virus particles. The specific infectivity, expressed as PFU per genome equivalent (PCR units), was used to evaluate the quality of replication. A value expressed as specific infectivity, indicated a good quality of replication. All cell cultures showed a high level of replication and highly comparable results (Figure 3.10c).

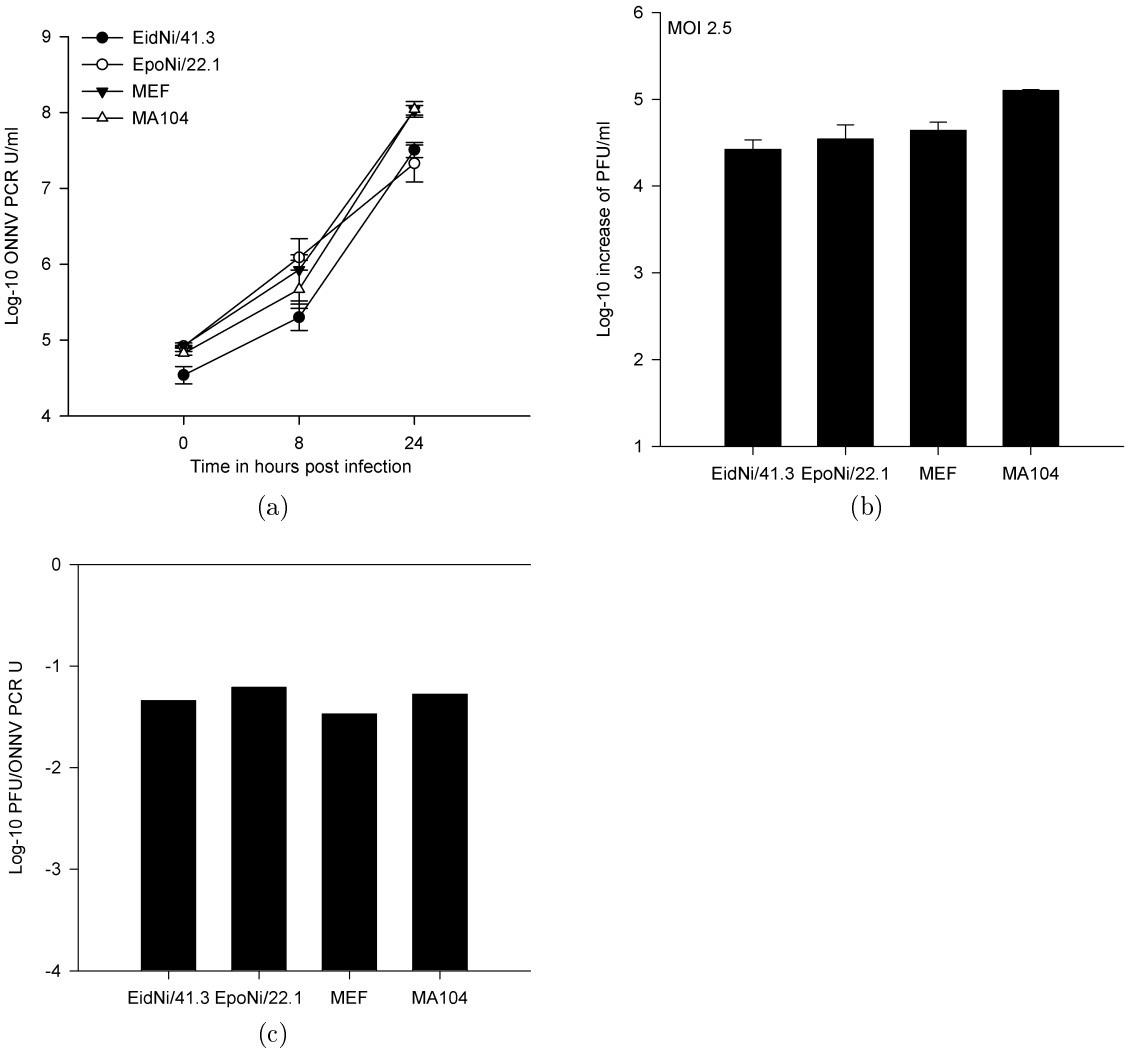

Figure 3.10: **ONNV replication in different mammalian cells using a high MOI.** (a) For a synchronized infection cells were inoculated with ONNV at an MOI of 2.5 and supernatants were harvested at 0, 8 and 24 hpi. After viral RNA isolation the concentration was measured by ONNV specific real-time RT-PCR assay (triplicates). ONNV PCR units (U) per mL were determined. The dilution end-point was defined as one PCR unit. Virus replication could be detected in all cell lines. The increase of genome equivalents per mL were approximately 1,000-fold after 24 hpi. (b) Titration of ONNV 24 hpi in supernatants. In all cells viral particles were formed. (c) The specific infectivity was estimated by calculating the ratio between PFU and ONNV PCR U. In all cell lines the specific infectivity was comparable.

3.4.2 IFN induction after ONNV infection

After confirming that all cells were efficiently infected and to similar levels the IFN responses of the different cell lines were analysed. IFN induction was determined

by correlation of IFN mRNA levels to expression levels of the housekeeping gene TBP. Samples were taken at 0, 24 hpi and, additionally, at 8 hpi since the mRNA transcription levels are prone to variation. In all cell lines an increase of IFN mRNA transcription was detectable and ranged between 7.3 to 8.0 logs (Figure3.11a).

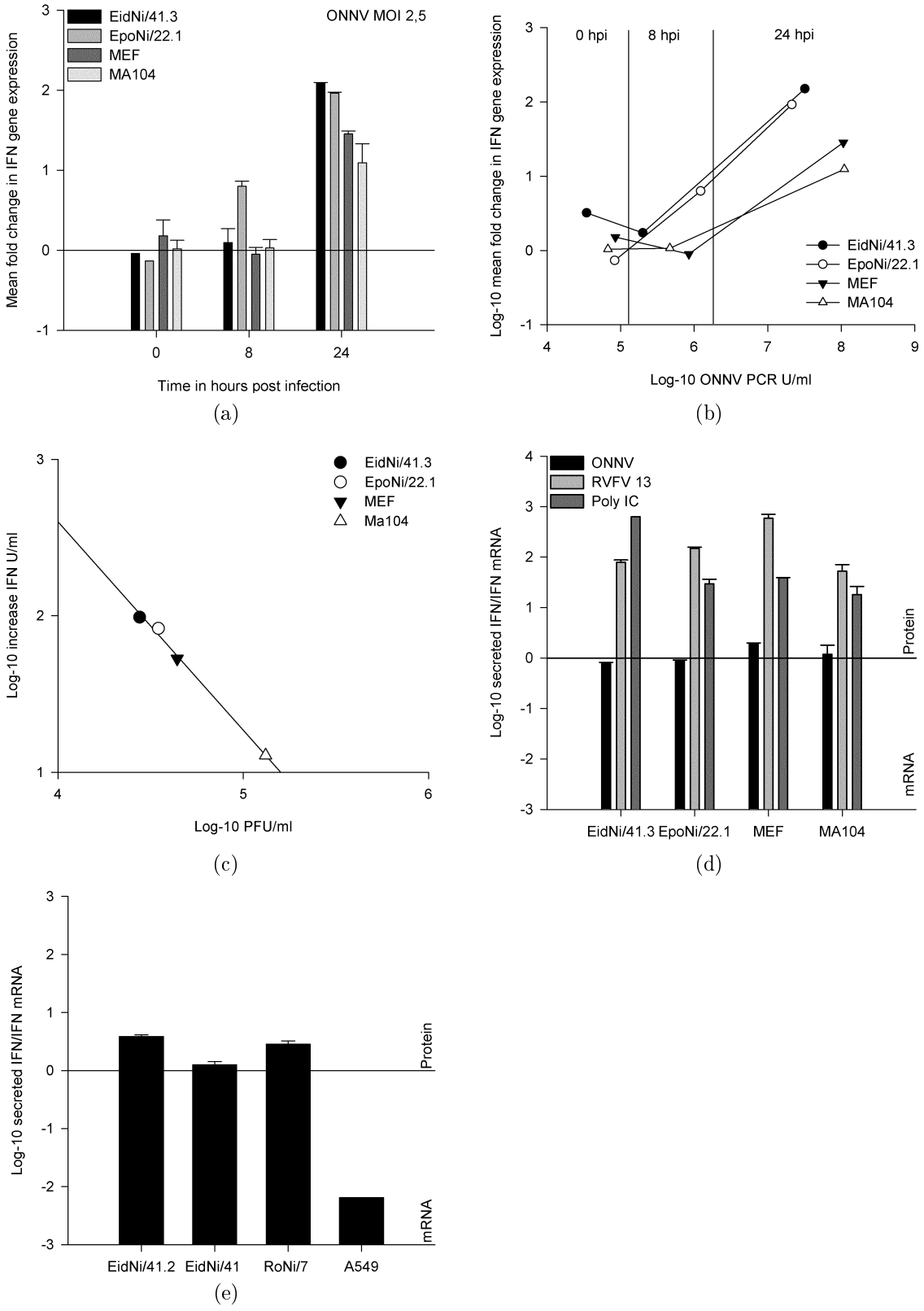

Figure 3.11: **IFN-β mRNA induction but IFN protein decrease in all mammalian cells upon ONNV infection.**
(a) Mean fold change in IFN-β gene expression detected by species-specific real-time RT-PCR 0, 8 and 24 hpi with ONNV. (b) The induced IFN-β mRNA levels were correlated to the amount of relative ONNV genome equivalents in PCR units per mL.

(c) At 24 hpi the increase of secreted IFN was correlated to ONNV plaque forming units indicating that higher virus titres led to a decreased amount of IFN in the supernatants. (d) Comparison of secreted IFN protein to IFN-β mRNA 24 hpi with ONNV, RVFV 13 infection and poly IC transfection. ONNV replication was related to IFN protein reduction.

The IFN induction was directly compared to ONNV infection. While no induction of IFN mRNA was detectable at 8 hpi, ONNV replication clearly induced IFN mRNA expression by 24 hpi for all cell lines (Figure 3.11b). The increased viral titers corresponded to lower amounts of secreted IFN protein after 24 hpi (Figure 3.11c). EidNi/41.3 cells showed highest levels of secreted IFN but lowest level of infectious particles, indicating that virus growth was limited in response to IFN. To differentiate whether virus control correlated with levels of secreted IFN or merely with the induction of genes under control of the IFN promoter, the ratios of secreted IFN versus IFN mRNA were determined in all cell lines. The ratios of secreted IFN versus IFN mRNA after stimulation by RVFV 13 or poly IC were in all cell lines comparable. In contrast, in all cell lines infected with ONNV the relative levels of secreted IFN were clearly reduced, while overall IFN mRNA induction was less affected (Figure 3.11d). This effect was independent from the cell species indicating a ONNV-specific IFN protein reduction. To exclude cell clone specific effects, EidNi/41.2 and the mixed culture EidNi/41 were additionally analysed. These cell lines showed the same reduction of relative IFN secretion upon ONNV infection (Figure 3.11e). Similar effects were also detected in a mixed culture generated from the related flying fox *R. aegyptiacus* (RoNi/7). The human cell line A549 showed a stronger reduction on IFN secretion than MEF and MA104 cell lines in similar experiments (Figure 3.11e).

3.4.3 mRNA levels of IFN and ISGs

Alphaviruses were shown to induce transcriptional shutoff affecting mainly the cellular but not the viral mRNAs [158]. While the reported results suggested similar effects in *E. helvum*, *Epo. buettikoferi* and *R. aegyptiacus* cells, control of ONNV replication seemed to be more efficient in the applied bat cells. The similarity of the reduction levels of secreted IFN could be explained by a more pronounced and efficient upregulation of ISGs in bat cells. To investigate this, the mRNA abundance of two different ISGs (MxA and ISG56) as well as two reference genes (beta actin and TBP) were analysed (Figure 3.12a and 3.12b) and compared to the amounts of

secreted IFN 0 and 24 hpi (Figure 3.12c and 3.12d).

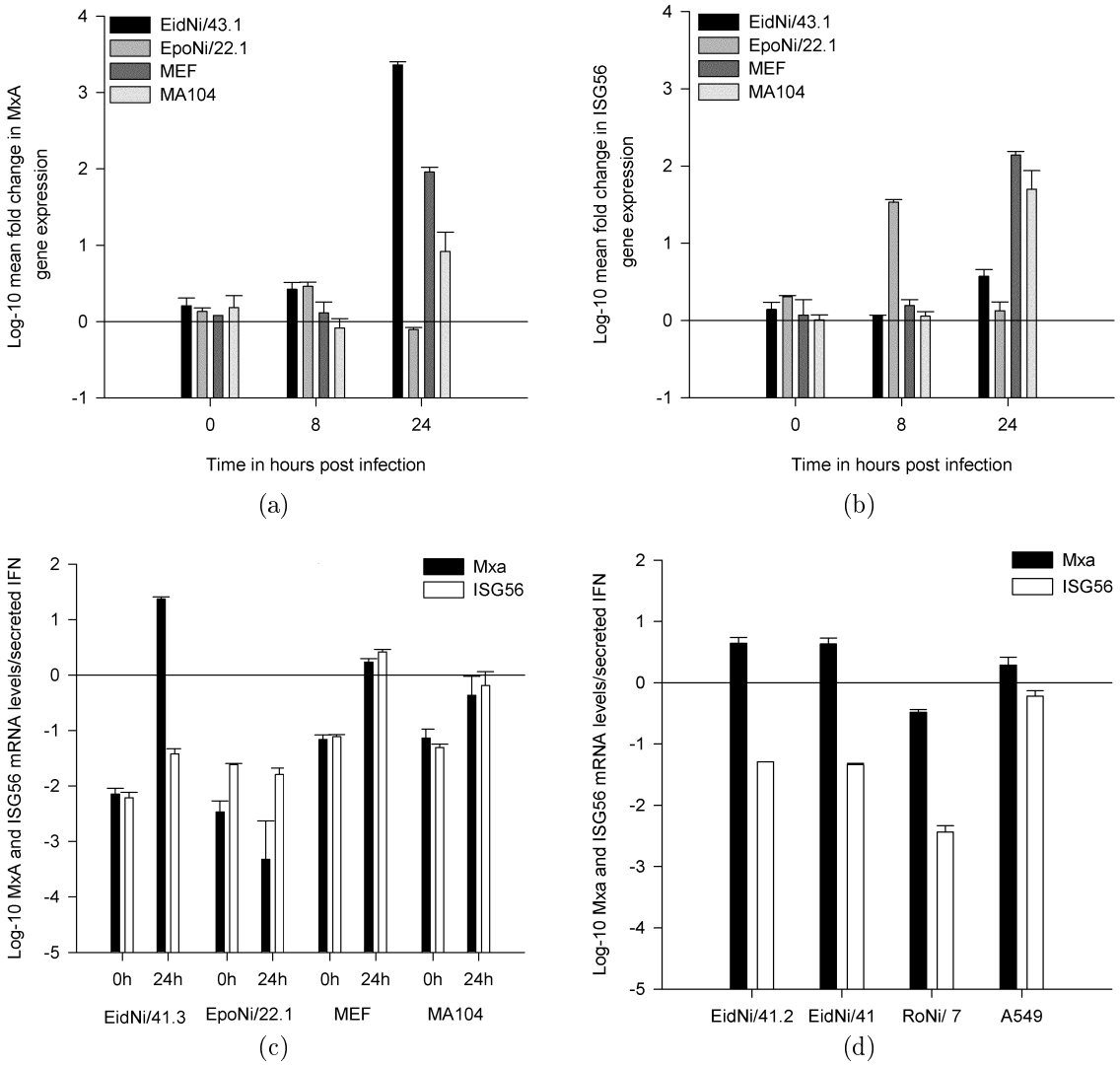

Figure 3.12: **IFN protein secretion and ISG expression.**
(a) Expression of MxA after 0, 8 and 24 hpi with ONNV in EidNi/41.3,EpoNi/22.1, MEF and MA104 cell lines measured by species-specific RT-PCR assay. (b) Expression ISG56 mRNA levels after ONNV infection measured by species-species RT-PCR. Both (a) and (b) show increasing levels of MxA and ISG56 mRNA expression over time. (c) Comparison of mRNA fold-induction of IFN stimulated genes (MxA and ISG56) to secreted IFN protein at time points 0 hpi and 24 hpi. Expression was not affected by IFN protein downregulation indicating that there was no general transcriptional shutoff. (d) Test of different cell clones and cell cultures 24 hpi showing that MxA mRNA was upregulated in bat cell cultures upon ONNV infection.

The absolute values of MxA and ISG56 mRNA increase over time are shown in Figure 3.12 a and b. In EidNi/41.3 cells the level of MxA mRNA induction in relation to IFN in the supernatant was more than 1,000-fold higher compared to the same ratio for ISG56. Only for EpoNi/22.1 highest amount of MxA and

ISG56 mRNA levels were detected at 8 hpi followed by a reduction of mRNA levels after 24 hpi. In contrast to IFN secretion the ratios showed an approximate 10-fold increase at 24 hpi indicating no general block of transcription after ONNV infection (Figure 3.12c). The clonal and mixed cultures EidNi/41.2 and EidNi/4 as well as RoNi/7 showed a 100-fold higher induction of MxA mRNA in comparison to ISG56, which indicated a related reaction pattern (Figure 3.12d). The results suggested a highly efficient IFN signalling-dependent induction of ISG mRNA in *E. helvum*, *Epo. buettikoferi* and *R. aegyptiacus* bat cells, which could explain a better control of ONNV replication in both applied bat cell lines.

3.4.4 ONNV infection ablates the expression of IFN stimulated genes

ONNV infection did not affect mRNA transcription. Since it was observed that alphaviruses can lead to translational shutoffs [65], protein expression was analysed by Western blot analysis (Figure 3.13). The protein expression of MxA, ISG56 (p56) and actin were compared to uninfected, RVFV 13 and ONNV infected cells. After RVFV 13 infection MxA expression was clearly higher or similar to the uninfected control cells, whereas for p56 protein the expression level maintained (Figure3.13). In contrast, ONNV infection resulted in decreased expression levels of MxA and p56 proteins. This effect was generally more pronounced for MxA than for p56. The data pointed to a virus-related effect on the IFN-dependent signalling via the JAK/STAT-pathway rather than a JAK/STAT-independent induction of ISGs. MEF cells formed an exception with no reduction in MxA expression (Figure 3.13). The bat cell lines EidNi/41.3, EpoNi/22.1 and RoNi/7 showed clear induction of MxA mRNA, but the production of the antiviral protein was antagonized by ONNV to a larger extent than in cells from rodents or primates.

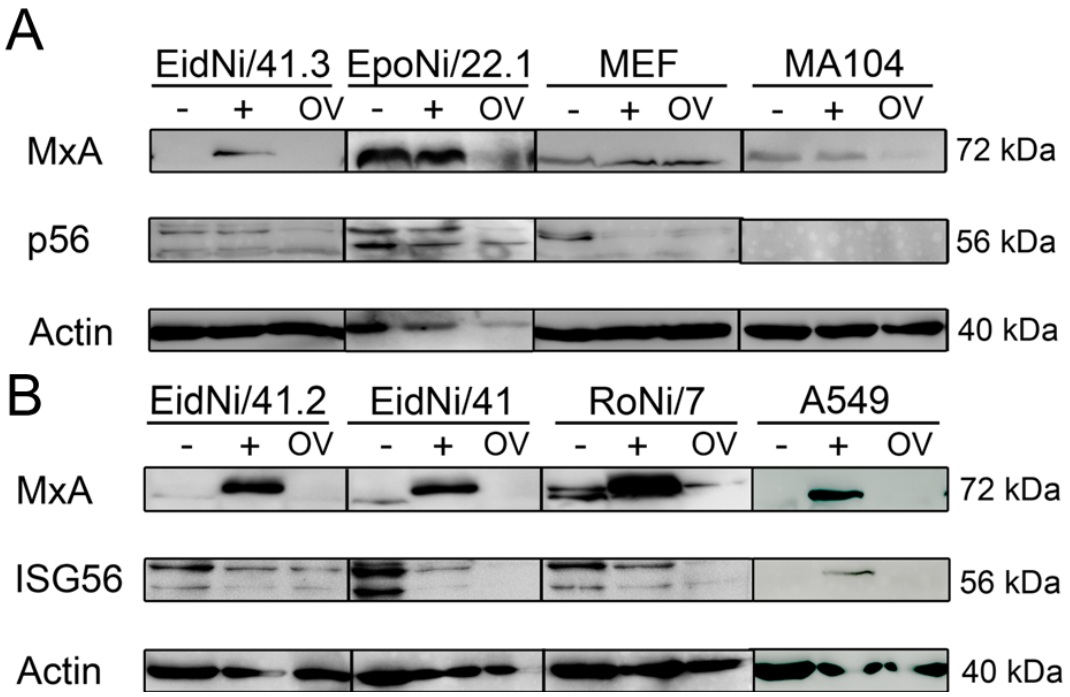

Figure 3.13: **ONNV infection ablates the expression of IFN stimulated genes.** (a) Cells were either left untreated (-) or infected with RVFV 13 (+) or ONNV (OV). After 24 h proteins were extracted from cells. Same amount of proteins were subjected to SDS-PAGE followed by a Western blot analysis. Mouse-anti-MxA, mouse-anti-ISG56 and mouse-anti-actin IgG antibodies were applied at dilutions 1:1000 followed by a peroxidase labelled goat-anti-mouse secondary antibody (1:20000). In all cell lines infection with ONNV did not induce the expression of MxA and p56 and was less or similar to untreated cells. (b) To exclude cell clone specific effects additional EidNi and RoNi bat cell cultures were included (EidNi/41.2; EidNi/41 and RoNi/7) as well as a human A549 cell line.

3.4.5 Efficient ONNV replication upon infection at low MOI

The effects on IFN and ISG protein reduction were found as results of ONNV replication. Alphaviruses, however, are prone to mutations in the 5‘UTR [103, 210], nsP3[13], or nsP2[53] genes which result in low replication levels enabling the virus´ persistence without IFN-dependent elimination. However, the observed increase of IFN mRNA expression upon ONNV infection (Figure 3.11a and 3.11b) and the high virus titers of up to 10^5 PFU per mL (Figure 3.10b) indicated that replication was not limited. To further exclude this, virus replication was studies upon infection with an MOI of 0.0025 in selected cell lines. At time point 0, 8 and 24 hpi virus replication was analysed by real-time RT-PCR (Figure 3.14a). Viral supernatants taken 24 hpi were titrated to determine the concentration of infectious particles (Figure 3.14b) and enable the definition of the specific infectivity of the virus (Fig-

ure 3.14c). Although the experiments were performed with 1,000-fold lower MOI, the virus growth was efficient in all cell cultures. The specific infectivity showed the same strong infectious particle formation. With this efficient particle formation in all cell lines tested it was concluded that the decrease in IFN and ISG protein levels was not a result of attenuated viral replication.

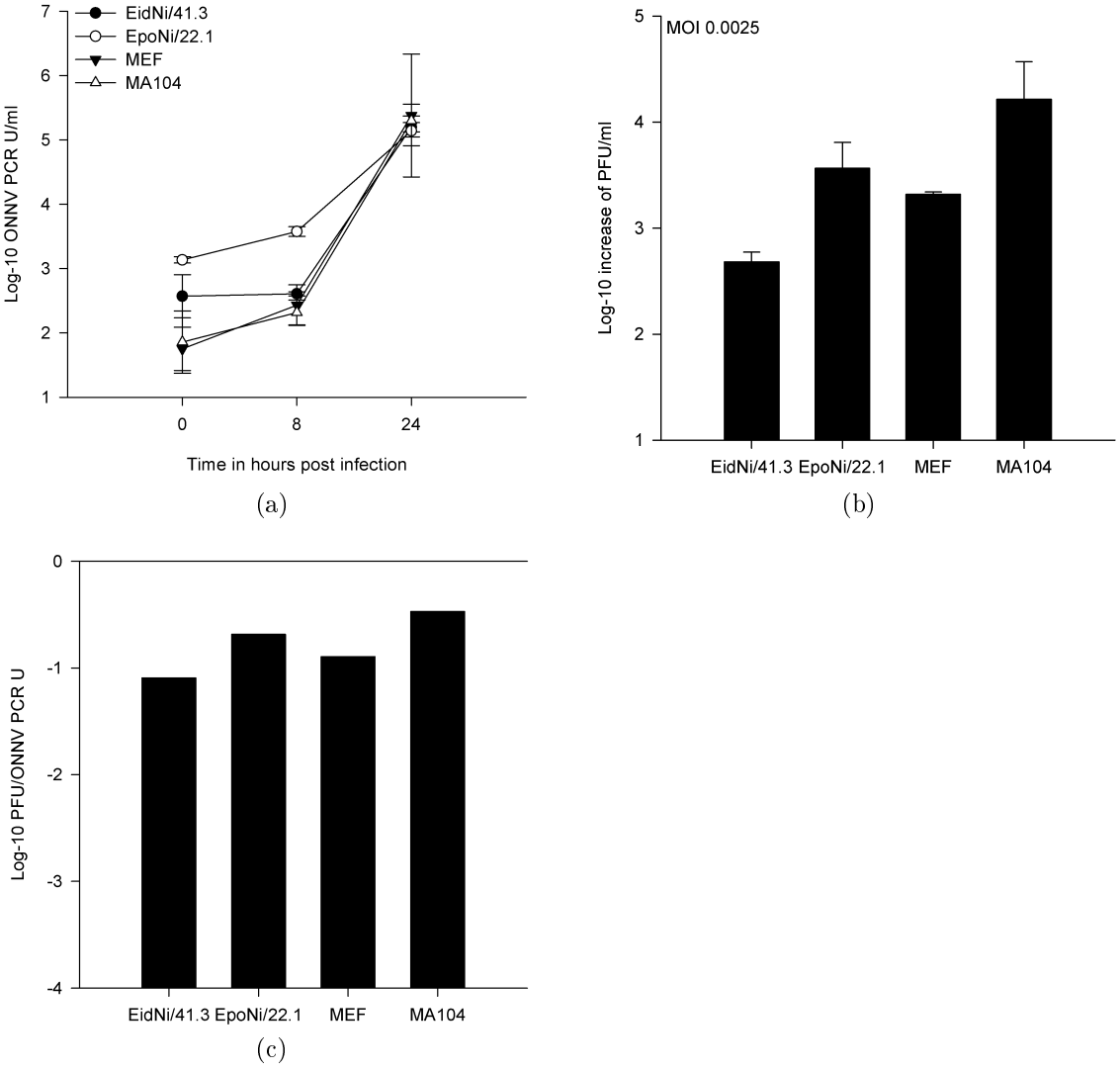

Figure 3.14: **Efficient ONNV replication upon infection at low MOI.**
(a) In order to access if insufficient viral replication led to a delayed or ablated IFN production in cells a growth kinetic at low MOI was performed (MOI 0.0025). Cells were inoculated with ONNV and supernatants analysed at 0, 8 and 24 hpi by real-time RT-PCR. Virus replication could be detected in all cell lines. (b) Supernatants were titrated after 24 hpi confirming the PCR results. (c) PFU to ONNV PCR unit (U) ratio after infection of cells with ONNV at an MOI of 0.0025.

3.5 Comparison with other Old World alphaviruses (SINV and CHIKV)

Bat cells as well as reference cell lines could be efficiently infected by ONNV. Despite elevated mRNA levels for IFN and ISGs the amount of corresponding proteins decreased suggesting an ONNV-related translational shutoff. In order to investigate whether this is a common feature upon alphavirus infection two other alphaviruses, SINV and CHIKV, were analysed for activation of the IFN response. The experiments were limited to one bat cell line (EidNi/41.3) and one rodent reference cell line (MEF).

3.5.1 CPE detection after SINV or CHIKV infection

SINV is one of the first described and therefore extensively characterized alphaviruses. CHIKV re-emerged in 2005 and 2006 illustrated the potential threat to public health and the necessity to understand mechanisms involved in alphavirus biology [112]. Earlier findings showed high replication rates for both viruses in cell culture systems [189]. In order to analyse the replication behaviour of SINV and CHIKV in EidNi/41.3 compared to MEF cells, the cell lines were infected with MOI 2.5 to ensure synchronised infection. Morphological signs of cell death were determined at 0, 4, 8, 10 and 24 hpi. After SINV infection first morphological signs of cell death were observed in EidNi/41.3 cells already 4 hpi. CPE were continuously stronger than in MEF cells over time. The cell monolayer was completely destroyed for EidNi/41.3 cells 24 hpi, while in MEF cells only first signs of CPE were detected (Figure 3.15a). Figure 3.15b shows the CPEs after CHIKV infection. In both cell lines morphological changes were first detected at 8 hpi with similar patterns of morphological change over time. A complete destruction of the cell monolayer in EidNi/41.3 cells was visible by 24 hpi (Figure 3.15b).

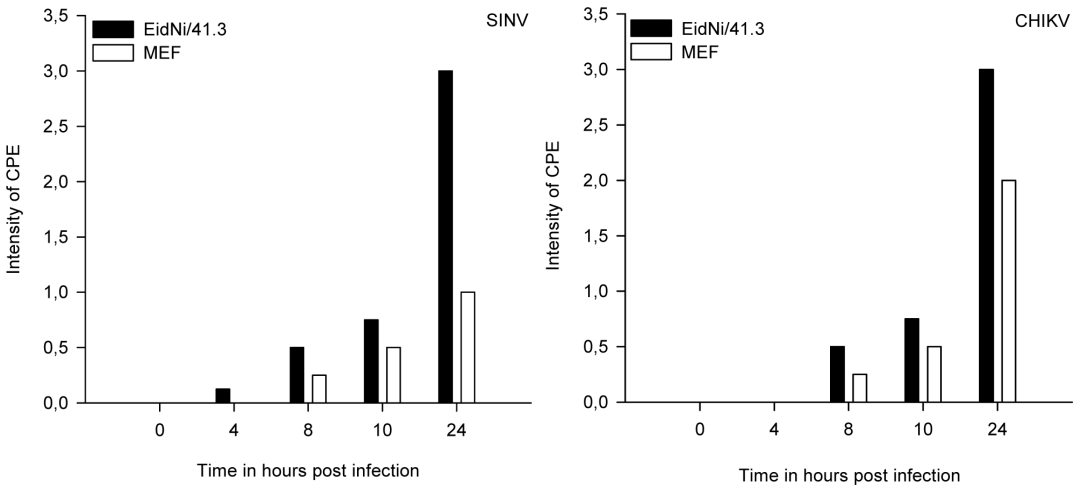

(a) (b)

Figure 3.15: **CPE detection after SINV or CHIKV infection.**
Various cells were infected with 3 different MOIs 2.5, 0.1 and 0.0025. The cells were observed and CPE appearance was validated (1= small changes to 3= all cells dead). A strong cytopathic effect was observed after SINV as well as CHIKV infection.

3.5.2 SINV and CHIKV replication in bat or MEF cells

The observed CPEs upon SINV and CHIKV infection revealed that an incubation time of 24 hpi was too long to generate reliable samples. To analyse virus replication and growth, induction of the IFN response and effects on the ISG expression sampling was reduced to 4 and 10 hpi with an MOI of 2.5 for both viruses. Viral replication was analysed with virus-specific RT-PCR assays. Figure 3.16a shows a 100-fold increase of genome equivalents between 4 and 10 hpi for both viruses. SINV already showed high amounts of GE after 4 hpi, indicating a more rapid replication in comparison to CHIKV infection, which showed RNA levels of at least 100-fold lower. But at 10 hpi an 10,000-fold increase in GE was detected in MEF cells after CHIKV infection and with this the replication rate was almost similar to SINV infection. Interestingly, in EidNi/41.3 cells CHIKV RNA levels were lowest. Since measured RNA levels only describe the replication but not the effective formation of viral particles, the supernatants taken 10 hpi were then titrated to determine the infectious particle formation. In both cell lines SINV was able to produce viral particles to very high titers (Figure 3.16b). In correlations with the difference in replication levels between SINV and CHIKV, SINV infection resulted in higher titers. The ratio between PFU and PCR U per mL expressing the specific infectivity was equal for SINV and CHIKV in both cell lines.

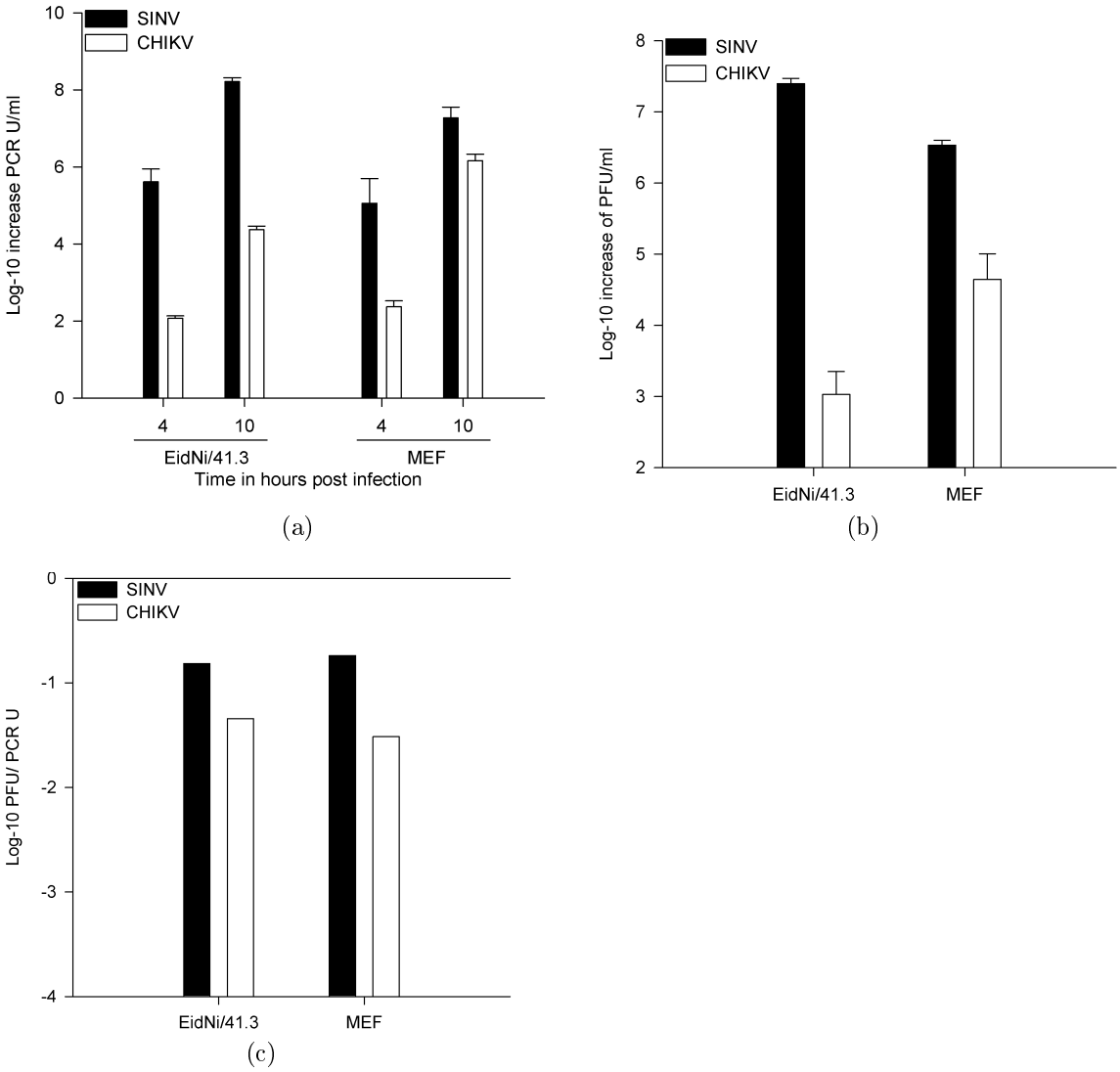

Figure 3.16: **SINV and CHIKV replication in bat or MEF cells.**
(a) For synchronized infection cells were inoculated with SINV at an MOI 2.5 and supernatants were harvested at 4 and 10 hpi. After viral RNA isolation (triplicates) the concentration was measured by SINV specific real-time RT-PCR assay. SINV and CHIKV PCR units (U) per mL were determined. The dilution end-point was defined as one PCR unit. Virus replication could be detected in both cell lines. The increase of genome equivalents per mL were approximately 100 to 1,000-fold at 10 hpi. (b) Titration of supernatants showed an increase of PFU per mL (titer of inoculum was subtracted) after 10 hpi of 1,000 to 10,000-fold. (c) The ratio of log-10 increase PFU/mL to SINV or CHIKV PCR units were similar in both cell lines indicating an efficient particle formation.

3.5.3 IFN induction after infection with SINV and CHIKV

After verifying viral growth, the IFN induction upon SINV or CHIKV infection was determined. IFN mRNA levels were measured by cell-specific IFN real-time RT-PCR assays and compared to the levels of TBP levels. In EidNi/41.3 cells the observed IFN induction after SINV infection increased over time, while the IFN induction after CHIKV infection was already induced to the same extent as after 4 hpi. This indicated a fast IFN response of the cells to virus infection (Figure 3.17a). In MEF cells IFN induction was similar to the SINV infection in EidNi/41.3 cells with highest IFN mRNA transcription levels at 10 hpi (Figure 3.17a). However the increase in IFN mRNA transcription was approximately 10,000-fold after CHIKV infection and only 1,000-fold after SINV infection.

In Figure 3.17b the comparison of secreted IFN to the levels of induced IFN mRNA is shown. The values for cells treated with RVFV 13 or poly IC indicated protein synthesis (Figure 3.17b). After SINV and CHIKV infection both cell lines clearly showed reduction of secreted IFN protein. For EidNi/41.3 cells a strong effect on mRNA levels was also observed (Figure 3.17b). This effect was less intense in MEF cells, which was similar to mRNA levels after infection with ONNV (Figure 3.11d). In conclusion, the IFN protein reduction was SINV- and CHIKV-specific.

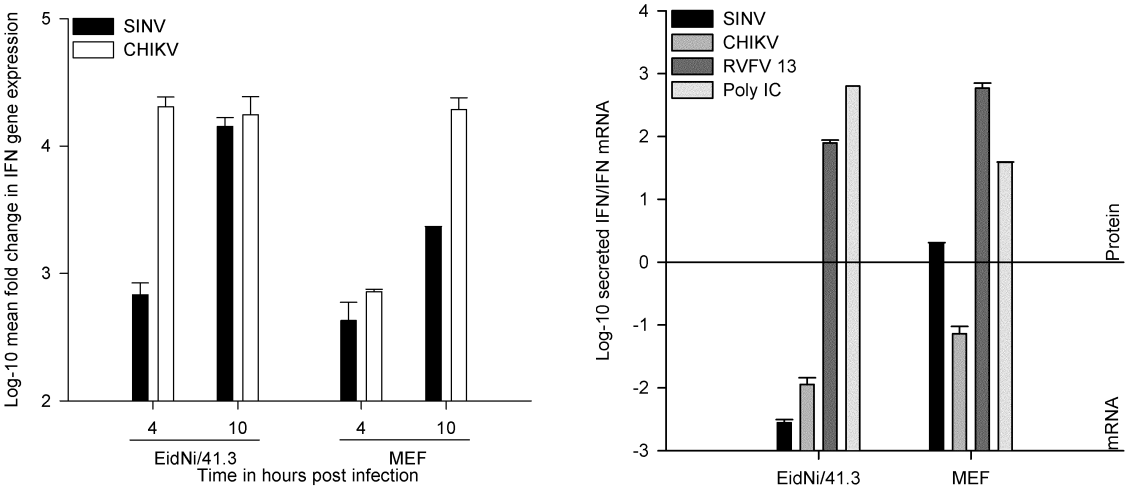

Figure 3.17: **IFN induction after SINV and CHIKV infection.**
(a) Mean fold change in IFN-β gene expression in EidNi/41.3 and MEF cells after 4 and 10 hpi with SINV and CHIKV. Both viruses lead to an increase of IFN-β after 10 hpi. Interestingly in EidNi/41.3 cells saturating expression amounts of IFN-β mRNA level are already reached after 4 hpi with CHIKV.(b) Comparison of secreted IFN protein to IFN-β mRNA 10 hpi with SINV and CHIKV, RVFV 13 infection and poly IC transfection. SINV and CHIKV replication could be related to IFN protein reduction.

3.5.4 ISG induction after SINV and CHIKV infection

Since ONNV did not induce a general transcriptional block proven by an increase in MxA mRNA levels (Figure 3.12), it was tested if this was also true after SINV and CHIKV could be confirmed. Therefore MxA and ISG56 expression levels were measured with specific real-time RT-PCR assays and compared to secreted IFN levels. The direct comparison demonstrated that in EidNi/41.3 cells the transcription of MxA was almost 100-fold higher compared to the same ratio for ISG56 (Figure 3.18a).

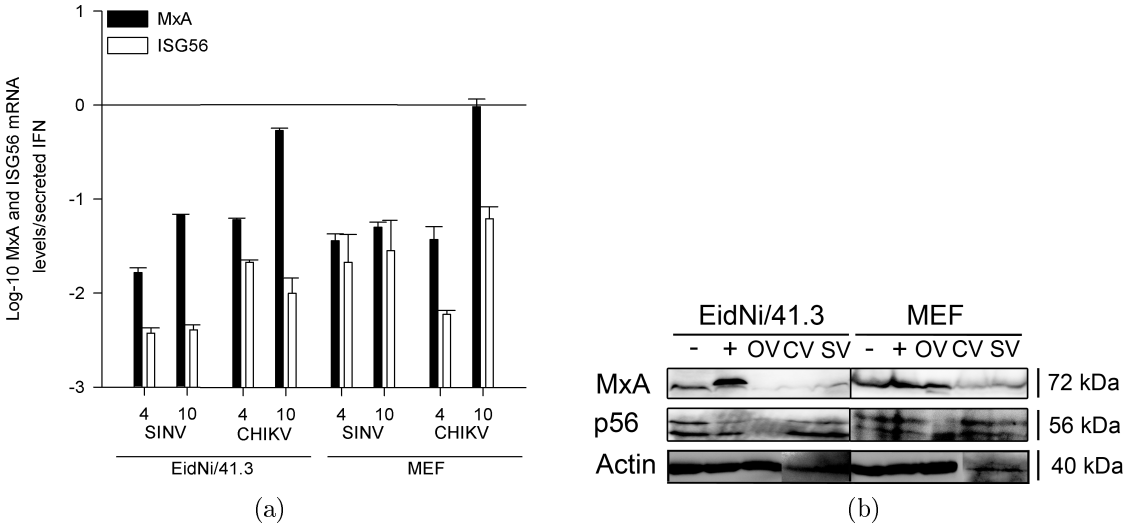

Figure 3.18: **ISG induction after SINV infection.**
(a) Comparison of mRNA fold-induction of IFN stimulated genes (MxA and ISG56) to secreted IFN protein at time points 4 and 10 hpi. Expression of MxA was stronger affected by IFN protein down regulation in both cell lines after infection with SINV. The effects on ISG56 expression were similar in both cell lines after SINV and CHIKV infection. (b) Cells were either left untreated (-) or infected with RVFV 13 (+), ONNV (OV), CHIKV (CV) or SINV (SV). After 10 h proteins were extracted from cells infected with SINV and CHIKV and at 24 hpi from cells infected with ONNV and RVFV and untreated. Equal amount of proteins were subjected to SDS-PAGE followed by a Western blot analysis. Mouse-anti-MxA, mouse-anti-ISG56 and mouse-anti-actin IgG antibodies were applied at dilutions 1:1000 followed by a peroxidase labelled goat-anti-mouse secondary antibody (1:20000). In all cell lines infection with ONNV did not induce the expression of MxA and p56 and was less or similar to untreated cells. After the infection with CHIKV or SINV MxA protein was only in reduced amounts detectable, while p56 abundance was similar to untreated cells.

In MEF cells the difference between MxA and ISG56 was only depicted after CHIKV infection. The results were similar to the ones after ONNV infection and confirmed that there was no general block of transcription and a highly efficient IFN signalling-dependent induction of the ISGs in the bat cell line EidNi/41.3.

To analyse if a translational shut off could explain reduced protein levels Western blot analysis was performed. It was shown that ONNV infection resulted in decreased expression levels of MxA and p56 (Figure 3.18b). This effect was also observed after SINV and CHIKV infection. In general the effect was more pronounced for MxA than for p56. Interestingly, in MEF cells the reduction of MxA protein expression after ONNV infection was not detected, but was clearly visible upon infection with SINV and CHIKV (Figure 3.18b). Overall the production of this antiviral protein was antagonized in EidNi/41.3 cells to a greater extent than in MEF cells.

4 Discussion

4.1 Bat cell culture characterization

With only two bat cell lines commercially available [68, 67], this study presents three new cell culture systems comprising different bat species. One major concern when using cell cultures from wild animals like bats are pathogenic contaminants. The severe impacts of contaminated cell cultures were shown in 1967 when wild captured monkeys were brought to Europe to generate cell cultures in diverse laboratories for vaccine research [181]. In Marburg, Frankfurt and Belgrade laboratory workers with direct contact with blood, organs, and cell cultures from *Cercopithecus aethiops* showed severe and fatal haemorrhagic fever [182, 172]. The cause of the disease was identified as the Marburg virus, which is a genus of the family *Filoviridae [181].* Since the bat cell lines were gained from captured wild bats, they were tested for lyssaviruses, filoviruses, mycoplasma and SV5 by RT-PCR and found to be negative for all. As contaminations might be introduced during passaging, mycoplasma and SV5 contaminations were frequently tested. In particular SV5 is an overlooked problem. The V protein of the virus targets STAT-1 and inducing its degradation, which blocks the IFN-signalling pathway [38, 82, 203]. In addition, the protein blocks the MDA5-mediated activation of the IFN-promoter and therefore inhibits IFN-induction [28, 27, 148]. Mycoplasmic contaminations have severe influences on several cell culture properties by leading to changes in cell metabolism, performance and viral activity [156, 117, 40]. The adverse effects on IFN production and activity show the great impact of mycoplasmas in virus-host interaction assays [40]. As the investigation of the IFN response was a major part of this study, these contaminations had to be ruled out.

All cells in the presented study were immortalised by lentiviral transduction of the large T antigen of SV40 [5]. The expression of the SV40 Large T-antigen inhibits the pRB- and p53-dependent responses in cellular pathways [5]. This effect results in the cells escaping apoptosis and permanent re-entering of the S-phase of the cell cycle [5]. The random integration of the large T-antigen can affect important genes and can lead to dysfunctions in cellular signalling cascades.

As the focus in this study was the IFN response upon virus infection, the integrity of IFN response signalling pathways had to be ensured. Cell lines EidNi/41.3 and EpoNi/22.1 were tested for their reactivity to IFN stimuli like poly IC and RVFV 13. The cells showed the same or higher sensitivity to commonly used stimulators of IFN gene expression compared to MEF and MA104 cell lines indicating that the IFN induction pathway within the cells was not affected by immortalisation. In addition, subclones and mixed cultures were included in some experiments to confirm the results and exclude subclone-specificity. The newly generated EidNi and EpoNi as well as additional RoNi bat cell lines are well-characterized and highly IFN competent by showing high IFN mRNA induction, efficient IFN protein secretion and highly efficient ISG induction.

4.2 Cell line specific VSV-bioassays to allow comparison of effective IFN response between different cell lines

For investigations into the IFN response, particularly the comparison of secreted IFN is challenging, since the commonly used methods are limited to certain species or different IFN specificities [125]. IFN bioassays which rely on the induction of an antiviral state by upregulated ISG, are restricted by the compatibility between the IFN of interest and the IFN receptors of the used cells [204, 25]. Also commercially available ELISA assays show similar restrictions to particular types of IFN or host species.

In this study a species-specific VSV-bioassay based on the determination of IFN concentration with the help of pan-species IFN, enabled the direct comparison of bioactive secreted IFN after challenging with the same pathogen. Each cell line has a defined EC_{50} value, which facilitates the exact determination of total IFN concentrations and enables direct comparison between species. The sensitivity to the pan-species IFN is not related to the origin of the cells and VSV enables a fast adaptation of the newly developed VSV-bioassay to cell lines of interest. Other methods for IFN detection such as ELISAs [115] or MxR-systems [120] are either limited in the IFN type and the host species or restricted to a specific host organism, which detects only species-specific IFN. These limitations to IFN types or cell lines can be prevented with the established assay, since the secreted IFN is recognized by the cell-specific IFN receptors. Additionally, the EC_{50} factor values, determined by

the help of a pan-specific IFN, enabled the correlation and direct comparison of the measured IFN values by excluding host-specific variations.

To enable the comparison of the IFN response to virus infections between bat, rodent and human cell lines promoted the development of an assay which is species-independent. In parallel with the group of F. Weber in Freiburg, the advantage of pan-species IFN was used to develop a bioassay with the ability to measure secreted IFN independently of the cell line origin [105]. Using a *Renilla* luciferase-expressing RVFV (RVFV-Ren) the group developed a bioassay with short incubation times and a high sensitivity up to 1 U/mL IFN [105]. They could show that the RVFV-Ren is species-independent which allows interspecies comparison [105]. Unfortunately, the RVFV-Ren is patented (personal communication with F. Weber), which limits its availability [105]. Furthermore, the read-out depends on the *Renilla* luciferase assay system provided by Promega®, which is expensive [105].

The modification of the VSV-bioassay with pan-species IFN optimized the assay as a tool to be able to measure species-independent secreted IFN concentrations. The establishment of the VSV-bioassay for additional cell lines of interest, like newly identified reservoirs of human pathogenic viruses or possible zoonotic viruses identified in, for example bats, is fast and uncomplicated. The advantages of using a modified version of the well established VSV-bioassay makes the assay available to any BSL 2 laboratory. The read-out is based on plaque formation and counting, which is independent of any company or measuring system and is therefore more cost-effective. With the EC_{50} value interspecies comparison of secreted IFN after challenging the same virus is possible and allows to draw conclusions about the specific IFN response.

Furthermore IFN response antagonists of viruses of interest can be studied, since increasing mRNA levels are not necessarily in accordance with bioactive secreted IFN [225].

4.3 Serology

Bats have been shown to carry a large diversity of highly pathogenic agents [78]. It is therefore important to obtain an estimate on the distribution of pathogens within bat colonies in particular in those that are living in proximity to humans. In this study a serological approach was chosen to get a broader view on the prevalence of alphaviruses in bats. The serological study included 16 different bat species. In total 5% of the bat serum samples showed cross-reactivities to either VEEV or CHIKV

antigens. Despite the fact that most studies are based on nucleic acid detection methods [42], we chose a serological approach. The main reason for this choice was that nucleic acid based methods have a major disadvantage by depending on the right sampling time point and on certain virus concentrations in the analysed specimens[45]. Viraemic phases can be very short and many pathogens might be overlooked due to low viral loads. Here the serological survey shows an advantage by detecting virus-specific antibodies, which can, in many cases, be detected a life time.

Compared to paramyxoviruses and CoV cross-reactivity to alphaviruses was low [42, 201]. For paramyxoviruses a prevalence of 40% (approximately 10,000 individuals) was determined, showing that the virus diversity in bats is larger than expected [43, 44, 219] and tempting bats to be the animal reservoir for mammalian paramyxoviruses [42]. For CoV a cross-reactivity of 10% was detected in bat serum samples from Africa [134], following investigations revealed that bats in Africa carry SARS-related agents [145]. Since SARS-CoV originated from the Chinese horseshoe bats, the findings of CoV prevalence in Africa underlined the reservoir function of the animals for this virus family [108]. These two examples show that the prevalence of a virus in the reservoir animal is high, which indicates that bats are most likely accidental hosts for alphaviruses but might play a role in the natural transmission cycle.

As early as 1973 Seymour *et al.* proposed that neotropical bats could serve as alternate hosts in the enzootic cycle maintaining VEEV transmission [168]. But the role of bats in the transmission cycle and ecology of this virus has not yet been described [168]. The bat species *A. jamaicensis* showed the highest prevalence among the neotropical bats with an average of 5% which complements the results of Ubico *et al.* from 1995 [202]. Interestingly, VEEV and CHIKV, which are defined to be distributed on separate continents [99], showed identical prevalences in almost all tested bat species. Reactivity of Old World bats with a New World alphavirus antigen could be explained by a cross-reactivity of sera with both antigens as observed for other alphaviruses by Vollmar *et al.* [211]. But since several sera reacted only with one antigen this can be ruled out as a general explanation. In fact, one reason could be that the actual diversity of alphaviruses might be much higher in bats as e.g. observed for paramyxoviruses and CoV. With an abundance of 20% for both viruses in the bat *M. torquata*, this bat species showed the highest prevalence within the Old World bat species. In comparison the species *R. aegyptiacus* showed an abundance of 1% for VEEV and 2% for CHIKV. Both species belong to the frugivorous bats but are differently distributed and have different roosting behaviours

[133, 14].

The geographical distribution and various habitats of bats could be a reason for the observed differences in alphavirus abundance between the different bat species. Phylogenetic analyses of Ebola virus identified in bats corresponded to the human epidemic strain (Zaire Ebola virus) and allowed the conclusion that the virus outbreaks can be linked to the geographic distribution and roosting behaviour of the reservoir bat species [151]. Since alphaviruses are transmitted by several mosquito genera like *Aedes* or *Culex* and others [99], the distribution of these viruses is probably primarily linked to the prevalence of these vectors. Mosquito prevalence has shown to be sensitive to ecological changes which influences the viral variety for the different regions [91]. With *M. torquata* being highly adaptive to new environments and merging to plantation regions [133], it is suggested that this species has a higher exposure to mosquitoes serving as alphavirus vectors instead of *R. aegyptiacus* roosting in caves [14].

It is tempting to speculate that the prevalences of alphavirus cross-reactivities in both bat species can probably be linked to the different habitats and roosting behaviours of the animals. The present study shows the relevance of serological studies to support nucleic acid detection assays or virus isolation by directing the focus of the research to positive samples. Since the relevance of bats in virus ecology has become a new focus in virology, working together with bat ecologists could complete interpretations and analyses of serological studies. This may also assist in explaining the causal connection between virus prevalence and geographical distribution of the animals.

4.4 Comparable mechanisms of IFN response between bat, murine and human model cell lines

The high diversity and quantity of pathogens detected in bats [24] indicates that these flying mammals and the missing overt clinical symptoms upon infection may have developed strategies to minimize viral pathogenesis. The IFN response, which is known to be the first barrier within the mammalian cells, could be one possibility for bats to escape the infection. Only a few aspects of bat IFN response are known, such as identified homologous genes of human IFN response pathway [55, 124, 164, 26].

In this study the IFN response of newly introduced immortalized bat cell lines was

compared to a murine cell line, MEF, and a human cell line, MA104. The cell lines showed the same IFN response to ONNV, SINV and CHIKV infections which was detected with species-specific methods on mRNA-detection and on bioactive protein analysis. After virus-induced IFN induction, the IFN protein synthesis was blocked. Partially synthesized IFN was able to induce MxA and ISG56 mRNA expression but the translational block diminished measurable protein levels. Although the ratios might differ to some extent between the various viruses, taken together the data suggest a translational rather than a transcriptional shutoff. Similar effects were shown for CHIKV in human fibroblasts by White *et al.* [215]. It could be proven that the innate immune activation was dependent on the adaptor molecule IFN promoter stimulator 1 (IPS-1) and that CHIKV induced a translational shutoff [215]. In this study newly generated bat cell lines were shown to be sensitive to IFN-induction and able to secrete bioactive IFN. IFN-signalling was demonstrated with species-specific RT-PCRs for the ISGs MxA and ISG56, which indicated similar mechanisms to well-characterized mammals.

Current research focuses largely on the various mechanisms employed by the host to control an invading virus. The fact that mammals like bats serve as reservoirs for viruses, indicates that virus-host interaction on the type I IFN response level might be crucial for the course of infection.

Therefore the IFN response of bats was analysed in detail upon virus infection in this study. The different IFN inducers like poly IC, attenuated virus RVFV 13 or wild type viruses like ONNV, SINV and CHIKV were considered for every cell culture background. While in EidNi/41.3, MEF and MA104 cell lines the sensitivity to poly IC and RVFV 13 were of similar extent, the EpoNi/22.1 cell line showed a higher sensitivity to RVFV 13 (Figure 3.7a). Not only the total amount of IFN was measured, but also the ratios of secreted IFN and mRNA levels. Both commonly used IFN inducers showed high relative levels of secreted IFN that were comparable for all cells (Figure 3.7b). However, in cells infected with ONNV, SINV or CHIKV, the levels of relative secreted IFN-β were clearly reduced. This can be explained by a induction of PKR-independent translational shutoff [215].

The IFN response in bat cells was similar or more sensitive compared to the IFN response in reference cell lines. The higher sensitivity to IFN in the signalling cascade suggests that smaller amounts of IFN might be enough to induce the antiviral state in bat cells. Earlier findings confess the IFN-β mRNA expression upon poly IC transfection for *P. alecto* and other bat species [225, 187], additionally IFN-λ expression was predicted to play a major role in bat IFN response [225]. After virus infection the type I IFN expression was suggested to be immediately blocked by

virus antagonists [224]. The type III IFN expression could compensate for the loss of the IFN-mediated antiviral activity, thereby making the antiviral strategy of bats less susceptible to suppression by viral immune evasion mechanisms. However, bioactive IFN was not analysed in those studies [224]. As shown in the present study the differences between type I IFN mRNA and effectively secreted IFN-β can vary to a very high degree. To draw conclusions about the IFN response of cell lines it is necessary to measure bioactive IFN. Interestingly, an IFN-independent virus control has been predicted by Virtue *et al.* [208] indicating great possibilities for alternative virus control. White *et al.* results underlined alternative virus control by showing a PKR-independent block of cellular protein synthesis.

The present study emphasises that the release of bioactive IFN must be considered in the interpretation of results to assess whether the cells are able to counteract the virus infection. All steps of the antiviral response have to be analysed to draw conclusions on which level viruses might intervene with the host IFN response. The results are important indications to understand the bat IFN response and but need to be further analysed in future studies, with focus on for example other ISGs or IFN antagonists.

Conclusion

Taken together the newly generated bat cell lines were IFN sensitive and therefore ideal tools for in-depth studies on the IFN response system upon viral infections. The optimized VSV-bioassay enabled together with the species-specific qRT-PCRs an detailed analysis of IFN -induction, -signalling and -secretion with considerations of viral antagonism strategies. With the help of a serological survey on alphavirus prevalence in bats it could be shown that bats are most likely not the reservoir of alphaviruses but may serve as hosts in the enzootic cycle. The induction of sero conversion and thus the ability to infect bats led to further investigations upon IFN response after alphavirus infection. Here it was shown that bat cell lines react in the same or even more sensitive way as the reference cell lines indicating a strong IFN mRNA expression, followed by inhibited protein secretion postulating a translational rather than a transcriptional shutoff.

5 Summary

Bats have been identified as reservoir for human pathogenic zoonotic viruses like Rabies, Marburg or Henipaviruses. The fact that bats carry viruses without showing clinical symptoms, raised the question if these flying mammals have evolved specific mechanisms to suppress virus replication. To address this question a bat cell culture model was established to investigate the IFN response upon virus infection.

First, cell lines of *E. helvum*, *Epo. buettikoferi* and *R. aegyptiacus* were generated, immortalised and characterized. IFN sensitivity upon viral and artificial IFN-stimuli was analysed by pan-bat IFN real-time RT-PCR assay. To enable comparative analysis of species-specificity and inter-species bioactive IFN secretion the VSV-bioassay was optimized. It was adapted to each cell line and the pan-species IFN enabled with the EC_{50} factor the determination of relative secreted bioactive IFN concentration.

To determine IFN-signalling, the mRNA expression levels of several IFN stimulated genes (ISGs) were determined with established species-specific real-time RT-PCR assays. These methods enabled comparable studies between bat, murine and human cell lines. The role of bats within the life cycle of arthropod borne alphaviruses is not clear. The prevalence of cross-reactive antibodies was determined by an Immunofluoresence assay, analysing bat sera from several continents and species. In average 5% of the serological samples were found positive which is a comparably low seroprevalence. Interestingly, some Old World bat samples showed exclusive reactivity with New World alphaviruses and vice versa. This cross-reactivity might indicate that the phylogenetic range of alphaviruses in bats could be much higher. In an alphavirus infection model with O´nyong-nyong virus (ONNV) high IFN-induction on mRNA level was detected in all cell lines. Conversely, IFN secretion was reduced. Although IFN-signalling seemed to be more sensitive on mRNA expression level in bat cell lines, this could not be confirmed on protein levels. These results indicated a translational rather than a transcriptional shutoff upon alphavirus infection in bat cell lines. To investigate if these results were ONNV-specific, two additional alphaviruses, Sindbis and Chikungunya virus (SINV and CHIKV), were tested. These infection experiments showed similar results suggesting a general mechanism of al-

phaviruses to antagonize the IFN response. Interestingly, bat cell lines showed similar IFN response as human cell lines. Generated bat cell lines, designed pan-bat or species-specific real-time RT-PCR assays and the optimized VSV-bioassay altogether enable a detailed analysis of the IFN response to virus infections in bat cell lines, which was especially on the bioactive IFN protein level in this comparable way not possible before.

Zusammenfassung

Fledermäuse wurden als Wirte von zoonotischen, humanpathogenen Viren, wie Tollwut, Marburg- oder Henipaviren, identifiziert. Als Träger von pathogenen Viren zeigen die Fledermäuse keine klinischen Symptome einer Erkrankung. Daher wurde spekuliert, ob sie im Laufe der Evolution spezielle Mechanismen zur Unterdrückung der Virusreplikation entwickelt haben. Zur Verifizierung dieser Frage, wurde die IFN-Antwort, bestehend aus IFN-Induktion, -Sezernierung und -Signalwirkung, auf Virusinfektionen in Fledermauszellen im Vergleich zu murinen und humanen Zellkulturmodellen untersucht.

Zunächst wurden Zellkulturen von *E. helvum*, *Epo. buettikoferi* und *R. aegyptiacus* generiert, immortalisiert und charakterisiert. Mit Hilfe eines pan-spezies IFN Real-Time RT-PCR Assays konnte gezeigt werden, dass die generierten Fledermauszelllinien in der Lage sind, sowohl auf virale als auch auf artifizielle IFN-Stimuli zu reagieren. Die Optimierung des VSV-Bioassays ermöglicht die Detektion von sezerniertem IFN unter Berücksichtigung der Spezienspezifität und Interspezifität. Dazu wurde das Assay individuell an jede Zelllinie angepasst und mit Hilfe des EC_{50}-Faktors die Vergleichbarkeit der Konzentration des sezernierten IFNs ermöglicht.

Zur Bestimmung der IFN-Signalwirkung wurden verschiedene ISG mRNA- Expressionen mittels Spezies-spezifischen Real-Time RT-PCR Assays bestimmt. Durch die Entwicklung der entsprechenden Assays war es möglich, vergleichende Experimente durchzuführen. Ob Fledermäuse ebenfalls als Wirte für Alphaviren in Frage kommen, wurde bisher nur vermutet. Mit Hilfe einer serologischen Studie wurde daher die Prävalenz von kreuzreagierenden Antikörpern gegen Alphaviren in Fledermäusen verschiedenster Kontinente bestimmt. Es wurde eine Prävalenz von durchschnittlich 5% festgestellt. Dies ist eine vergleichsweise niedrige Seroprävalenz. Einige Altweltfledermausproben waren interessanterweise nur für Neuweltalphaviren positiv und umgekehrt. Dies lässt vermuten, dass die phylogenetische Spanne innerhalb der Alphaviren in Fledermäusen größer ist, als bis jetzt angenommen.

In einem Alphavirusinfektionsmodell konnte gezeigt werden, dass die Infektion mit ONNV in allen Zellen eine hohe IFN-Induktion zur Folge hatte. Kontrovers hierzu

konnte eine Reduktion der IFN-Sezernierung gemessen werden. Obwohl die IFN-Signalwirkung bei Fledermäusen auf mRNA-Ebene sensibler zu sein schien, konnte dies auf Proteinebene nicht bestätigt werden. Daher kann auch bei Fledermäusen auf einen Translationsabbruch nach Alphavirusinfektion geschlossen werden. Zur Klärung, ob die Ergebnisse ONNV-spezifisch waren, wurden die gleichen Versuche noch mit zwei weiteren Alphaviren (SINV und CHIKV) durchgeführt. Die Ergebnisse hieraus bestätigen, dass Fledermauszellen eine der humanen ähnliche IFN-Antwort besitzen und die beobachteten Mechanismen wahrscheinlich allgemeingültig für Alphaviren sind.

Künftig kann also die IFN-Antwort auf Virusinfektionen zwischen Fledermaus- und humanen Zelllinien vergleichend auf allen Ebenen untersucht werden. Die generierten Zelllinien, die entwickelten Spezies-spezifischen Real-Time RT-PCR Assays und das optimierte VSV-Bioassay ermöglichen im Zusammenspiel detaillierte Erkenntnisse über die IFN-Antwort der Fledermauszellen auf Virusinfektionen, die im Besonderen auf der bioaktiven Proteinebene noch nahezu unerforscht ist.

Bibliography

[1] Andrea Ablasser, Franz Bauernfeind, Gunther Hartmann, Eicke Latz, Katherine A. Fitzgerald, and Veit Hornung. Rig-i-dependent sensing of poly(da:dt) through the induction of an rna polymerase iii-transcribed rna intermediate. *Nat Immunol*, 10(10):1065–1072, Oct 2009.

[2] P.N. Acha and B. Szyfres (Eds.). *Zoonoses and Communicable Diseases Common to Man and Animals*. Pan American Health Organization; Washington, D.C., 1989.

[3] N. H. Acheson and I. Tamm. Replication of semliki forest virus: an electron microscopic study. *Virology*, 32(1):128–143, May 1967.

[4] T. Ahola and L. Kääriäinen. Reaction in alphavirus mrna capping: formation of a covalent complex of nonstructural protein nsp1 with 7-methyl-gmp. *Proc Natl Acad Sci U S A*, 92(2):507–511, Jan 1995.

[5] Deepika Ahuja, M Teresa Sáenz-Robles, and James M. Pipas. Sv40 large t antigen targets multiple cellular pathways to elicit cellular transformation. *Oncogene*, 24(52):7729–7745, Nov 2005.

[6] Shizuo Akira, Satoshi Uematsu, and Osamu Takeuchi. Pathogen recognition and innate immunity. *Cell*, 124(4):783–801, Feb 2006.

[7] G. Aliperti and M. J. Schlesinger. Evidence for an autoprotease activity of sindbis virus capsid protein. *Virology*, 90(2):366–369, Oct 1978.

[8] Altringham. *Bats-biology and behaviour*. New York: Oxford University Press, 1996.

[9] Svetlana Atasheva, Alexander Fish, Maarten Fornerod, and Elena I. Frolova. Venezuelan equine encephalitis virus capsid protein forms a tetrameric complex with crm1 and importin alpha/beta that obstructs nuclear pore complex function. *J Virol*, 84(9):4158–4171, May 2010.

[10] Svetlana Atasheva, Natalia Garmashova, Ilya Frolov, and Elena Frolova. Venezuelan equine encephalitis virus capsid protein inhibits nuclear import in mammalian but not in mosquito cells. *J Virol*, 82(8):4028–4041, Apr 2008.

[11] Svetlana Atasheva, Valentina Krendelchtchikova, Anton Liopo, Elena Frolova, and Ilya Frolov. Interplay of acute and persistent infections caused by venezuelan equine encephalitis virus encoding mutated capsid protein. *J Virol*, 84(19):10004–10015, Oct 2010.

[12] S. K. Bandyopadhyay, GT Leonard, Jr, T. Bandyopadhyay, G. R. Stark, and G. C. Sen. Transcriptional induction by double-stranded rna is mediated by interferon-stimulated response elements without activation of interferon-stimulated gene factor 3. *J Biol Chem*, 270(33):19624–19629, Aug 1995.

[13] Brett F. Beitzel, Russell R. Bakken, Jeffrey M. Smith, and Connie S. Schmaljohn. High-resolution functional mapping of the venezuelan equine encephalitis virus genome by insertional mutagenesis and massively parallel sequencing. *PLoS Pathog*, 6(10):e1001146, 2010.

[14] Aulagnier S. Hutson A.M. Amr Z.S. Kock D. Sharifi M. Karata? A. Mickleburgh S. Bergmans W. & Howell K Benda, P. Rousettus aegyptiacus. In: IUCN 2011. IUCN Red List of Threatened Species, Downloaded on 09 June 2012. 2008. Version 2011.

[15] Marianne Berger Rentsch and Gert Zimmer. A vesicular stomatitis virus replicon-based bioassay for the rapid and sensitive determination of multi-species type i interferon. *PLoS One*, 6(10):e25858, 2011.

[16] Juan J. Berlanga, Iván Ventoso, Heather P. Harding, Jing Deng, David Ron, Nahum Sonenberg, Luis Carrasco, and César de Haro. Antiviral effect of the mammalian translation initiation factor 2alpha kinase gcn2 against rna viruses. *EMBO J*, 25(8):1730–1740, Apr 2006.

[17] Paul D. Bieniasz. Intrinsic immunity: a front-line defense against viral attack. *Nat Immunol*, 5(11):1109–1115, Nov 2004.

[18] Agnès Billecocq, Martin Spiegel, Pierre Vialat, Alain Kohl, Friedemann Weber, Michèle Bouloy, and Otto Haller. Nss protein of rift valley fever virus blocks interferon production by inhibiting host gene transcription. *J Virol*, 78(18):9798–9806, Sep 2004.

[19] N. K. Blackburn, C. M. Foggin, L. Searle, and P. N. Smith. Isolation of sindbis virus from bat organs. *Cent Afr J Med*, 28(8):201, Aug 1982.

[20] A. R. Bluyssen, J. E. Durbin, and D. E. Levy. Isgf3 gamma p48, a specificity switch for interferon activated transcription factors. *Cytokine Growth Factor Rev*, 7(1):11–17, Jun 1996.

[21] W. M. Boggs, C. S. Hahn, E. G. Strauss, J. H. Strauss, and D. E. Griffin. Low ph-dependent sindbis virus-induced fusion of bhk cells: differences between strains correlate with amino acid changes in the e1 glycoprotein. *Virology*, 169(2):485–488, Apr 1989.

[22] D. F. Bowers, B. A. Abell, and D. T. Brown. Replication and tissue tropism of the alphavirus sindbis in the mosquito aedes albopictus. *Virology*, 212(1):1–12, Sep 1995.

[23] Lucy Breakwell, Pia Dosenovic, Gunilla B. Karlsson Hedestam, Mauro D'Amato, Peter Liljeström, John Fazakerley, and Gerald M. McInerney. Semliki forest virus nonstructural protein 2 is involved in suppression of the type i interferon response. *J Virol*, 81(16):8677–8684, Aug 2007.

[24] Charles H. Calisher, James E. Childs, Hume E. Field, Kathryn V. Holmes, and Tony Schountz. Bats: important reservoir hosts of emerging viruses. *Clin Microbiol Rev*, 19(3):531–545, Jul 2006.

[25] U. Canosi, M. Mascia, L. Gazza, O. Serlupi-Crescenzi, S. Donini, F. Antonetti, and G. Galli. A highly precise reporter gene bioassay for type i interferon. *J Immunol Methods*, 199(1):69–76, Nov 1996.

[26] A. K. Chakravarty and S. K. Sarkar. Immunofluorescence analysis of immunoglobulin bearing lymphocytes in the indian fruit bat: Pteropus giganteus. *Lymphology*, 27(2):97–104, Jun 1994.

[27] K. S. Childs, J. Andrejeva, R. E. Randall, and S. Goodbourn. Mechanism of mda-5 inhibition by paramyxovirus v proteins. *J Virol*, 83(3):1465–1473, Feb 2009.

[28] Kay Childs, Nicola Stock, Craig Ross, Jelena Andrejeva, Louise Hilton, Michael Skinner, Richard Randall, and Stephen Goodbourn. mda-5, but not rig-i, is a common target for paramyxovirus v proteins. *Virology*, 359(1):190–200, Mar 2007.

[29] David A. Coil and A Dusty Miller. Phosphatidylserine is not the cell surface receptor for vesicular stomatitis virus. *J Virol*, 78(20):10920–10926, Oct 2004.

[30] P. S. CORBET, M. C. WILLIAMS, and J. D. GILLETT. O'nyong-nyong fever: an epidemic virus disease in east africa. iv. vector studies at epidemic sites. *Trans R Soc Trop Med Hyg*, 55:463–480, Sep 1961.

[31] P. Correa-Giron, C. H. Calisher, and G. M. Baer. Epidemic strain of venezuelan equine encephalomyelitis virus from a vampire bat captured in oaxaca, mexico, 1970. *Science*, 175(4021):546–547, Feb 1972.

[32] Gary Crameri, Shawn Todd, Samantha Grimley, Jennifer A. McEachern, Glenn A. Marsh, Craig Smith, Mary Tachedjian, Carol De Jong, Elena R. Virtue, Meng Yu, Dieter Bulach, Jun-Ping Liu, Wojtek P. Michalski, Deborah Middleton, Hume E. Field, and Lin-Fa Wang. Establishment, immortalisation and characterisation of pteropid bat cell lines. *PLoS One*, 4(12):e8266, 2009.

[33] I. Dé, S. G. Sawicki, and D. L. Sawicki. Sindbis virus rna-negative mutants that fail to convert from minus-strand to plus-strand synthesis: role of the nsp2 protein. *J Virol*, 70(5):2706–2719, May 1996.

[34] JE Darnell, Jr. Stats and gene regulation. *Science*, 277(5332):1630–1635, Sep 1997.

[35] JE Darnell, Jr, I. M. Kerr, and G. R. Stark. Jak-stat pathways and transcriptional activation in response to ifns and other extracellular signaling proteins. *Science*, 264(5164):1415–1421, Jun 1994.

[36] R. J. de Groot, W. R. Hardy, Y. Shirako, and J. H. Strauss. Cleavage-site preferences of sindbis virus polyproteins containing the non-structural proteinase. evidence for temporal regulation of polyprotein processing in vivo. *EMBO J*, 9(8):2631–2638, Aug 1990.

[37] M. Diallo, J. Thonnon, M. Traore-Lamizana, and D. Fontenille. Vectors of chikungunya virus in senegal: current data and transmission cycles. *Am J Trop Med Hyg*, 60(2):281–286, Feb 1999.

[38] L. Didcock, D. F. Young, S. Goodbourn, and R. E. Randall. The v protein of simian virus 5 inhibits interferon signalling by targeting stat1 for proteasome-mediated degradation. *J Virol*, 73(12):9928–9933, Dec 1999.

[39] DeeAnn M. Reeder Don E. Wilson. *Mammal Species of the World a taxonomic and geographic reference*. Johns Hopkins University Press, 2005.

[40] Hans G. Drexler and Cord C. Uphoff. Mycoplasma contamination of cell cultures: Incidence, sources, effects, detection, elimination, prevention. *Cytotechnology*, 39(2):75–90, Jul 2002.

[41] Jan Felix Drexler, Victor Max Corman, Florian Gloza-Rausch, Antje Seebens, Augustina Annan, Anne Ipsen, Thomas Kruppa, Marcel A. Müller, Elisabeth K V. Kalko, Yaw Adu-Sarkodie, Samuel Oppong, and Christian Drosten. Henipavirus rna in african bats. *PLoS One*, 4(7):e6367, 2009.

[42] Jan Felix Drexler, Victor Max Corman, Marcel Alexander Müller, Gael Darren Maganga, Peter Vallo, Tabea Binger, Florian Gloza-Rausch, Andrea Rasche, Stoian Yordanov, Antje Seebens, Samuel Oppong, Yaw Adu Sarkodie, Célestin Pongombo, Alexander N. Lukashev, Jonas Schmidt-Chanasit, Andreas Stöcker, Aroldo José Borges Carneiro, Stephanie Erbar, Andrea Maisner, Florian Fronhoffs, Reinhard Buettner, Elisabeth K V. Kalko, Thomas Kruppa, Carlos Roberto Franke, René Kallies, Emmanuel R N. Yandoko, Georg Herrler, Chantal Reusken, Alexandre Hassanin, Detlev H. Krüger, Sonja Matthee, Rainer G. Ulrich, Eric M. Leroy, and Christian Drosten. Bats host major mammalian paramyxoviruses. *Nat Commun*, 3:796, 2012.

[43] Jan Felix Drexler, Victor Max Corman, Tom Wegner, Adriana Fumie Tateno, Rodrigo Melim Zerbinati, Florian Gloza-Rausch, Antje Seebens, Marcel A. Müller, and Christian Drosten. Amplification of emerging viruses in a bat colony. *Emerg Infect Dis*, 17(3):449–456, Mar 2011.

[44] Jan Felix Drexler, Florian Gloza-Rausch, Jörg Glende, Victor Max Corman, Doreen Muth, Matthias Goettsche, Antje Seebens, Matthias Niedrig, Susanne Pfefferle, Stoian Yordanov, Lyubomir Zhelyazkov, Uwe Hermanns, Peter Vallo, Alexander Lukashev, Marcel Alexander Müller, Hongkui Deng, Georg Herrler, and Christian Drosten. Genomic characterization of severe acute respiratory syndrome-related coronavirus in european bats and classification of coronaviruses based on partial rna-dependent rna polymerase gene sequences. *J Virol*, 84(21):11336–11349, Nov 2010.

[45] Jan Felix Drexler, Angelika Helmer, Heike Kirberg, Ulrike Reber, Marcus Panning, Marcel Müller, Katja Höfling, Bertfried Matz, Christian Drosten, and Anna Maria Eis-Hübinger. Poor clinical sensitivity of rapid antigen test for influenza a pandemic (h1n1) 2009 virus. *Emerg Infect Dis*, 15(10):1662–1664, Oct 2009.

[46] P. C. Familletti, S. Rubinstein, and S. Pestka. A convenient and rapid cytopathic effect inhibition assay for interferon. *Methods Enzymol*, 78(Pt A):387–394, 1981.

[47] O. Fernandes, R. H. Mangia, C. V. Lisboa, A. P. Pinho, C. M. Morel, B. Zingales, D. A. Campbell, and A. M. Jansen. The complexity of the sylvatic cycle of trypanosoma cruzi in rio de janeiro state (brazil) revealed by the non-transcribed spacer of the mini-exon gene. *Parasitology*, 118 (Pt 2):161–166, Feb 1999.

[48] Cristina Ferro, Jorge Boshell, Abelardo C. Moncayo, Marta Gonzalez, Marta L. Ahumada, Wenli Kang, and Scott C. Weaver. Natural enzootic vectors of venezuelan equine encephalitis virus, magdalena valley, colombia. *Emerg Infect Dis*, 9(1):49–54, Jan 2003.

[49] H. E. Field, J. S. Mackenzie, and P. Daszak. Henipaviruses: emerging paramyxoviruses associated with fruit bats. *Curr Top Microbiol Immunol*, 315:133–159, 2007.

[50] Katherine A Fitzgerald, Sarah M McWhirter, Kerrie L Faia, Daniel C Rowe, Eicke Latz, Douglas T Golenbock, Anthony J Coyle, Sha-Mei Liao, and Tom Maniatis. Ikkepsilon and tbk1 are essential components of the irf3 signaling pathway. *Nat Immunol*, 4(5):491–496, May 2003.

[51] I. Frolov and S. Schlesinger. Comparison of the effects of sindbis virus and sindbis virus replicons on host cell protein synthesis and cytopathogenicity in bhk cells. *J Virol*, 68(3):1721–1727, Mar 1994.

[52] I. Frolov and S. Schlesinger. Translation of sindbis virus mrna: analysis of sequences downstream of the initiating aug codon that enhance translation. *J Virol*, 70(2):1182–1190, Feb 1996.

[53] Elena I. Frolova, Rafik Z. Fayzulin, Susan H. Cook, Diane E. Griffin, Charles M. Rice, and Ilya Frolov. Roles of nonstructural protein nsp2 and alpha/beta interferons in determining the outcome of sindbis virus infection. *J Virol*, 76(22):11254–11264, Nov 2002.

[54] X. Y. Fu, D. S. Kessler, S. A. Veals, D. E. Levy, and JE Darnell, Jr. Isgf3, the transcriptional activator induced by interferon alpha, consists of multiple interacting polypeptide chains. *Proc Natl Acad Sci U S A*, 87(21):8555–8559, Nov 1990.

[55] Hikaru Fujii, Shumpei Watanabe, Daisuke Yamane, Naoya Ueda, Koichiro Iha, Satoshi Taniguchi, Kentaro Kato, Yukinobu Tohya, Shigeru Kyuwa, Yasuhiro Yoshikawa, and Hiroomi Akashi. Functional analysis of rousettus aegyptiacus "signal transducer and activator of transcription 1" (stat1). *Dev Comp Immunol*, 34(5):598–602, May 2010.

[56] S. D. Fuller. The t=4 envelope of sindbis virus is organized by interactions with a complementary t=3 capsid. *Cell*, 48(6):923–934, Mar 1987.

[57] K. Gaedigk-Nitschko and M. J. Schlesinger. The sindbis virus 6k protein can be detected in virions and is acylated with fatty acids. *Virology*, 175(1):274–281, Mar 1990.

[58] Natalia Garmashova, Rodion Gorchakov, Elena Frolova, and Ilya Frolov. Sindbis virus nonstructural protein nsp2 is cytotoxic and inhibits cellular transcription. *J Virol*, 80(12):5686–5696, Jun 2006.

[59] Natalia Garmashova, Rodion Gorchakov, Eugenia Volkova, Slobodan Paessler, Elena Frolova, and Ilya Frolov. The old world and new world alphaviruses use different virus-specific proteins for induction of transcriptional shutoff. *J Virol*, 81(5):2472–2484, Mar 2007.

[60] H. Garoff, A. M. Frischauf, K. Simons, H. Lehrach, and H. Delius. Nucleotide sequence of cdna coding for semliki forest virus membrane glycoproteins. *Nature*, 288(5788):236–241, Nov 1980.

[61] H. Garoff, K. Simons, and B. Dobberstein. Assembly of the semliki forest virus membrane glycoproteins in the membrane of the endoplasmic reticulum in vitro. *J Mol Biol*, 124(4):587–600, Oct 1978.

[62] N. Glanville, M. Ranki, J. Morser, L. Kääriäinen, and A. E. Smith. Initiation of translation directed by 42s and 26s rnas from semliki forest virus in vitro. *Proc Natl Acad Sci U S A*, 73(9):3059–3063, Sep 1976.

[63] Florian Gloza-Rausch, Anne Ipsen, Antje Seebens, Matthias Göttsche, Marcus Panning, Jan Felix Drexler, Nadine Petersen, Augustina Annan, Klaus Grywna, Marcel Müller, Susanne Pfefferle, and Christian Drosten. Detection and prevalence patterns of group i coronaviruses in bats, northern germany. *Emerg Infect Dis*, 14(4):626–631, Apr 2008.

[64] M. Gomez de Cedrón, N. Ehsani, M. L. Mikkola, J. A. García, and L. Kääriäinen. Rna helicase activity of semliki forest virus replicase protein nsp2. *FEBS Lett*, 448(1):19–22, Apr 1999.

[65] Rodion Gorchakov, Elena Frolova, and Ilya Frolov. Inhibition of transcription and translation in sindbis virus-infected cells. *J Virol*, 79(15):9397–9409, Aug 2005.

[66] Y. Guan, B. J. Zheng, Y. Q. He, X. L. Liu, Z. X. Zhuang, C. L. Cheung, S. W. Luo, P. H. Li, L. J. Zhang, Y. J. Guan, K. M. Butt, K. L. Wong, K. W. Chan, W. Lim, K. F. Shortridge, K. Y. Yuen, J. S M Peiris, and L. L M Poon. Isolation and characterization of viruses related to the sars coronavirus from animals in southern china. *Science*, 302(5643):276–278, Oct 2003.

[67] K. Hagmaier, N. Stock, B. Precious, K. Childs, L-F. Wang, S. Goodbourn, and R. E. Randall. Mapuera virus, a rubulavirus that inhibits interferon signalling in a wide variety of mammalian cells without degrading stats. *J Gen Virol*, 88(Pt 3):956–966, Mar 2007.

[68] Kathrin Hagmaier, Nicola Stock, Steve Goodbourn, Lin-Fa Wang, and Richard Randall. A single amino acid substitution in the v protein of nipah virus alters its ability to block interferon signalling in cells from different species. *J Gen Virol*, 87(Pt 12):3649–3653, Dec 2006.

[69] Y. S. Hahn, A. Grakoui, C. M. Rice, E. G. Strauss, and J. H. Strauss. Mapping of rna- temperature-sensitive mutants of sindbis virus: complementation group f mutants have lesions in nsp4. *J Virol*, 63(3):1194–1202, Mar 1989.

[70] O. Haller and F. Weber. The interferon response circuit in antiviral host defense. *Verh K Acad Geneeskd Belg*, 71(1-2):73–86, 2009.

[71] Otto Haller and Georg Kochs. Interferon-induced mx proteins: dynamin-like gtpases with antiviral activity. *Traffic*, 3(10):710–717, Oct 2002.

[72] Otto Haller, Peter Staeheli, and Georg Kochs. Interferon-induced mx proteins in antiviral host defense. *Biochimie*, 89(6-7):812–818, 2007.

[73] Kim Halpin, Alexander D Hyatt, Raina K Plowright, Jonathan H Epstein, Peter Daszak, Hume E Field, Linfa Wang, Peter W Daniels, and Henipavirus Ecology Research Group. Emerging viruses: coming in on a wrinkled wing and a prayer. *Clin Infect Dis*, 44(5):711–717, Mar 2007.

[74] W. R. Hardy and J. H. Strauss. Processing the nonstructural polyproteins of sindbis virus: nonstructural proteinase is in the c-terminal half of nsp2 and functions both in cis and in trans. *J Virol*, 63(11):4653–4664, Nov 1989.

[75] David T S. Hayman, Anthony R. Fooks, Daniel Horton, Richard Suu-Ire, Andrew C. Breed, Andrew A. Cunningham, and James L N. Wood. Antibodies against lagos bat virus in megachiroptera from west africa. *Emerg Infect Dis*, 14(6):926–928, Jun 2008.

[76] P. R. Heaton, P. Johnstone, L. M. McElhinney, R. Cowley, E. O'Sullivan, and J. E. Whitby. Heminested pcr assay for detection of six genotypes of rabies and rabies-related viruses. *J Clin Microbiol*, 35(11):2762–2766, Nov 1997.

[77] Hiroaki Hemmi, Osamu Takeuchi, Shintaro Sato, Masahiro Yamamoto, Tsuneyasu Kaisho, Hideki Sanjo, Taro Kawai, Katsuaki Hoshino, Kiyoshi Takeda, and Shizuo Akira. The roles of two ikappab kinase-related kinases in lipopolysaccharide and double stranded rna signaling and viral infection. *J Exp Med*, 199(12):1641–1650, Jun 2004.

[78] Hill and Smith. *Bats: a natural history*. University of texas press, 1984.

[79] Andreas Hofmann, Barbara Kessler, Sonja Ewerling, Andrea Kabermann, Gottfried Brem, Eckhard Wolf, and Alexander Pfeifer. Epigenetic regulation of lentiviral transgene vectors in a large animal model. *Mol Ther*, 13(1):59–66, Jan 2006.

[80] Dirk Holzinger, Carl Jorns, Silke Stertz, Stéphanie Boisson-Dupuis, Robert Thimme, Manfred Weidmann, Jean-Laurent Casanova, Otto Haller, and Georg Kochs. Induction of mxa gene expression by influenza a virus requires type i or type iii interferon signaling. *J Virol*, 81(14):7776–7785, Jul 2007.

[81] C. M. Horvath, G. R. Stark, I. M. Kerr, and JE Darnell, Jr. Interactions between stat and non-stat proteins in the interferon-stimulated gene factor 3 transcription complex. *Mol Cell Biol*, 16(12):6957–6964, Dec 1996.

[82] Curt M. Horvath. Weapons of stat destruction. interferon evasion by paramyxovirus v protein. *Eur J Biochem*, 271(23-24):4621–4628, Dec 2004.

[83] Koichiro Iha, Tsutomu Omatsu, Shumpei Watanabe, Naoya Ueda, Satoshi Taniguchi, Hikaru Fujii, Yoshiyuki Ishii, Shigeru Kyuwa, Hiroomi Akashi, and Yasuhiro Yoshikawa. Molecular cloning and expression analysis of bat toll-like receptors 3, 7 and 9. *J Vet Med Sci*, 72(2):217–220, Feb 2010.

[84] D. M. Irwin, T. D. Kocher, and A. C. Wilson. Evolution of the cytochrome b gene of mammals. *J Mol Evol*, 32(2):128–144, Feb 1991.

[85] A. Isaacs and J. Lindenmann. Virus interference. i. the interferon. *Proc R Soc Lond B Biol Sci*, 147(927):258–267, Sep 1957.

[86] Konstantin A Ivanov, Tobias Hertzig, Mikhail Rozanov, Sonja Bayer, Volker Thiel, Alexander E Gorbalenya, and John Ziebuhr. Major genetic marker of nidoviruses encodes a replicative endoribonuclease. *Proc Natl Acad Sci U S A*, 101(34):12694–12699, Aug 2004.

[87] C. A. Janeway, K. Murphy, P. Travers, and M. Walport. *Immunobiology*. Garland Science, 2008.

[88] A. M. Jansen, A. P. Santos de Pinho, C. V. Lisboa, E. Cupolillo, R. H. Mangia, and O. Fernandes. The sylvatic cycle of trypanosoma cruzi: a still unsolved puzzle. *Mem Inst Oswaldo Cruz*, 94 Suppl 1:203–204, 1999.

[89] Gareth Jones and Emma C. Teeling. The evolution of echolocation in bats. *Trends Ecol Evol*, 21(3):149–156, Mar 2006.

[90] Ingo Jordan, Deborah Horn, Stefanie Oehmke, Fabian H. Leendertz, and Volker Sandig. Cell lines from the egyptian fruit bat are permissive for modified vaccinia ankara. *Virus Res*, 145(1):54–62, Oct 2009.

[91] S. Junglen, A. Kurth, H. Kuehl, P-L. Quan, H. Ellerbrok, G. Pauli, A. Nitsche, C. Nunn, S. M. Rich, W. I. Lipkin, T. Briese, and F. H. Leendertz. Examining landscape factors influencing relative distribution of mosquito genera and frequency of virus infection. *Ecohealth*, 6(2):239–249, Jun 2009.

[92] McIntosh BM. Jupp PG. *Chikungunya virus disease. In: .* The Arbovirus: Epidemiology and Ecology. II. CRC Press; Boca Raton, Florida ., 1988.

[93] Thirumala-Devi Kanneganti, Mohamed Lamkanfi, and Gabriel Núñez. Intracellular nod-like receptors in host defense and disease. *Immunity*, 27(4):549–559, Oct 2007.

[94] N. Karabatsos. *International Catalogue of Arboviruses including certain other viruses of vertebrates*. American Society for tropical medicine and hygiene, 1985.

[95] Hiroki Kato, Osamu Takeuchi, Eriko Mikamo-Satoh, Reiko Hirai, Tomoji Kawai, Kazufumi Matsushita, Akane Hiiragi, Terence S. Dermody,

Takashi Fujita, and Shizuo Akira. Length-dependent recognition of double-stranded ribonucleic acids by retinoic acid-inducible gene-i and melanoma differentiation-associated gene 5. *J Exp Med*, 205(7):1601–1610, Jul 2008.

[96] Hiroki Kato, Osamu Takeuchi, Shintaro Sato, Mitsutoshi Yoneyama, Masahiro Yamamoto, Kosuke Matsui, Satoshi Uematsu, Andreas Jung, Taro Kawai, Ken J. Ishii, Osamu Yamaguchi, Kinya Otsu, Tohru Tsujimura, Chang-Sung Koh, Caetano Reis e Sousa, Yoshiharu Matsuura, Takashi Fujita, and Shizuo Akira. Differential roles of mda5 and rig-i helicases in the recognition of rna viruses. *Nature*, 441(7089):101–105, May 2006.

[97] Taro Kawai, Ken Takahashi, Shintaro Sato, Cevayir Coban, Himanshu Kumar, Hiroki Kato, Ken J. Ishii, Osamu Takeuchi, and Shizuo Akira. Ips-1, an adaptor triggering rig-i- and mda5-mediated type i interferon induction. *Nat Immunol*, 6(10):981–988, Oct 2005.

[98] Jonathan Kingdon. *East African Mammals vol. 2A (Insectivors and Bats)*. University of Chicago Press, 1984.

[99] Peter M. und Griffin Diane E. Knipe, David M.; Howley. *Fields Virology*. Lippincott Williams & Wilkins, 2007.

[100] Sergei V. Kotenko, Grant Gallagher, Vitaliy V. Baurin, Anita Lewis-Antes, Meiling Shen, Nital K. Shah, Jerome A. Langer, Faruk Sheikh, Harold Dickensheets, and Raymond P. Donnelly. Ifn-lambdas mediate antiviral protection through a distinct class ii cytokine receptor complex. *Nat Immunol*, 4(1):69–77, Jan 2003.

[101] V. Kubes and F. A. Ríos. The causative agent of infectious equine encephalomyelitis in venezuela. *Science*, 90(2323):20–21, Jul 1939.

[102] S A M. Kularatne, M. C. Gihan, S. C. Weerasinghe, and S. Gunasena. Concurrent outbreaks of chikungunya and dengue fever in kandy, sri lanka, 2006-07: a comparative analysis of clinical and laboratory features. *Postgrad Med J*, 85(1005):342–346, Jul 2009.

[103] Raghavendran Kulasegaran-Shylini, Varatharasa Thiviyanathan, David G. Gorenstein, and Ilya Frolov. The 5'utr-specific mutation in veev tc-83 genome has a strong effect on rna replication and subgenomic rna synthesis, but not on translation of the encoded proteins. *Virology*, 387(1):211–221, Apr 2009.

[104] T. H. Kunz and M. B. Fenton. *Bat Ecology*. The University of Chicago Press, London, 2003.

[105] Thomas Kuri, Matthias Habjan, Nicola Penski, and Friedemann Weber. Species-independent bioassay for sensitive quantification of antiviral type i interferons. *Virol J*, 7:50, 2010.

[106] R. Laine, H. Söderlund, and O. Renkonen. Chemical composition of semliki forest virus. *Intervirology*, 1(2):110–118, 1973.

[107] J. R. Lamb, S. Tugendreich, and P. Hieter. Tetratrico peptide repeat interactions: to tpr or not to tpr? *Trends Biochem Sci*, 20(7):257–259, Jul 1995.

[108] Susanna K P Lau, Patrick C Y Woo, Kenneth S M Li, Yi Huang, Hoi-Wah Tsoi, Beatrice H L Wong, Samson S Y Wong, Suet-Yi Leung, Kwok-Hung Chan, and Kwok-Yung Yuen. Severe acute respiratory syndrome coronavirus-like virus in chinese horseshoe bats. *Proc Natl Acad Sci U S A*, 102(39):14040–14045, Sep 2005.

[109] Agnes Le Bon and David F. Tough. Links between innate and adaptive immunity via type i interferon. *Curr Opin Immunol*, 14(4):432–436, Aug 2002.

[110] J. A. Lemm, T. Rümenapf, E. G. Strauss, J. H. Strauss, and C. M. Rice. Polypeptide requirements for assembly of functional sindbis virus replication complexes: a model for the temporal regulation of minus- and plus-strand rna synthesis. *EMBO J*, 13(12):2925–2934, Jun 1994.

[111] W. J. Leonard and J. J. O'Shea. Jaks and stats: biological implications. *Annu Rev Immunol*, 16:293–322, 1998.

[112] Jason Yat-Sing Leung, Mary Mah-Lee Ng, and Justin Jang Hann Chu. Replication of alphaviruses: a review on the entry process of alphaviruses into cells. *Adv Virol*, 2011:249640, 2011.

[113] D. Levy, A. Larner, A. Chaudhuri, L. E. Babiss, and JE Darnell, Jr. Interferon-stimulated transcription: isolation of an inducible gene and identification of its regulatory region. *Proc Natl Acad Sci U S A*, 83(23):8929–8933, Dec 1986.

[114] D. E. Levy. Physiological significance of stat proteins: investigations through gene disruption in vivo. *Cell Mol Life Sci*, 55(12):1559–1567, Sep 1999.

[115] J. A. Lewis. A sensitive biological assay for interferons. *J Immunol Methods*, 185(1):9–17, Sep 1995.

[116] G. Li and C. M. Rice. The signal for translational readthrough of a uga codon in sindbis virus rna involves a single cytidine residue immediately downstream of the termination codon. *J Virol*, 67(8):5062–5067, Aug 1993.

[117] C. K. Lincoln and M. G. Gabridge. Cell culture contamination: sources, consequences, prevention, and elimination. *Methods Cell Biol*, 57:49–65, 1998.

[118] N. Liu and D. T. Brown. Transient translocation of the cytoplasmic (endo) domain of a type i membrane glycoprotein into cellular membranes. *J Cell Biol*, 120(4):877–883, Feb 1993.

[119] K. J. Livak and T. D. Schmittgen. Analysis of relative gene expression data using real-time quantitative pcr and the 2(-delta delta c(t)) method. *Methods*, 25(4):402–408, Dec 2001.

[120] R. Lleonart, D. Näf, H. Browning, and C. Weissmann. A novel, quantitative bioassay for type i interferon using a recombinant indicator cell line. *Biotechnology (N Y)*, 8(12):1263–1267, Dec 1990.

[121] M. Lobigs, H. X. Zhao, and H. Garoff. Function of semliki forest virus e3 peptide in virus assembly: replacement of e3 with an artificial signal peptide abolishes spike heterodimerization and surface expression of e1. *J Virol*, 64(9):4346–4355, Sep 1990.

[122] Hélène Malet, Bruno Coutard, Saïd Jamal, Hélène Dutartre, Nicolas Papageorgiou, Maarit Neuvonen, Tero Ahola, Naomi Forrester, Ernest A. Gould, Daniel Lafitte, Francois Ferron, Julien Lescar, Alexander E. Gorbalenya, Xavier de Lamballerie, and Bruno Canard. The crystal structures of chikungunya and venezuelan equine encephalitis virus nsp3 macro domains define a conserved adenosine binding pocket. *J Virol*, 83(13):6534–6545, Jul 2009.

[123] E. J. Mancini, M. Clarke, B. E. Gowen, T. Rutten, and S. D. Fuller. Cryo-electron microscopy reveals the functional organization of an enveloped virus, semliki forest virus. *Mol Cell*, 5(2):255–266, Feb 2000.

[124] D. N. McMurray, J. Stroud, J. J. Murphy, M. A. Carlomagno, and D. L. Greer. Role of immunoglobulin classes in experimental histoplasmosis in bats. *Dev Comp Immunol*, 6(3):557–567, 1982.

[125] Anthony Meager. Biological assays for interferons. *J Immunol Methods*, 261(1-2):21–36, Mar 2002.

[126] Ruslan Medzhitov. Recognition of microorganisms and activation of the immune response. *Nature*, 449(7164):819–826, Oct 2007.

[127] P. Melancon and H. Garoff. Processing of the semliki forest virus structural polyprotein: role of the capsid protease. *J Virol*, 61(5):1301–1309, May 1987.

[128] Jesper Melchjorsen and Søren R. Paludan. Induction of rantes/ccl5 by herpes simplex virus is regulated by nuclear factor kappa b and interferon regulatory factor 3. *J Gen Virol*, 84(Pt 9):2491–2495, Sep 2003.

[129] Julian V. Melton, Gary D. Ewart, Ronald C. Weir, Philip G. Board, Eva Lee, and Peter W. Gage. Alphavirus 6k proteins form ion channels. *J Biol Chem*, 277(49):46923–46931, Dec 2002.

[130] K. Metsikkö and H. Garoff. Oligomers of the cytoplasmic domain of the p62/e2 membrane protein of semliki forest virus bind to the nucleocapsid in vitro. *J Virol*, 64(10):4678–4683, Oct 1990.

[131] F. P. Möhres and E.. Z. Kulzer. Über die orientierung der flughunde (chiroptera-pteropodidae). *vergl. Physiol.*, 38:1–29, 1956.

[132] S. Mi and V. Stollar. Expression of sindbis virus nsp1 and methyltransferase activity in escherichia coli. *Virology*, 184(1):423–427, Sep 1991.

[133] Hutson A.M. Bergmans W. & Fahr J. Mickleburgh, S. Myonycteris torquata. Downloaded on 29 May 2012, 2008.

[134] Marcel A. Müller, Janusz T. Paweska, Patricia A. Leman, Christian Drosten, Klaus Grywna, Alan Kemp, Leo Braack, Karen Sonnenberg, Matthias Niedrig, and Robert Swanepoel. Coronavirus antibodies in african bat species. *Emerg Infect Dis*, 13(9):1367–1370, Sep 2007.

[135] C. MORGAN, C. HOWE, and H. M. ROSE. Structure and development of viruses as observed in the electron microscope. v. western equine encephalomyelitis virus. *J Exp Med*, 113:219–234, Jan 1961.

[136] Ronald M. Nowak. *Walkers Mammals of the World*. Johns Hopkins University Press, 1999.

[137] A. Omar and H. Koblet. Semliki forest virus particles containing only the e1 envelope glycoprotein are infectious and can induce cell-cell fusion. *Virology*, 166(1):17–23, Sep 1988.

[138] K. E. Owen and R. J. Kuhn. Identification of a region in the sindbis virus nucleocapsid protein that is involved in specificity of rna encapsidation. *J Virol*, 70(5):2757–2763, May 1996.

[139] K. E. Owen and R. J. Kuhn. Alphavirus budding is dependent on the interaction between the nucleocapsid and hydrophobic amino acids on the cytoplasmic domain of the e2 envelope glycoprotein. *Virology*, 230(2):187–196, Apr 1997.

[140] Marcus Panning, Klaus Grywna, Marjan van Esbroeck, Petra Emmerich, and Christian Drosten. Chikungunya fever in travelers returning to europe from the indian ocean region, 2006. *Emerg Infect Dis*, 14(3):416–422, Mar 2008.

[141] Marcus Panning, Thomas Laue, Stephan Olschlager, Markus Eickmann, Stephan Becker, Sabine Raith, Marie-Claude Georges Courbot, Mikael Nilsson, Robin Gopal, Ake Lundkvist, Antonino di Caro, David Brown, Hermann Meyer, Graham Lloyd, Beate M. Kummerer, Stephan Gunther, and Christian Drosten. Diagnostic reverse-transcription polymerase chain reaction kit for filoviruses based on the strain collections of all european biosafety level 4 laboratories. *J Infect Dis*, 196 Suppl 2:S199–S204, Nov 2007.

[142] J. Peränen, P. Laakkonen, M. Hyvönen, and L. Kääriäinen. The alphavirus replicase protein nsp1 is membrane-associated and has affinity to endocytic organelles. *Virology*, 208(2):610–620, Apr 1995.

[143] Sidney Pestka, Christopher D. Krause, and Mark R. Walter. Interferons, interferon-like cytokines, and their receptors. *Immunol Rev*, 202:8–32, Dec 2004.

[144] Susanne Pfefferle, Verena Krähling, Vanessa Ditt, Klaus Grywna, Elke Mühlberger, and Christian Drosten. Reverse genetic characterization of the natural genomic deletion in sars-coronavirus strain frankfurt-1 open reading frame 7b reveals an attenuating function of the 7b protein in-vitro and in-vivo. *Virol J*, 6:131, 2009.

[145] Susanne Pfefferle, Samuel Oppong, Jan Felix Drexler, Florian Gloza-Rausch, Anne Ipsen, Antje Seebens, Marcel A. Müller, Augustina Annan, Peter Vallo, Yaw Adu-Sarkodie, Thomas F. Kruppa, and Christian Drosten. Distant relatives of severe acute respiratory syndrome coronavirus and close relatives of human coronavirus 229e in bats, ghana. *Emerg Infect Dis*, 15(9):1377–1384, Sep 2009.

[146] Andreas Pichlmair and Caetano Reis e Sousa. Innate recognition of viruses. *Immunity*, 27(3):370–383, Sep 2007.

[147] M. R. Player and P. F. Torrence. The 2-5a system: modulation of viral and cellular processes through acceleration of rna degradation. *Pharmacol Ther*, 78(2):55–113, May 1998.

[148] Emma Poole, Biao He, Robert A. Lamb, Richard E. Randall, and Stephen Goodbourn. The v proteins of simian virus 5 and other paramyxoviruses inhibit induction of interferon-beta. *Virology*, 303(1):33–46, Nov 2002.

[149] L L M. Poon, D K W. Chu, K. H. Chan, O. K. Wong, T. M. Ellis, Y H C. Leung, S K P. Lau, P C Y. Woo, K. Y. Suen, K. Y. Yuen, Y. Guan, and J S M. Peiris. Identification of a novel coronavirus in bats. *J Virol*, 79(4):2001–2009, Feb 2005.

[150] X. Pourrut, A. Délicat, P. E. Rollin, T. G. Ksiazek, J-P. Gonzalez, and E. M. Leroy. Spatial and temporal patterns of zaire ebolavirus antibody prevalence in the possible reservoir bat species. *J Infect Dis*, 196 Suppl 2:S176–S183, Nov 2007.

[151] Xavier Pourrut, Marc Souris, Jonathan S. Towner, Pierre E. Rollin, Stuart T. Nichol, Jean-Paul Gonzalez, and Eric Leroy. Large serological survey showing cocirculation of ebola and marburg viruses in gabonese bat populations, and a high seroprevalence of both viruses in rousettus aegyptiacus. *BMC Infect Dis*, 9:159, 2009.

[152] Virginie Pétrilli, Catherine Dostert, Daniel A. Muruve, and Jürg Tschopp. The inflammasome: a danger sensing complex triggering innate immunity. *Curr Opin Immunol*, 19(6):615–622, Dec 2007.

[153] J. S. Reif, P. A. Webb, T. P. Monath, J. K. Emerson, J. D. Poland, G. E. Kemp, and G. Cholas. Epizootic vesicular stomatitis in colorado, 1982: infection in occupational risk groups. *Am J Trop Med Hyg*, 36(1):177–182, Jan 1987.

[154] M. Rikkonen, J. Peränen, and L. Kääriäinen. Atpase and gtpase activities associated with semliki forest virus nonstructural protein nsp2. *J Virol*, 68(9):5804–5810, Sep 1994.

[155] J. M. Rose, C. K. Crowley, and WR Fleischmann, Jr. Evidence that ifn-alph/beta induces two antiviral states active against different viruses. *J Gen Virol*, 66 (Pt 5):1153–1158, May 1985.

[156] S. Rottem and M. F. Barile. Beware of mycoplasmas. *Trends Biotechnol*, 11(4):143–151, Apr 1993.

[157] S. Rubinstein, P. C. Familletti, and S. Pestka. Convenient assay for interferons. *J Virol*, 37(2):755–758, Feb 1981.

[158] Kate D. Ryman and William B. Klimstra. Host responses to alphavirus infection. *Immunol Rev*, 225:27–45, Oct 2008.

[159] Takeshi Saito, Reiko Hirai, Yueh-Ming Loo, David Owen, Cynthia L. Johnson, Sangita C. Sinha, Shizuo Akira, Takashi Fujita, and Michael Gale, Jr. Regulation of innate antiviral defenses through a shared repressor domain in rig-i and lgp2. *Proc Natl Acad Sci U S A*, 104(2):582–587, Jan 2007.

[160] C. E. Samuel. Antiviral actions of interferons. *Clin Microbiol Rev*, 14(4):778–809, table of contents, Oct 2001.

[161] Jussi Sane, Satu Kurkela, Lev Levanov, Simo Nikkari, Antti Vaheri, and Olli Vapalahti. Development and evaluation of a real-time rt-pcr assay for sindbis virus detection. *J Virol Methods*, 179(1):185–188, Jan 2012.

[162] M. A. Sanz, L. Pérez, and L. Carrasco. Semliki forest virus 6k protein modifies membrane permeability after inducible expression in escherichia coli cells. *J Biol Chem*, 269(16):12106–12110, Apr 1994.

[163] Miguel Angel Sanz, Vanessa Madan, Luis Carrasco, and José Luis Nieva. Interfacial domains in sindbis virus 6k protein. detection and functional characterization. *J Biol Chem*, 278(3):2051–2057, Jan 2003.

[164] S. K. Sarkar and A. K. Chakravarty. Analysis of immunocompetent cells in the bat, pteropus giganteus: isolation and scanning electron microscopic characterization. *Dev Comp Immunol*, 15(4):423–430, 1991.

[165] M. Sato, H. Suemori, N. Hata, M. Asagiri, K. Ogasawara, K. Nakao, T. Nakaya, M. Katsuki, S. Noguchi, N. Tanaka, and T. Taniguchi. Distinct and essential roles of transcription factors irf-3 and irf-7 in response to viruses for ifn-alpha/beta gene induction. *Immunity*, 13(4):539–548, Oct 2000.

[166] Olivier Schwartz and Matthew L. Albert. Biology and pathogenesis of chikungunya virus. *Nat Rev Microbiol*, 8(7):491–500, Jul 2010.

[167] Rashu B. Seth, Lijun Sun, Chee-Kwee Ea, and Zhijian J. Chen. Identification and characterization of mavs, a mitochondrial antiviral signaling protein that activates nf-kappab and irf 3. *Cell*, 122(5):669–682, Sep 2005.

[168] C. Seymour, R. W. Dickerman, and M. S. Martin. Venezuelan encephalitis virus infection in neotropical bats. i. natural infection in a guatemalan enzootic focus. *Am J Trop Med Hyg*, 27(2 Pt 1):290–296, Mar 1978.

[169] Zhengli Shi. Bat and virus. *Protein Cell*, 1(2):109–114, Feb 2010.

[170] Y. Shirako, E. G. Strauss, and J. H. Strauss. Suppressor mutations that allow sindbis virus rna polymerase to function with nonaromatic amino acids at the n-terminus: evidence for interaction between nsp1 and nsp4 in minus-strand rna synthesis. *Virology*, 276(1):148–160, Oct 2000.

[171] Y. Shirako and J. H. Strauss. Regulation of sindbis virus rna replication: uncleaved p123 and nsp4 function in minus-strand rna synthesis, whereas cleaved products from p123 are required for efficient plus-strand rna synthesis. *J Virol*, 68(3):1874–1885, Mar 1994.

[172] R. Siegert, H. L. Shu, W. Slenczka, D. Peters, and G. Müller. [on the etiology of an unknown human infection originating from monkeys]. *Dtsch Med Wochenschr*, 92(51):2341–2343, Dec 1967.

[173] Björn M. Siemers and Hans-Ulrich Schnitzler. Echolocation signals reflect niche differentiation in five sympatric congeneric bat species. *Nature*, 429(6992):657–661, Jun 2004.

[174] C. Sim, Y. S. Hong, D. L. Vanlandingham, B. W. Harker, G. K. Christophides, F. C. Kafatos, S. Higgs, and F. H. Collins. Modulation of anopheles gambiae gene expression in response to o'nyong-nyong virus infection. *Insect Mol Biol*, 14(5):475–481, Oct 2005.

[175] B. Simizu, K. Yamamoto, K. Hashimoto, and T. Ogata. Structural proteins of chikungunya virus. *J Virol*, 51(1):254–258, Jul 1984.

[176] D. T. Simmons and J. H. Strauss. Replication of sindbis virus. ii. multiple forms of double-stranded rna isolated from infected cells. *J Mol Biol*, 71(3):615–631, Nov 1972.

[177] Jason D. Simmons, Laura J. White, Thomas E. Morrison, Stephanie A. Montgomery, Alan C. Whitmore, Robert E. Johnston, and Mark T. Heise. Venezuelan equine encephalitis virus disrupts stat1 signaling by distinct mechanisms independent of host shutoff. *J Virol*, 83(20):10571–10581, Oct 2009.

[178] Jason D. Simmons, Amy C. Wollish, and Mark T. Heise. A determinant of sindbis virus neurovirulence enables efficient disruption of jak/stat signaling. *J Virol*, 84(21):11429–11439, Nov 2010.

[179] N.B Simmons. *Order Chiroptera. In Mammal species of the world: a taxonomic and geographic reference, 3 edn, pp. 312–529.* John Hopkins University Press, 2005.

[180] F. Simon, H. Tolou, and P. Jeandel. [the unexpected chikungunya outbreak]. *Rev Med Interne*, 27(6):437–441, Jun 2006.

[181] W. G. Slenczka. The marburg virus outbreak of 1967 and subsequent episodes. *Curr Top Microbiol Immunol*, 235:49–75, 1999.

[182] Werner Slenczka and Hans Dieter Klenk. Forty years of marburg virus. *J Infect Dis*, 196 Suppl 2:S131–S135, Nov 2007.

[183] T. J. Smith, R. H. Cheng, N. H. Olson, P. Peterson, E. Chase, R. J. Kuhn, and T. S. Baker. Putative receptor binding sites on alphaviruses as visualized by cryoelectron microscopy. *Proc Natl Acad Sci U S A*, 92(23):10648–10652, Nov 1995.

[184] Huai-Dong Song, Chang-Chun Tu, Guo-Wei Zhang, Sheng-Yue Wang, Kui Zheng, Lian-Cheng Lei, Qiu-Xia Chen, Yu-Wei Gao, Hui-Qiong Zhou, Hua Xiang, Hua-Jun Zheng, Shur-Wern Wang Chern, Feng Cheng, Chun-Ming Pan, Hua Xuan, Sai-Juan Chen, Hui-Ming Luo, Duan-Hua Zhou, Yu-Fei Liu, Jian-Feng He, Peng-Zhe Qin, Ling-Hui Li, Yu-Qi Ren, Wen-Jia Liang, Ye-Dong Yu, Larry Anderson, Ming Wang, Rui-Heng Xu, Xin-Wei Wu, Huan-Ying Zheng, Jin-Ding Chen, Guodong Liang, Yang Gao, Ming Liao, Ling Fang, Li-Yun Jiang, Hui Li, Fang Chen, Biao Di, Li-Juan He, Jin-Yan Lin, Suxiang Tong, Xiangang Kong, Lin Du, Pei Hao, Hua Tang, Andrea Bernini, Xiao-Jing Yu, Ottavia Spiga, Zong-Ming Guo, Hai-Yan Pan, Wei-Zhong He, Jean-Claude Manuguerra, Arnaud Fontanet, Antoine Danchin, Neri Niccolai, Yi-Xue Li, Chung-I. Wu, and Guo-Ping Zhao. Cross-host evolution of severe acute respiratory syndrome coronavirus in palm civet and human. *Proc Natl Acad Sci U S A*, 102(7):2430–2435, Feb 2005.

[185] D. E. Stallknecht, E. W. Howerth, C. L. Reeves, and B. S. Seal. Potential for contact and mechanical vector transmission of vesicular stomatitis virus new jersey in pigs. *Am J Vet Res*, 60(1):43–48, Jan 1999.

[186] G. R. Stark, I. M. Kerr, B. R. Williams, R. H. Silverman, and R. D. Schreiber. How cells respond to interferons. *Annu Rev Biochem*, 67:227–264, 1998.

[187] WE Stewart, 2nd, W. D. Scott, and S. E. Sulkin. Relative sensitivities of viruses to different species of interferon. *J Virol*, 4(2):147–153, Aug 1969.

[188] E. G. Strauss, C. M. Rice, and J. H. Strauss. Complete nucleotide sequence of the genomic rna of sindbis virus. *Virology*, 133(1):92–110, Feb 1984.

[189] J. H. Strauss and E. G. Strauss. The alphaviruses: gene expression, replication, and evolution. *Microbiol Rev*, 58(3):491–562, Sep 1994.

[190] Melanie Störmer, Tanja Vollmer, Birgit Henrich, Knut Kleesiek, and Jens Dreier. Broad-range real-time pcr assay for the rapid identification of cell-line contaminants and clinically important mollicute species. *Int J Med Microbiol*, 299(4):291–300, Apr 2009.

[191] R. Swanepoel, P. A. Leman, F. J. Burt, N. A. Zachariades, L. E. Braack, T. G. Ksiazek, P. E. Rollin, S. R. Zaki, and C. J. Peters. Experimental inoculation of plants and animals with ebola virus. *Emerg Infect Dis*, 2(4):321–325, 1996.

[192] Robert Swanepoel, Sheilagh B. Smit, Pierre E. Rollin, Pierre Formenty, Patricia A. Leman, Alan Kemp, Felicity J. Burt, Antoinette A. Grobbelaar, Janice Croft, Daniel G. Bausch, Hervé Zeller, Herwig Leirs, L E O. Braack, Modeste L. Libande, Sherif Zaki, Stuart T. Nichol, Thomas G. Ksiazek, Janusz T. Paweska, International Scientific , and Technical Committee for Marburg Hemorrhagic Fever Control in the Democratic Republic of Congo. Studies of reservoir hosts for marburg virus. *Emerg Infect Dis*, 13(12):1847–1851, Dec 2007.

[193] Kiyohiro Takahasi, Mitsutoshi Yoneyama, Tatsuya Nishihori, Reiko Hirai, Hiroyuki Kumeta, Ryo Narita, Michael Gale, Jr, Fuyuhiko Inagaki, and Takashi Fujita. Nonself rna-sensing mechanism of rig-i helicase and activation of antiviral immune responses. *Mol Cell*, 29(4):428–440, Feb 2008.

[194] Osamu Takeuchi and Shizuo Akira. Mda5/rig-i and virus recognition. *Curr Opin Immunol*, 20(1):17–22, Feb 2008.

[195] Emma C Teeling, Mark S Springer, Ole Madsen, Paul Bates, Stephen J O'brien, and William J Murphy. A molecular phylogeny for bats illuminates biogeography and the fossil record. *Science*, 307(5709):580–584, Jan 2005.

[196] Fulvia Terenzi, Daniel J. Hui, William C. Merrick, and Ganes C. Sen. Distinct induction patterns and functions of two closely related interferon-inducible human genes, isg54 and isg56. *J Biol Chem*, 281(45):34064–34071, Nov 2006.

[197] R. B. Tesh. Arthritides caused by mosquito-borne viruses. *Annu Rev Med*, 33:31–40, 1982.

[198] R. Tjian and T. Maniatis. Transcriptional activation: a complex puzzle with few easy pieces. *Cell*, 77(1):5–8, Apr 1994.

[199] Jonathan S. Towner, Brian R. Amman, Tara K. Sealy, Serena A Reeder Carroll, James A. Comer, Alan Kemp, Robert Swanepoel, Christopher D. Paddock, Stephen Balinandi, Marina L. Khristova, Pierre B H. Formenty, Cesar G. Albarino, David M. Miller, Zachary D. Reed, John T. Kayiwa, James N. Mills, Deborah L. Cannon, Patricia W. Greer, Emmanuel Byaruhanga, Eileen C. Farnon, Patrick Atimnedi, Samuel Okware, Edward Katongole-Mbidde, Robert Downing, Jordan W. Tappero, Sherif R. Zaki, Thomas G. Ksiazek, Stuart T. Nichol, and Pierre E. Rollin. Isolation of genetically diverse marburg viruses from egyptian fruit bats. *PLoS Pathog*, 5(7):e1000536, Jul 2009.

[200] Jonathan S. Towner, Xavier Pourrut, César G. Albariño, Chimène Nze Nkogue, Brian H. Bird, Gilda Grard, Thomas G. Ksiazek, Jean-Paul Gonzalez, Stuart T. Nichol, and Eric M. Leroy. Marburg virus infection detected in a common african bat. *PLoS One*, 2(8):e764, 2007.

[201] Shumpei Tsuda, Shumpei Watanabe, Joseph S. Masangkay, Tetsuya Mizutani, Phillip Alviola, Naoya Ueda, Koichiro Iha, Satoshi Taniguchi, Hikaru Fujii, Kentaro Kato, Taisuke Horimoto, Shigeru Kyuwa, Yasuhiro Yoshikawa, and Hiroomi Akashi. Genomic and serological detection of bat coronavirus from bats in the philippines. *Arch Virol*, Jul 2012.

[202] S. R. Ubico and R. G. McLean. Serologic survey of neotropical bats in guatemala for virus antibodies. *J Wildl Dis*, 31(1):1–9, Jan 1995.

[203] Christina M. Ulane, Alex Kentsis, Cristian D. Cruz, Jean-Patrick Parisien, Kristi L. Schneider, and Curt M. Horvath. Composition and assembly of

stat-targeting ubiquitin ligase complexes: paramyxovirus v protein carboxyl terminus is an oligomerization domain. *J Virol*, 79(16):10180–10189, Aug 2005.

[204] K. Uno, T. Sato, Y. Takada, K. Fujioka, Y. Suginoshita, K. Kakimi, F. Moriyasu, and T. Kishida. A bioassay for serum interferon based on induction of 2'5'-oligoadenylate synthetase activity. *J Interferon Cytokine Res*, 18(12):1011–1018, Dec 1998.

[205] Dana L. Vanlandingham, Chao Hong, Kimberly Klingler, Konstantin Tsetsarkin, Kate L. McElroy, Ann M. Powers, Michael J. Lehane, and Stephen Higgs. Differential infectivities of o'nyong-nyong and chikungunya virus isolates in anopheles gambiae and aedes aegypti mosquitoes. *Am J Trop Med Hyg*, 72(5):616–621, May 2005.

[206] L. Vasiljeva, A. Merits, P. Auvinen, and L. Kääriäinen. Identification of a novel function of the alphavirus capping apparatus. rna 5'-triphosphatase activity of nsp2. *J Biol Chem*, 275(23):17281–17287, Jun 2000.

[207] D. J. Vaux, A. Helenius, and I. Mellman. Spike–nucleocapsid interaction in semliki forest virus reconstructed using network antibodies. *Nature*, 336(6194):36–42, Nov 1988.

[208] Elena R. Virtue, Glenn A. Marsh, Michelle L. Baker, and Lin-Fa Wang. Interferon production and signaling pathways are antagonized during henipavirus infection of fruit bat cell lines. *PLoS One*, 6(7):e22488, 2011.

[209] R. H. Vogel, S. W. Provencher, C. H. von Bonsdorff, M. Adrian, and J. Dubochet. Envelope structure of semliki forest virus reconstructed from cryo-electron micrographs. *Nature*, 320(6062):533–535, 1986.

[210] Eugenia Volkova, Elena Frolova, Justin R. Darwin, Naomi L. Forrester, Scott C. Weaver, and Ilya Frolov. Ires-dependent replication of venezuelan equine encephalitis virus makes it highly attenuated and incapable of replicating in mosquito cells. *Virology*, 377(1):160–169, Jul 2008.

[211] P. Vollmar and G. Dobler. Serological cross-reactions between alphaviruses by indirect immunofluorescence assay. In *Medical Biodefense conference*, 2011.

[212] Scott C. Weaver, Cristina Ferro, Roberto Barrera, Jorge Boshell, and Juan-Carlos Navarro. Venezuelan equine encephalitis. *Annu Rev Entomol*, 49:141–174, 2004.

[213] Hana M. Weingartl, Yohannes Berhane, and Markus Czub. Animal models of henipavirus infection: a review. *Vet J*, 181(3):211–220, Sep 2009.

[214] B. Weiss, H. Nitschko, I. Ghattas, R. Wright, and S. Schlesinger. Evidence for specificity in the encapsidation of sindbis virus rnas. *J Virol*, 63(12):5310–5318, Dec 1989.

[215] Laura K. White, Tina Sali, David Alvarado, Evelina Gatti, Philippe Pierre, Daniel Streblow, and Victor R. Defilippis. Chikungunya virus induces ips-1-dependent innate immune activation and protein kinase r-independent translational shutoff. *J Virol*, 85(1):606–620, Jan 2011.

[216] Gudrun Wibbelt, Marianne S. Moore, Tony Schountz, and Christian C. Voigt. Emerging diseases in chiroptera: why bats? *Biol Lett*, 6(4):438–440, Aug 2010.

[217] B. R. Williams. Signal integration via pkr. *Sci STKE*, 2001(89):re2, Jul 2001.

[218] M. C. WILLIAMS, J. P. WOODALL, P. S. CORBET, and J. D. GILLETT. O'nyong-nyong fever: An epidemic virus disease in east africa. 8. virus isolations from anopheles mosquitoes. *Trans R Soc Trop Med Hyg*, 59:300–306, May 1965.

[219] Koon Chu Yaiw, Gary Crameri, Linfa Wang, Heng Thay Chong, Kaw Bing Chua, Chong Tin Tan, Khean Jin Goh, Devi Shamala, and K Thong Wong. Serological evidence of possible human infection with tioman virus, a newly described paramyxovirus of bat origin. *J Infect Dis*, 196(6):884–886, Sep 2007.

[220] J. M. Yob, H. Field, A. M. Rashdi, C. Morrissy, B. van der Heide, P. Rota, A. bin Adzhar, J. White, P. Daniels, A. Jamaluddin, and T. Ksiazek. Nipah virus infection in bats (order chiroptera) in peninsular malaysia. *Emerg Infect Dis*, 7(3):439–441, 2001.

[221] Mitsutoshi Yoneyama and Takashi Fujita. Rna recognition and signal transduction by rig-i-like receptors. *Immunol Rev*, 227(1):54–65, Jan 2009.

[222] Mitsutoshi Yoneyama, Mika Kikuchi, Kanae Matsumoto, Tadaatsu Imaizumi, Makoto Miyagishi, Kazunari Taira, Eileen Foy, Yueh-Ming Loo, Michael Gale, Jr, Shizuo Akira, Shin Yonehara, Atsushi Kato, and Takashi Fujita. Shared and unique functions of the dexd/h-box helicases rig-i, mda5, and lgp2 in antiviral innate immunity. *J Immunol*, 175(5):2851–2858, Sep 2005.

[223] Peng Zhou, Chris Cowled, Glenn A. Marsh, Zhengli Shi, Lin-Fa Wang, and Michelle L. Baker. Type iii ifn receptor expression and functional characterisation in the pteropid bat, pteropus alecto. *PLoS One*, 6(9):e25385, 2011.

[224] Peng Zhou, Chris Cowled, Glenn A. Marsh, Zhengli Shi, Lin-Fa Wang, and Michelle L. Baker. Type iii ifn receptor expression and functional characterisation in the pteropid bat, pteropus alecto. *PLoS One*, 6(9):e25385, 2011.

[225] Peng Zhou, Chris Cowled, Shawn Todd, Gary Crameri, Elena R. Virtue, Glenn A. Marsh, Reuben Klein, Zhengli Shi, Lin-Fa Wang, and Michelle L. Baker. Type iii ifns in pteropid bats: differential expression patterns provide evidence for distinct roles in antiviral immunity. *J Immunol*, 186(5):3138–3147, Mar 2011.

6 Abbreviation

	Abbreviation	Meaning
A	α	Anti
	A	Adenine
	APS	Ammoniumperoxodisulfat
	aa	Amino acid
	A549	Adenocarcinomic human alveolar basal epithelial cells
B	β-ME	β-Mercaptoethanol
	b	Bat
	bp	Base pair
	BSA	Bovines Serum Albumin
	BSL	Biosafety level
C	C	Cytosin
	cDNA	copy DNA
	CHIKV	Chikungunya virus
	CO_2	Kohlendioxid
	CoV	Coronavirus
	Cy	Cyanine
D	D	Aspartic acid
	DLA	Dual Luciferase Assay
	DMEM	Dulbecco's Modified Eagles Medium
	DNA	Desoxyribonucleic acid
	dNTP	Desoxyribonukleosid-Triphosphat
	dsRNA	Double stranded RNA
	DTT	Dithiothreitol
E	EC_{50}	Half maximal effective concentration
	EDTA	Ethylenediaminetetraacetic acid
	EGFP	Enhanced Green Fluorescent Protein
	E. helvum	*Eidolon helvum*
	Epo.	*Epomops*

	ER	Endoplasmatic Reticulum
	EtBr	Ethidiumbromid
	EtOH	Ethanol
F	For	forward primer
	FF	Firefly-Luciferase
	FITC	fluorescein isothiocyanate
	F.W.	Friedemann Weber
G	G	Guanine
	g	gravitational force
	GE	Genome equivalents
H	h	hour
	hpi	hours post infection
	hu	human
	H_2O	Water
	HA	Haemaglutinine
	HCl	Hydrochloric acid
	HEP2	Human epidermoid carcinoma cells
	hpi	hours post infection
	HRP	horseradish peroxidase
I	IF	Immuno fluorescence
	IFN	Interferon
	IFN-β	Interferon-β
	IGEPAL CA-630	octylphenoxypolyethoxyethanol
	IOV	Instiute of Virology
	IP	Immunoprecipitation
	ISG	IFN stimulated gene
	ISGF	Interferon stimulated gene factor
	ISRE	Interferon-stimulated response element
K	Kb	Kilo base pairs
	kDa	Kilo Dalton
L	LBV	Lagos bat virus
	lp	low passage
M	M	Mouse
	MA104	African green monkey fibroblast cells
	MDA5	Melanoma differentiation factor-5

	MEF	Mouse embryonic fibroblast cells
	MeOH	Methanol
	MOI	Multiplicity of infection
	mRNA	messenger RNA
	MxA	Myxovirus-resistance A
N	Ni	Kidney
	Nsp	non-structural protein
O	OAS	2´,5´-Oligoadenylate synthetase
	ORF	Open reading frame
	ONNV	O'nyong-nyong virus
P	PAGE	Polyacrylamid Gelelektrophoresis
	PBS	Newline Phosphate buffered saline
	PCR	Polymerase chain reaction
	PFU	Plaque forming units
	pH	pondus hydrogenii
	PI III	Proteinase Inhibitor III
	β-PL	β-Propiolactone
	Poly IC	Polyinosin:Polycytidyl acid
	Prb	Probe
	PVDF	Polyvinylidenfluorid
R	Rev	Reverse Primer
	RIPA	Radio immuno precipitation assay
	RIG-I	Retinoic acid inducible gene-I
	RL	Renilla-Luciferase
	RLU	Relative light units
	RNA	Ribonucleic acid
	RPM	Rotation per minute
	Ro	Rousettus
	RT	Room temperature
	RT-PCR	Reverse transcriptase PCR
	RVFV	Rift Valley Fever Virus
S	SARS	Severe Acute Respiratory Syndrome
	SDS	Sodium dodecylsulfate
	sgRNA	subgenomic RNA
	SINV	Sindbis virus
	SS III	SuperScript III Reverse Transkriptase
	ssRNA	Single strand RNA

	STAT	signal transducer and activator of transcription
	SV40	Simian Virus 40
T	T	Thymin
	TEMED	N,N,N‘,N‘-Tetramethyl-ethylendiamin
	TAE	Tris-Acetate-EDTA Buffer
	Tbp	TATA-box binding protein
	Tris	Tris(hydroxymethyl)-aminomethan
U	U	Uracil
	UV	Ultraviolett
V	v	Volume
	VEEV	Venuzuelan equine encephalitis virus
	Vero e6	African green monkey kidney cells
	vRNA	viral RNA
	VSV	Vesicular stomatits virus
W	w	Weight
	WB	Western Blot
	wt	Wild type
Z		

Curriculum vitae

Personal information	born on 16th October 1982 in Leverkusen
02.2009-2012	University of Bonn Medical Centre PhD student at the Institute of Virology ´Investigations into interferon response of novel bat cell cultures upon alphavirus infection´
06.2007-05.2008	University of Cologne Diploma thesis at the Institute for Genetics ´Mitochondrial ribosomal proteins as putative substrates of the m-AAA protease´
10.2005-05.2007	Advanced studies in Biology at the University of Cologne. Main subjects: genetics, biochemistry and physiology of plants
08.2004-07.2005	Erasmus scholarship following studies in Biology at the University of Leiden, the Netherlands Study project: ´Regulatory DNA binding peptides as novel tools for plant functional genomics´
10.2002-07.2004	University of Göttingen Basic studies in Biology including pre-degree
08.1992-05.2002	Johann-Gottfried-Herder Gymnasium, Cologne Degree: Qualification for entrance to universities (Abitur)

Publications and Posters

Susanne E. Biesold, Daniel Ritz, Florian Gloza-Rausch, Robert Wollny, Jan F. Drexler, Victor M. Corman, Elisabeth K. V. Kalko, Samuel Oppong, Christian Drosten, Marcel A. Müller 2011; Type I Interferon Reaction to Viral Infection in Interferon-Competent, Immortalized Cell Lines from the African Fruit Bat Eidolon helvum. PLoS ONE 6(11)

Susanne E. Biesold, Daniel Ritz, Florian Gloza-Rausch, Robert Wollny, Jan F. Drexler, Victor M. Corman, Friedemann. Weber, Elisabeth K. V. Kalko, Samuel Oppong, Christian Drosten and Marcel A. Müller, Annual Meeting of the Society for Virology 2012(3) Comparison of the interferon response of bat cells with prototypic mammalian cell cultures.

Susanne E. Biesold, Daniel Ritz, Florian Gloza-Rausch, Robert Wollny, Jan F. Drexler, Victor M. Corman, Friedemann Weber, Elisabeth K. V. Kalko, Samuel Oppong, Christian Drosten and Marcel A. Müller, National Symposium on Zoonoses Research 2011(10) Comparison of the interferon response of bat cells with prototypic mammalian cell cultures.

Susanne E. Biesold, Marcel A. Müller and Christian Drosten, National Symposium on Zoonoses Research 2010(10) Development and evaluation of a bat interferon specific bioassay.

Marcel A. Müller, Daniel Ritz, **Susanne E. Biesold**, Robert Wollny and Christian Drosten, National Symposium on Zoonoses Research 2010(10) Development of tools to characterize interferon induction and response in bat cells.

Erklärung zur Dissertation

Ich erkläre, dass ich

- die Dissertation persönlich, selbstständig und ohne unerlaubte fremde Hilfe angefertigt habe,

- keine anderen, als die von mir angegebenen Quellen und Hilfsmittel benutzt habe,

- diese oder eine ähnliche Arbeit an keiner anderen Universität zur Erlangung eines Titels eingereicht habe,

- noch keinen Promotionsversuch unternommen habe.

Bonn, den

Susanne E. Biesold

Danksagung

An erster Stelle möchte ich mich bei Prof. Christian Drosten dafür bedanken, dass er mir die Arbeit an einem so unberührten, spannenden Thema ermöglicht hat. Des weiteren bedanke ich mich für die vielen Ideen, verschiedenen Blickwinkel und wertvollen Diskussionen.

Bei Prof. Sahl bedanke ich mich für die unverzügliche Bereitschaft meine Arbeit zu begutachten.

Zusätzlich geht mein Dank an Prof. Eis-Hübinger und Prof. Misof für die Bereitschaft zur Teilnahme an meiner Promotionskommission.

Von Herzen bedanke ich mich bei Marcel Müller, der mit mir durch alle Dimensionen dieser Arbeit geschritten ist und mit mir gemeinsam den Kreis geschlossen hat. Vielen lieben Dank für deine Fürsorge, ich habe mich immer sehr wohl bei dir gefühlt.

Auch geht mein Dank an alle meine Kollegen, die jeden Tag aufs Neue ein Arbeitsklima geschaffen haben, indem so eine Arbeit überhaupt erst möglich war. Bei Robert und Daniel möchte ich mich für die gute und unkomplizierte Zusammenarbeit bei der Entwicklung der RT-PCR Assays und des Bioassays bedanken. Bei Tasmin möchte ich mich für die Ausdauer bei der Korrektur meines englischen Ausdrucks und für die liebevollen kleinen "Ausflüge" nach Tazland bedanken. Im Besonderen bedanke ich mich bei Dany für die unermüdliche Begeisterung ihr Wissen über Fledermäuse mit mir zu teilen und natürlich für ihr herzerfüllendes Lachen. Ich bedanke mich bei Nina und Janett für die liebevolle Umgebung beim Ankommen und bei Tabea vorm Weiterziehen.

Meiner lieben Ines danke ich für die vielen Schritte und Routen zum Kopf freimachen und das andere Licht auf das, was da ist. Ich danke meiner lieben Verena und meiner lieben Sarah für ihre Geduld, Liebe und die kleine Nase frische Luft. Lieber Papa, grandios, dass du mit nach Berlin gefahren bist. Das hat mir gezeigt, dass du hinter mir stehst. Liebe Rena, vielen Dank fürs Möwen füttern. Lieber Jan Willem, dir danke ich natürlich auch für deine Geduld und Liebe, aber auch die Kraft mich davon zu tragen und mit mir weiter zu gehen.

Ich gucke nach oben und sehe dein Lächeln.